The Search For Dark Matter with ACTs

James Buckley
Washington University, St. Louis

UCLA DM Conference

Feb 20, 2018

Dark Matter Complementarity

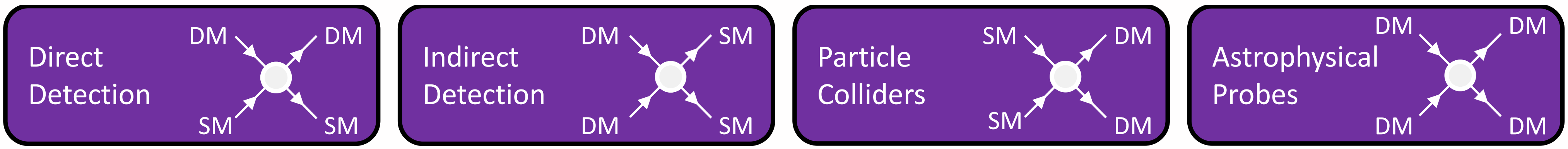

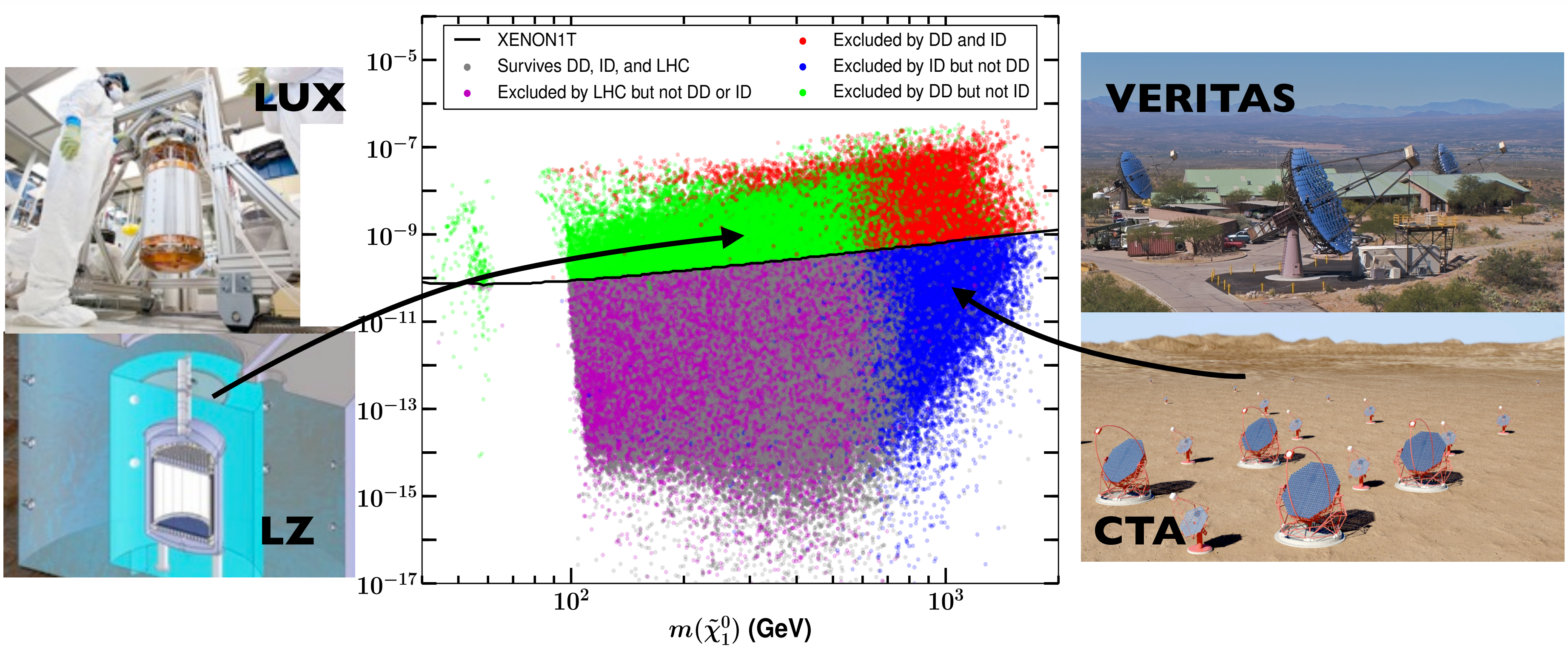

VERITAS Array

VERITAS Array

- *10 mCrab sensitivity* - 5σ detection at 1% Crab (2×10^{-13} erg cm^{-2} s^{-1} @ 1 TeV) in 28 hrs.
- *Effective area 10^5 m^2* above 500 GeV
- *Angular resolution <0.1 deg*
- *Energy range 150 GeV - 30 TeV, 15% resolution* (for spectral measurements)

VERITAS Array

- *10 mCrab sensitivity* - 5σ detection at 1% Crab (2×10^{-13} erg cm^{-2} s^{-1} @ 1 TeV) in 28 hrs.
- *Effective area 10^5 m^2* above 500 GeV
- *Angular resolution <0.1 deg*
- *Energy range 150 GeV - 30 TeV, 15% resolution* (for spectral measurements)

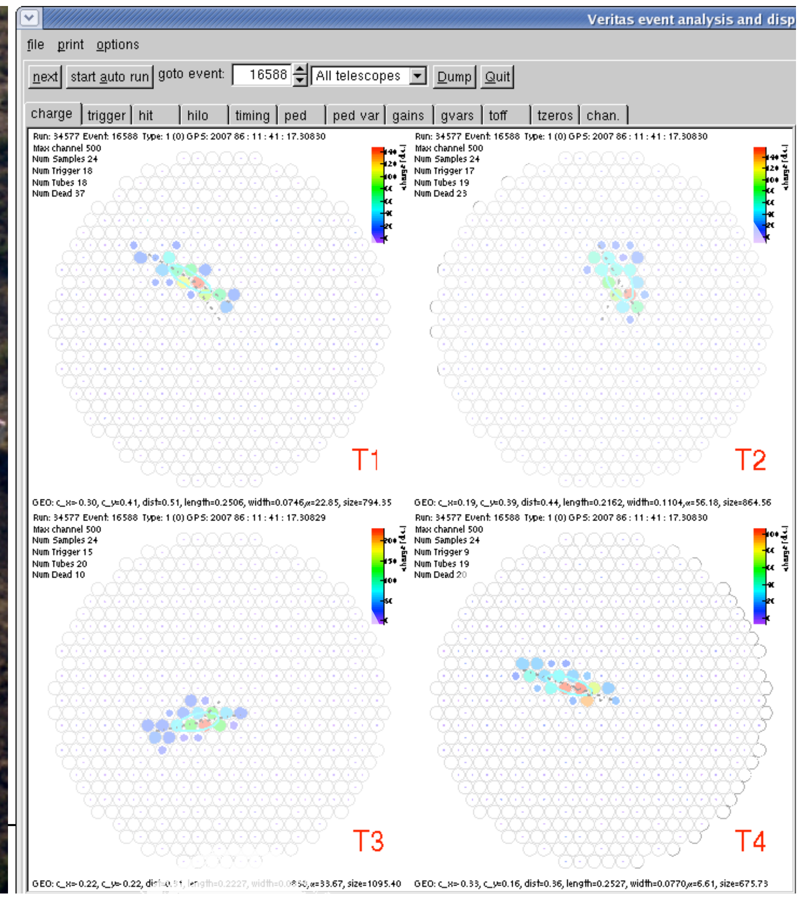

VERITAS Array

- *10 mCrab sensitivity* - 5σ detection at 1% Crab (2×10^{-13} erg cm^{-2} s^{-1} @ 1 TeV) in 28 hrs.
- *Effective area 10^5 m^2* above 500 GeV
- *Angular resolution <0.1 deg*
- *Energy range 150 GeV - 30 TeV, 15% resolution* (for spectral measurements)

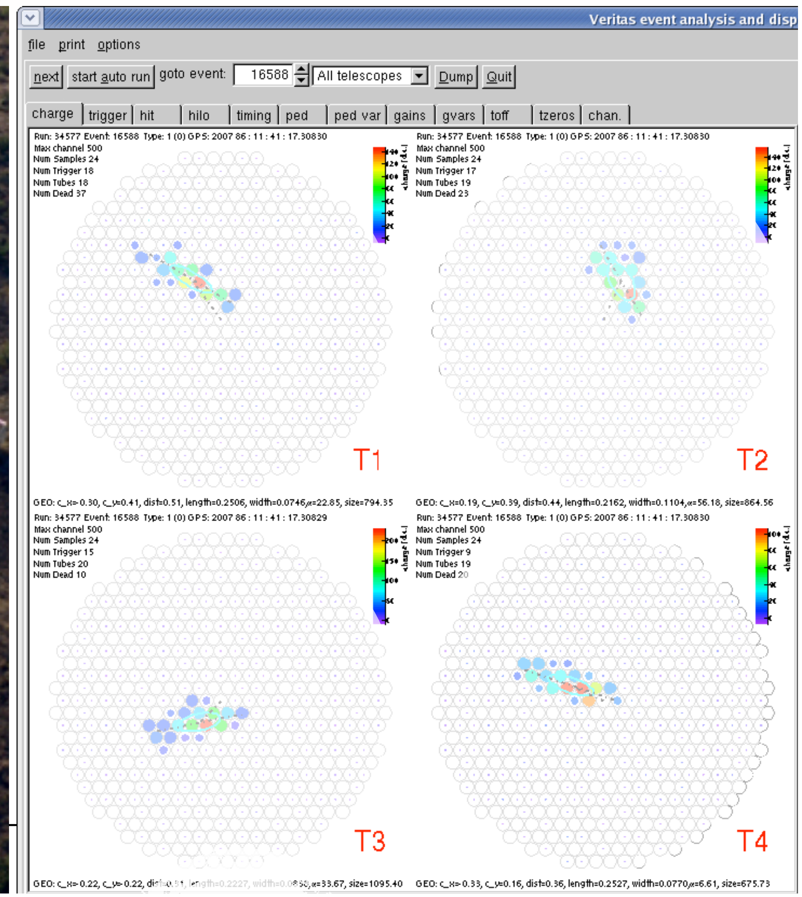

VERITAS Array

- *10 mCrab sensitivity* - 5σ detection at 1% Crab (2×10^{-13} erg cm^{-2} s^{-1} @ 1 TeV) in 28 hrs.
- *Effective area 10^5 m^2* above 500 GeV
- *Angular resolution <0.1 deg*
- *Energy range 150 GeV - 30 TeV, 15% resolution* (for spectral measurements)

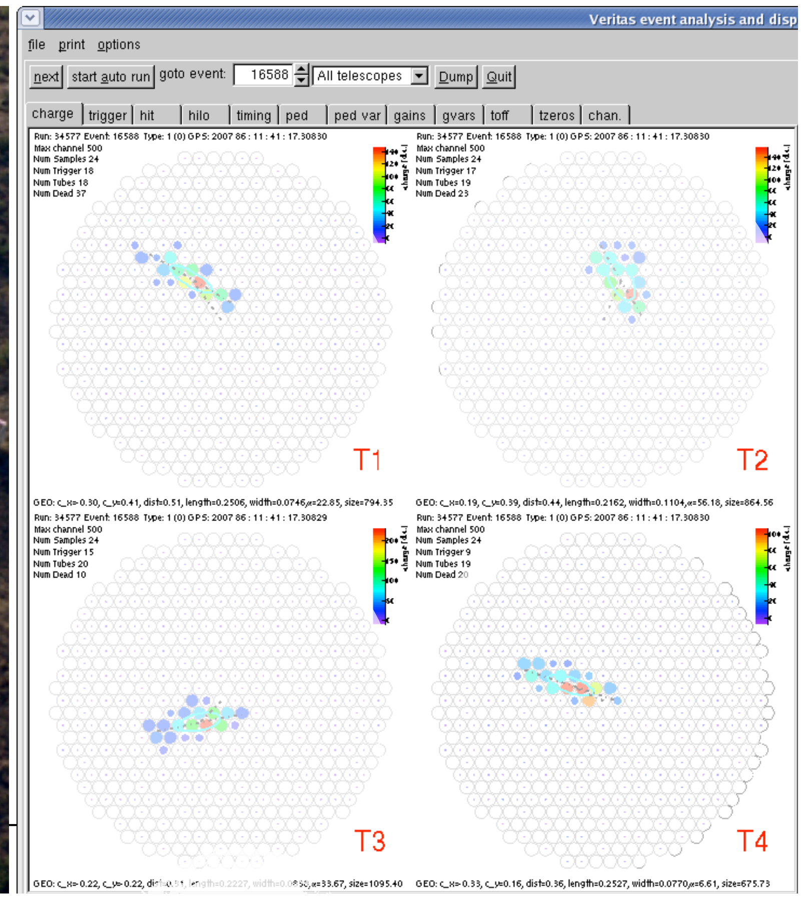

VERITAS Array

- *10 mCrab sensitivity* - 5σ detection at 1% Crab (2×10^{-13} erg cm^{-2} s^{-1} @ 1 TeV) in 28 hrs.
- *Effective area 10^5 m^2* above 500 GeV
- *Angular resolution <0.1 deg*
- *Energy range 150 GeV - 30 TeV, 15% resolution* (for spectral measurements)

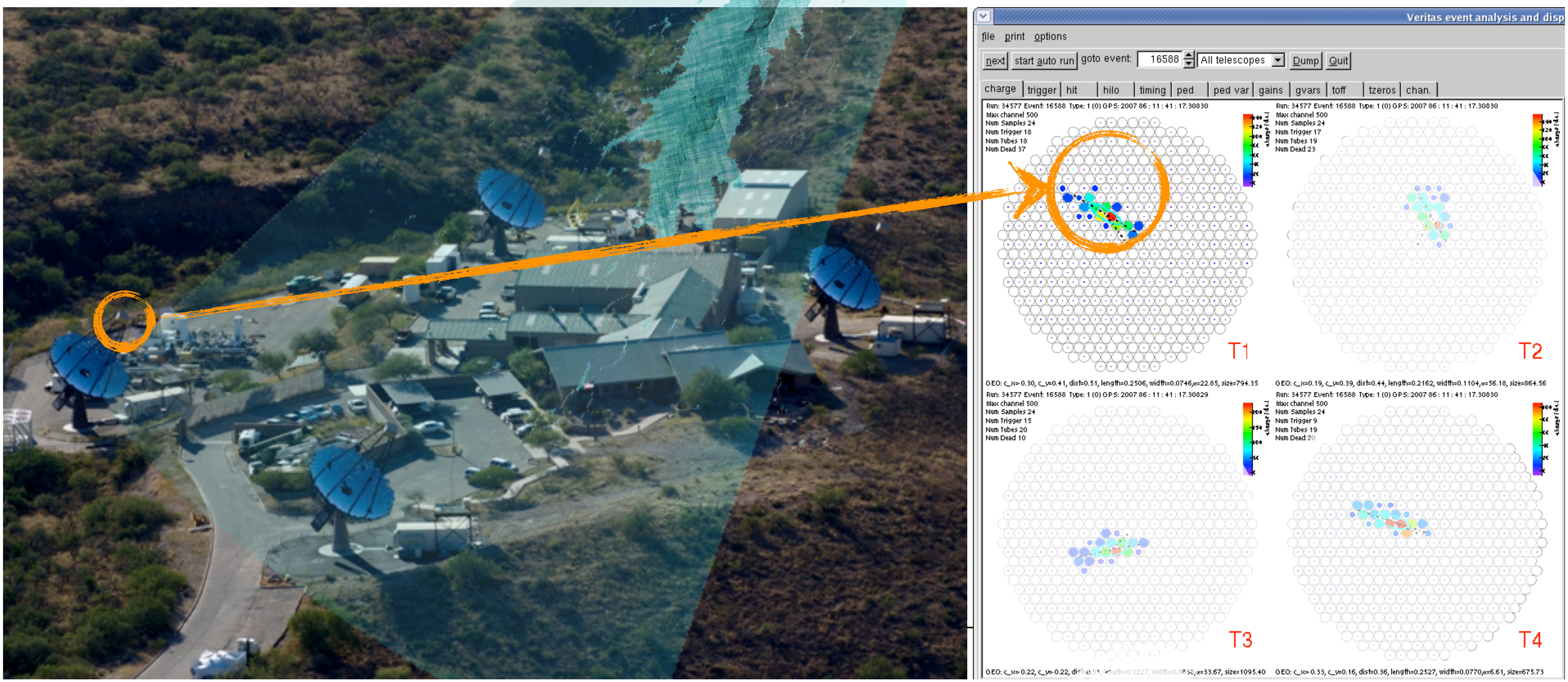

VERITAS Array

- *10 mCrab sensitivity* - 5σ detection at 1% Crab (2×10^{-13} erg cm^{-2} s^{-1} @ 1 TeV) in 28 hrs.
- *Effective area 10^5 m^2* above 500 GeV
- *Angular resolution <0.1 deg*
- *Energy range 150 GeV - 30 TeV, 15% resolution* (for spectral measurements)

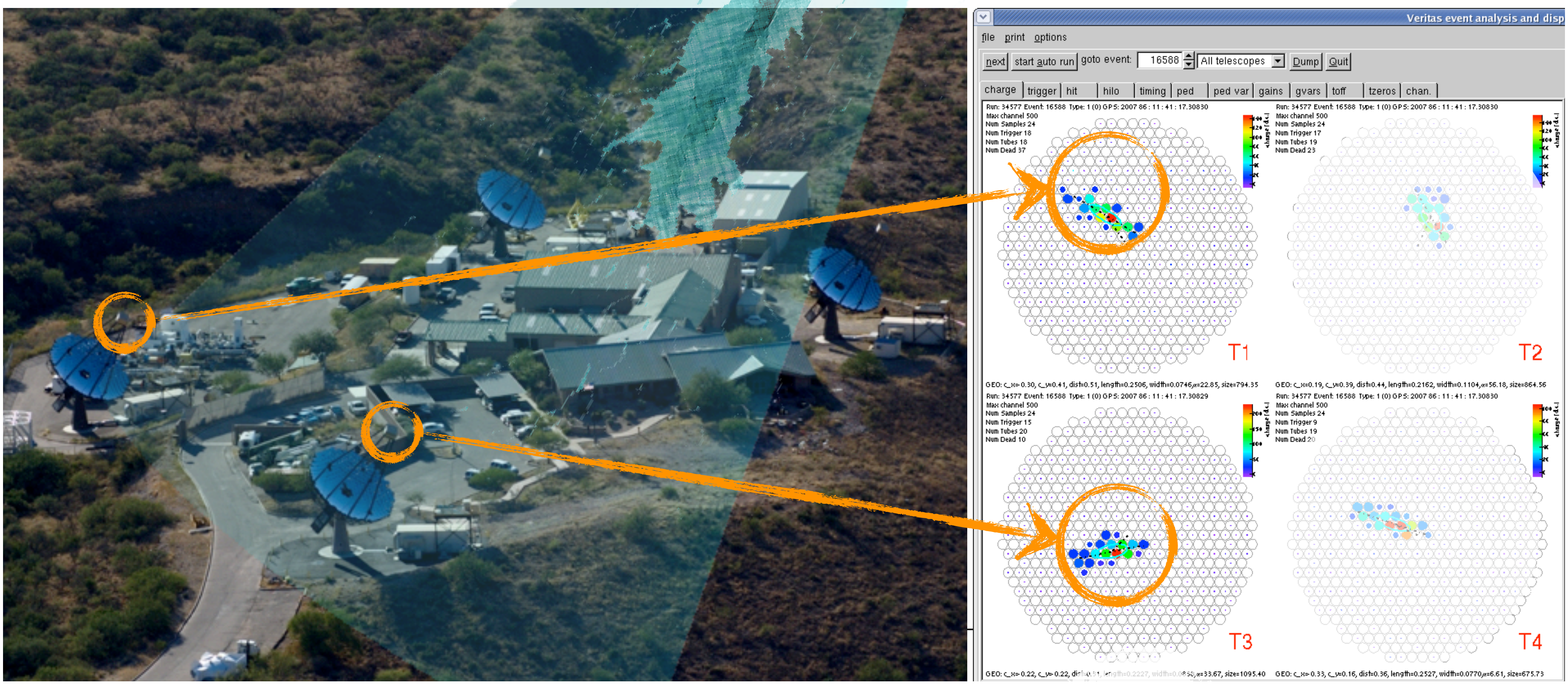

VERITAS Array

- *10 mCrab sensitivity* - 5σ detection at 1% Crab (2×10^{-13} erg cm^{-2} s^{-1} @ 1 TeV) in 28 hrs.
- *Effective area 10^5 m^2* above 500 GeV
- *Angular resolution <0.1 deg*
- *Energy range 150 GeV - 30 TeV, 15% resolution* (for spectral measurements)

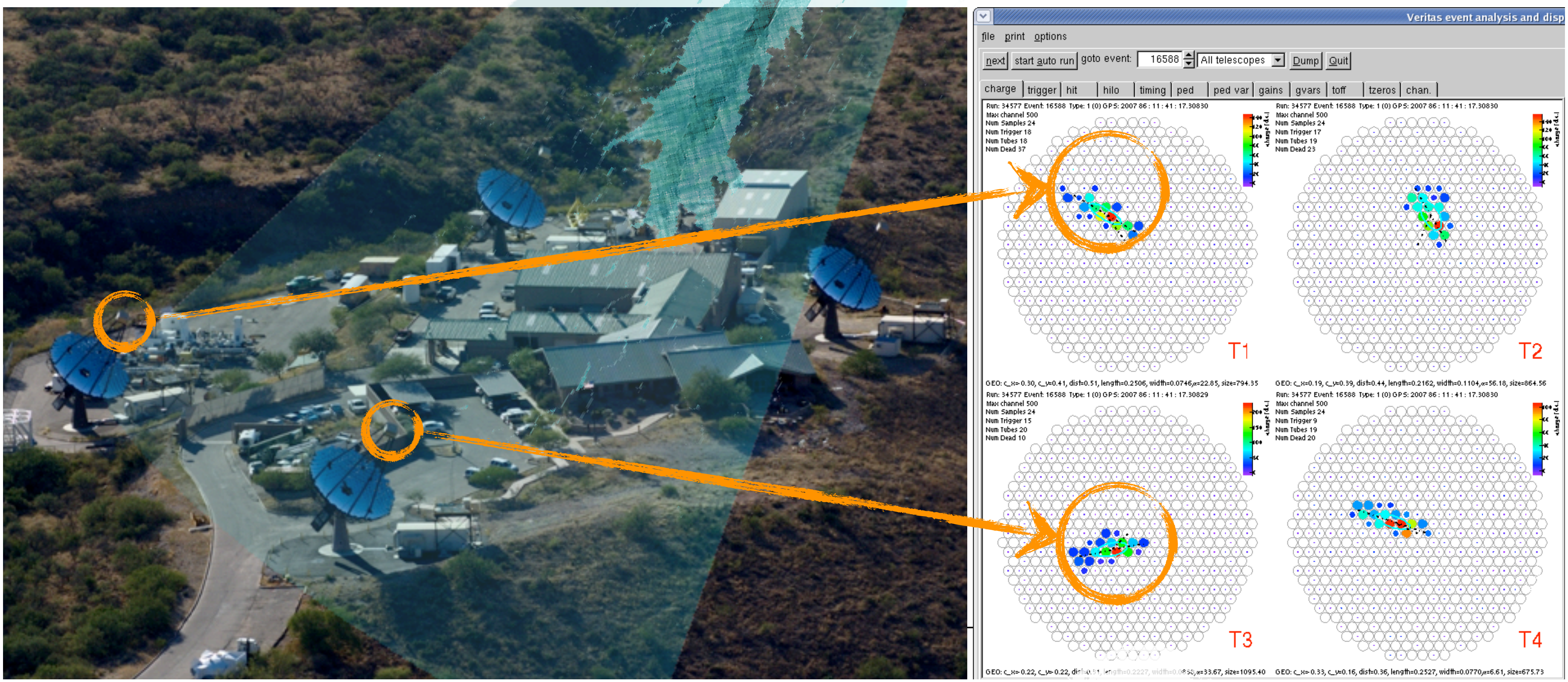

TeV Constellations

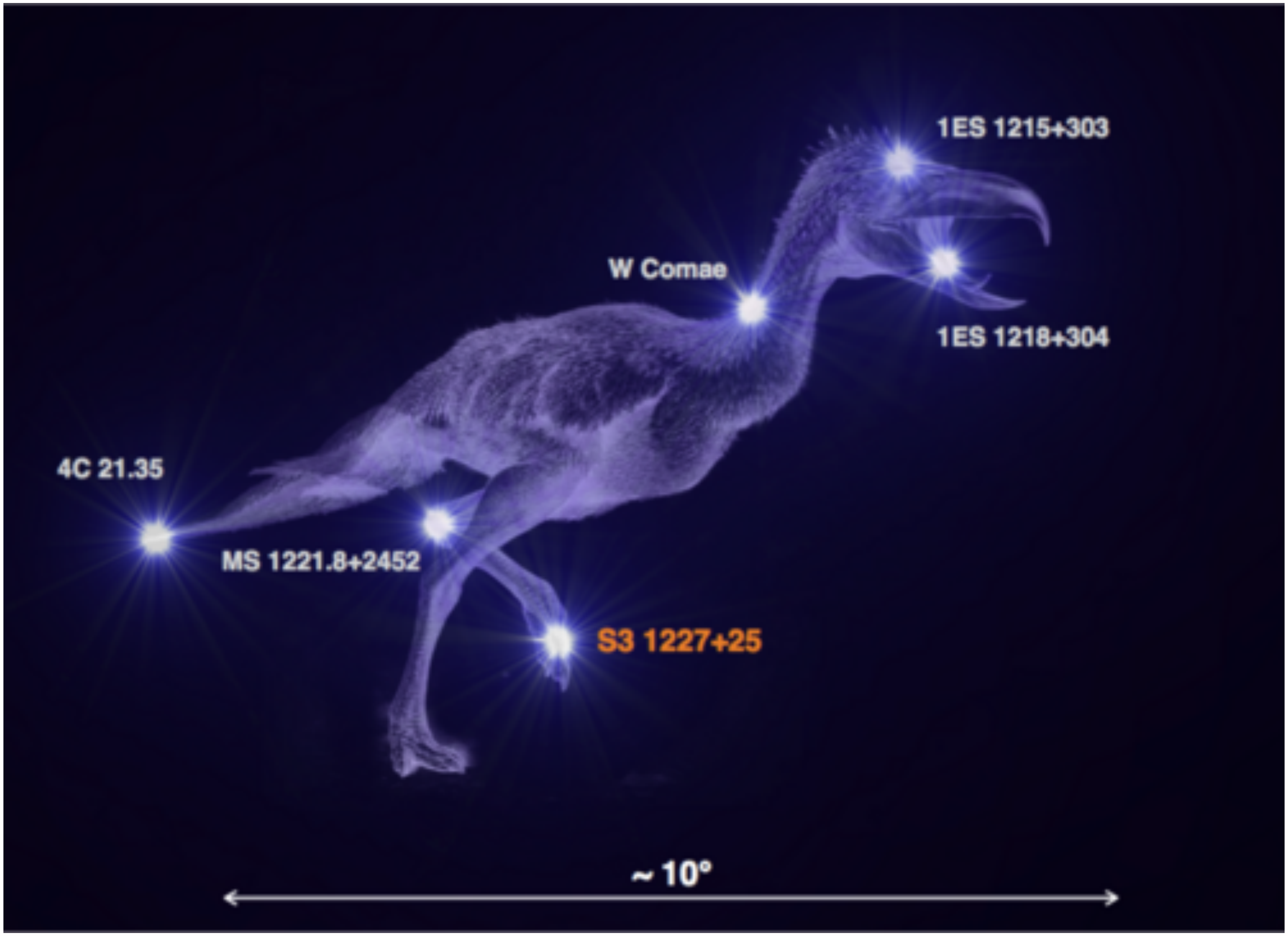

ACTs have now detected so many sources, we can make a constellation (the TeraBird Constellation of TeV sources!)

ACTs and Ground Arrays

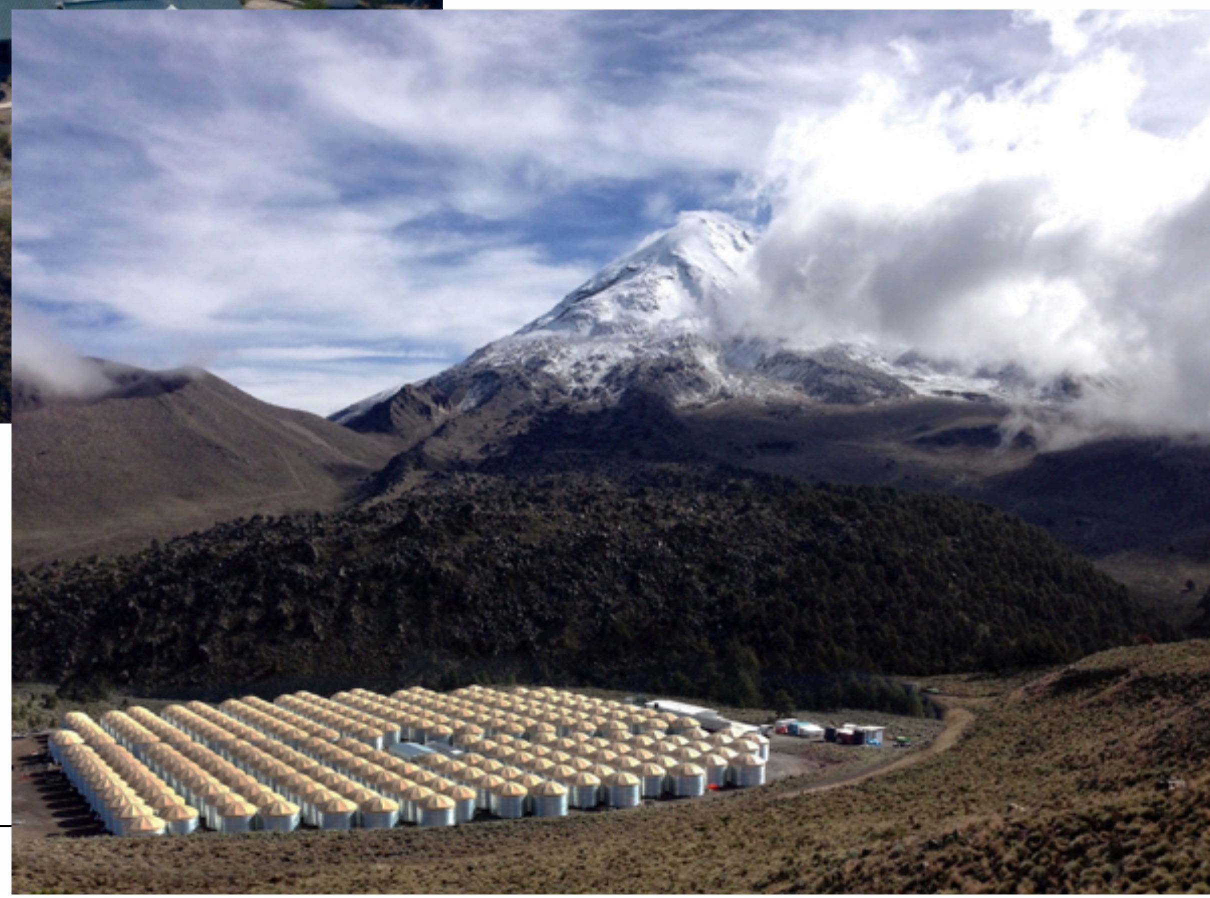

ACTs and Ground Arrays

- ACTs like **VERITAS** detect Cherenkov light from air showers with a narrow FoV on dark/moonless nights

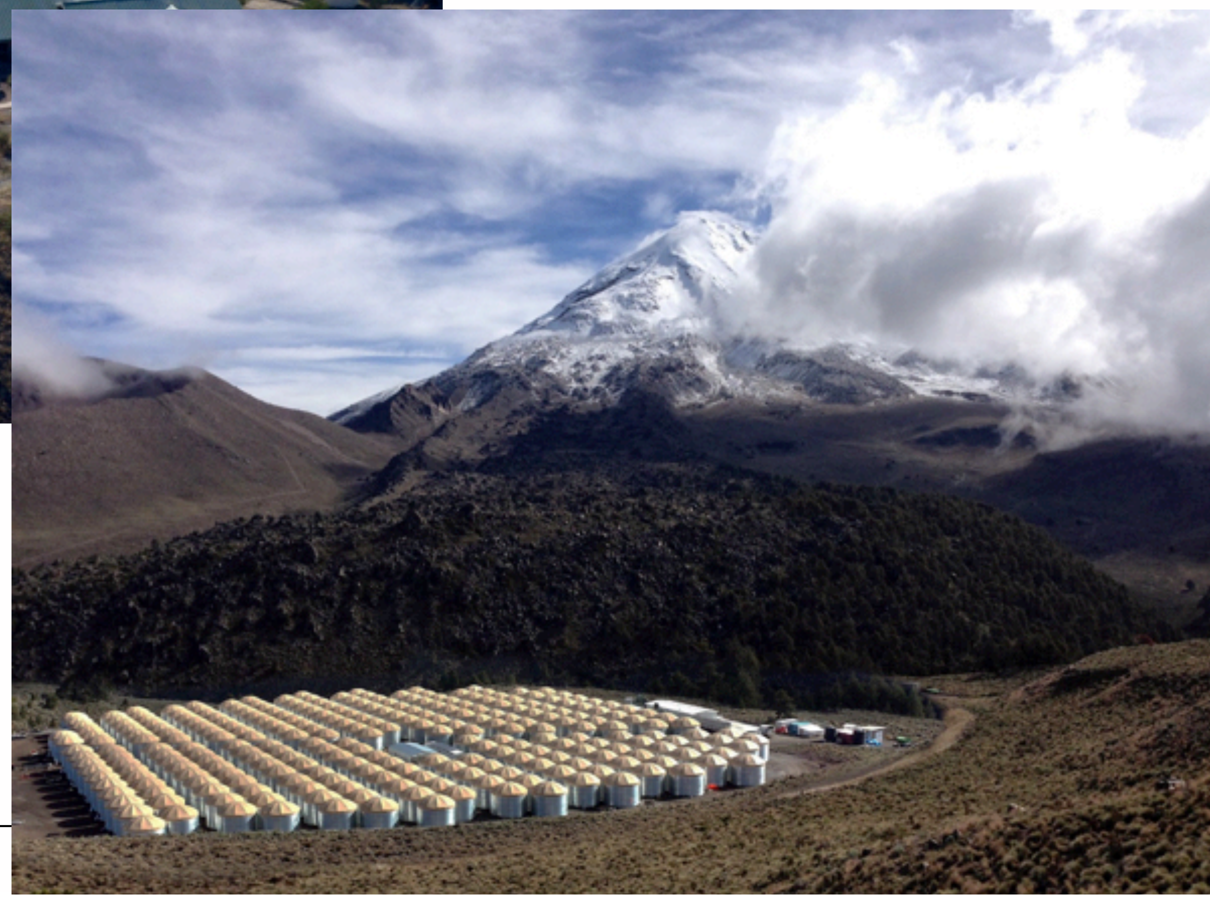

ACTs and Ground Arrays

- ACTs like **VERITAS** detect Cherenkov light from air showers with a narrow FoV on dark/moonless nights

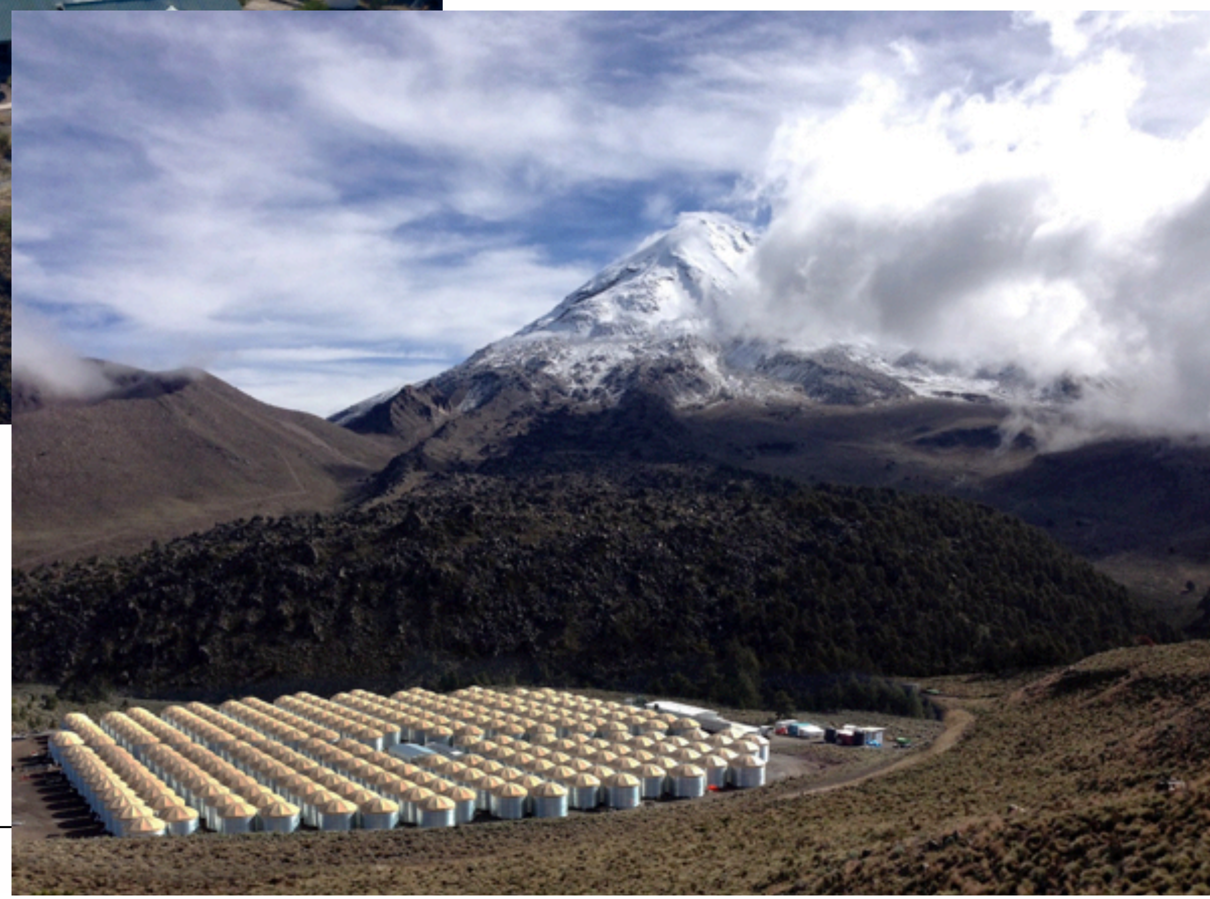

- Ground arrays like **HAWC** detect shower particles reaching the ground (albeit at high altitudes). These have higher energy threshold, and lower angular resolution, but are wide field, high duty cycle

The WIMP Miracle

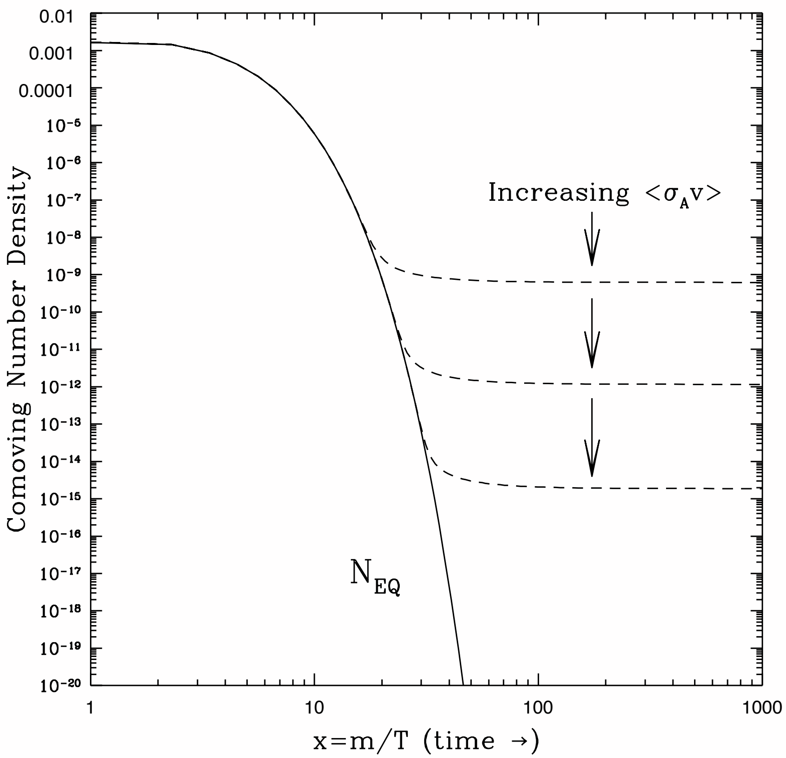

- In the beginning the universe was very hot, DM particles and SM particles were in thermal equilibrium.
- Particles in equilibrium were Boltzmann suppressed $\sim e^{-mc^2/kT}$
- annihilation and recombination rates $\Gamma \sim n^2\langle\sigma v\rangle$
- As the number density n dropped due to expansion, particles with the smallest $\langle\sigma v\rangle$ fell out of equilibrium first
- *the weak survive* with a relic density

The WIMP Miracle

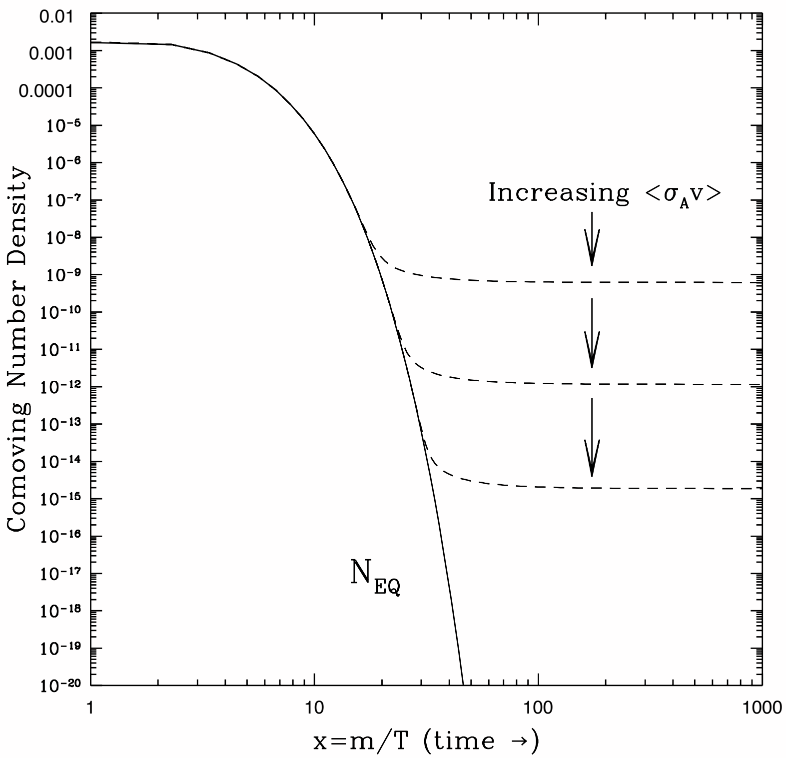

$$\Omega_{\rm DM} \approx 0.30 \left(\frac{2\times 10^{-26}{\rm cm}^3{\rm sec}^{-1}}{\langle \sigma v\rangle} \right)$$

- In the beginning the universe was very hot, DM particles and SM particles were in thermal equilibrium.
- Particles in equilibrium were Boltzmann suppressed $\sim e^{-mc^2/kT}$
- annihilation and recombination rates $\Gamma \sim n^2 \langle \sigma v \rangle$
- As the number density n dropped due to expansion, particles with the smallest $\langle \sigma v \rangle$ fell out of equilibrium first
- *the weak survive* with a relic density

The WIMP Miracle

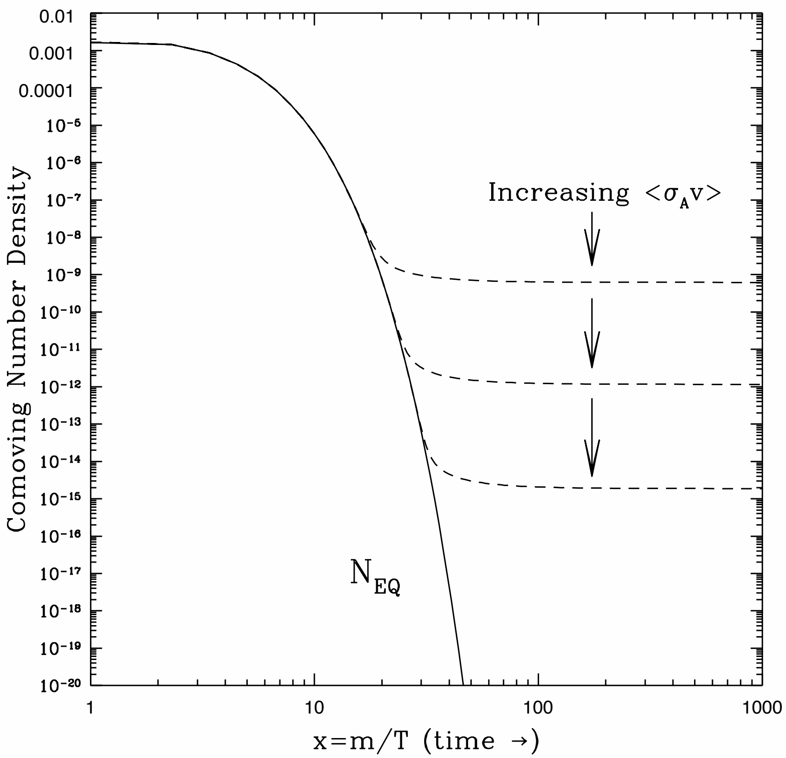

- In the beginning the universe was very hot, DM particles and SM particles were in thermal equilibrium.
- Particles in equilibrium were Boltzmann suppressed $\sim e^{-mc^2/kT}$
- annihilation and recombination rates $\Gamma \sim n^2 \langle \sigma v \rangle$
- As the number density n dropped due to expansion, particles with the smallest $\langle \sigma v \rangle$ fell out of equilibrium first
- *the weak survive* with a relic density

$$\Omega_{\rm DM} \approx 0.30 \left(\frac{2 \times 10^{-26} {\rm cm}^3 {\rm sec}^{-1}}{\langle \sigma v \rangle} \right)$$

Any theory with a new stable weakly interacting particle will work. Theorists (used to) really like SUSY - for every fermion loop there is a boson loop to cancel contributions to amplitudes, getting rid of embarrassing divergences in Higgs mass, gauge coupling unification, etc.

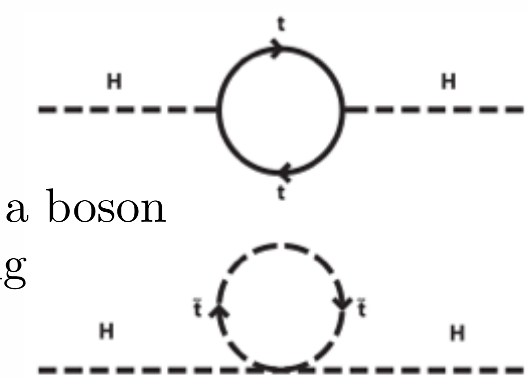

Gamma-rays from DM

$$E_\gamma \Phi_\gamma(\theta) \approx 10^{-10} \underbrace{\left(E_{\gamma,\mathrm{TeV}} \frac{dN}{dE_{\gamma,\mathrm{TeV}}}\right) \left(\frac{\langle \sigma v \rangle}{10^{-26}\mathrm{cm}^{-3}\mathrm{s}^{-1}}\right) \left(\frac{100\,\mathrm{GeV}}{M_\chi}\right)^2}_{\text{Particle Physics Input}} \underbrace{J(\theta)} \,\mathrm{erg\,cm^{-2}s^{-1}sr^{-1}}$$

$$J(\theta) = \underbrace{\frac{1}{8.5\,\mathrm{kpc}} \left(\frac{1}{0.3\,\mathrm{GeV/cm^3}}\right)^2 \int_{\text{line of sight}} \rho^2(l)\,dl(\theta)}_{\text{Astrophysics/Cosmology Input}}$$

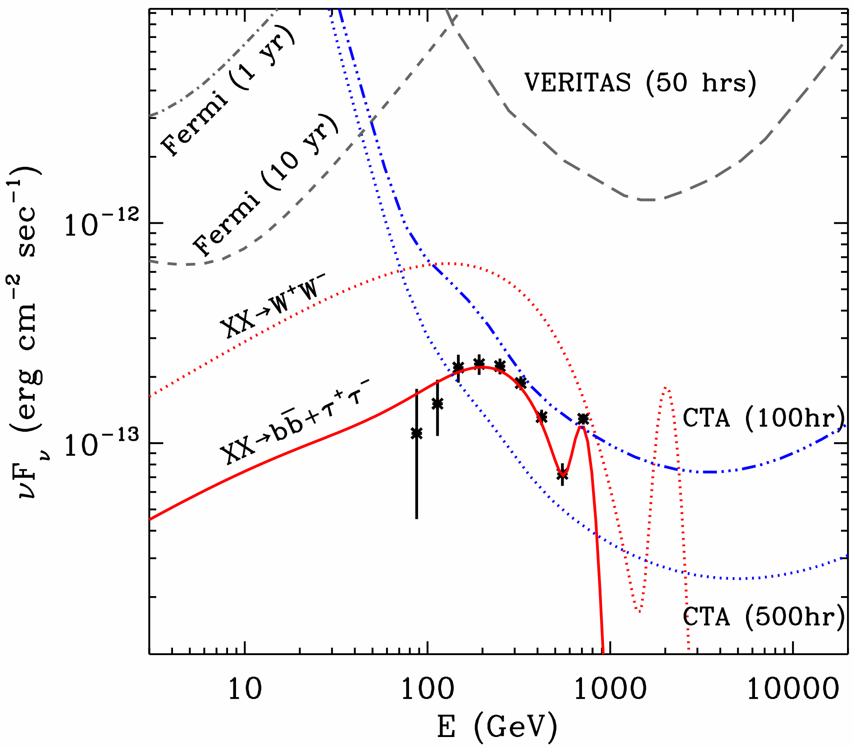

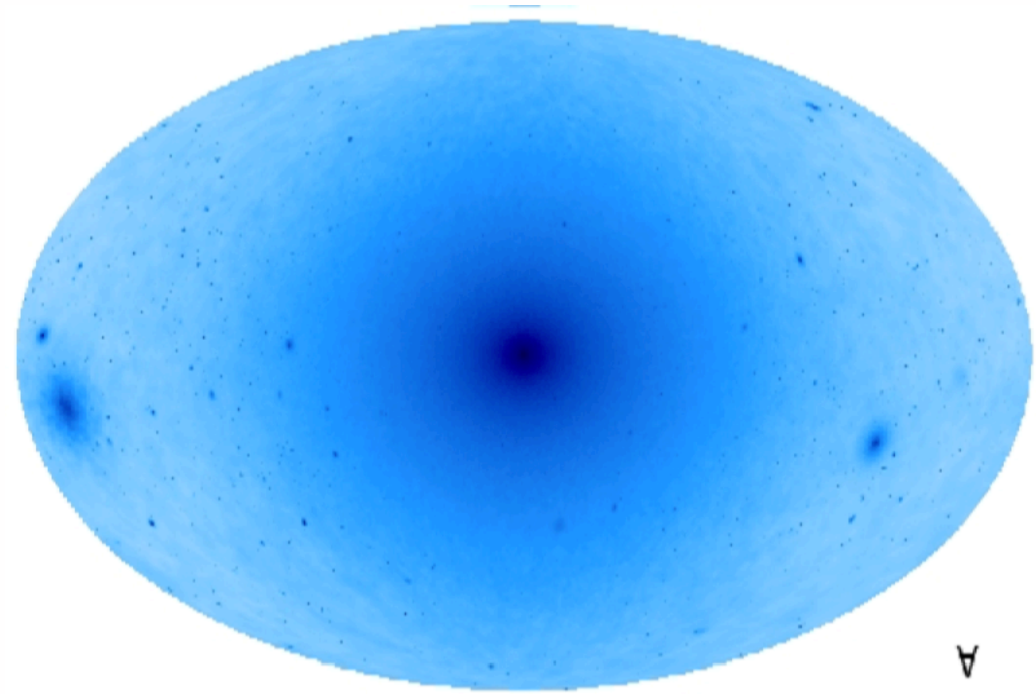

Line-of-sight integral of ρ^2 for a Milky-Way-like halo in the VL Lactea II ΛCDM N-body simulations (Kuhlen et al.)

Gamma-rays from DM

$$E_\gamma \Phi_\gamma(\theta) \approx 10^{-10} \underbrace{\left(E_{\gamma,\mathrm{TeV}} \frac{dN}{dE_{\gamma,\mathrm{TeV}}}\right) \left(\frac{\langle \sigma v \rangle}{10^{-26}\mathrm{cm}^{-3}\mathrm{s}^{-1}}\right) \left(\frac{100\,\mathrm{GeV}}{M_\chi}\right)^2}_{\text{Particle Physics Input}} \underbrace{J(\theta)} \;\mathrm{erg\,cm^{-2}s^{-1}sr^{-1}}$$

$$J(\theta) = \underbrace{\frac{1}{8.5\,\mathrm{kpc}} \left(\frac{1}{0.3\,\mathrm{GeV/cm^3}}\right)^2 \int_{\text{line of sight}} \rho^2(l)dl(\theta)}_{\text{Astrophysics/Cosmology Input}}$$

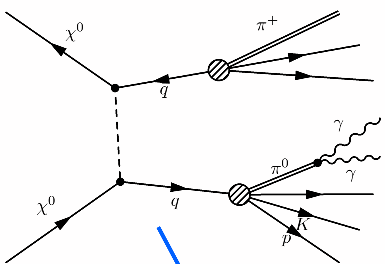

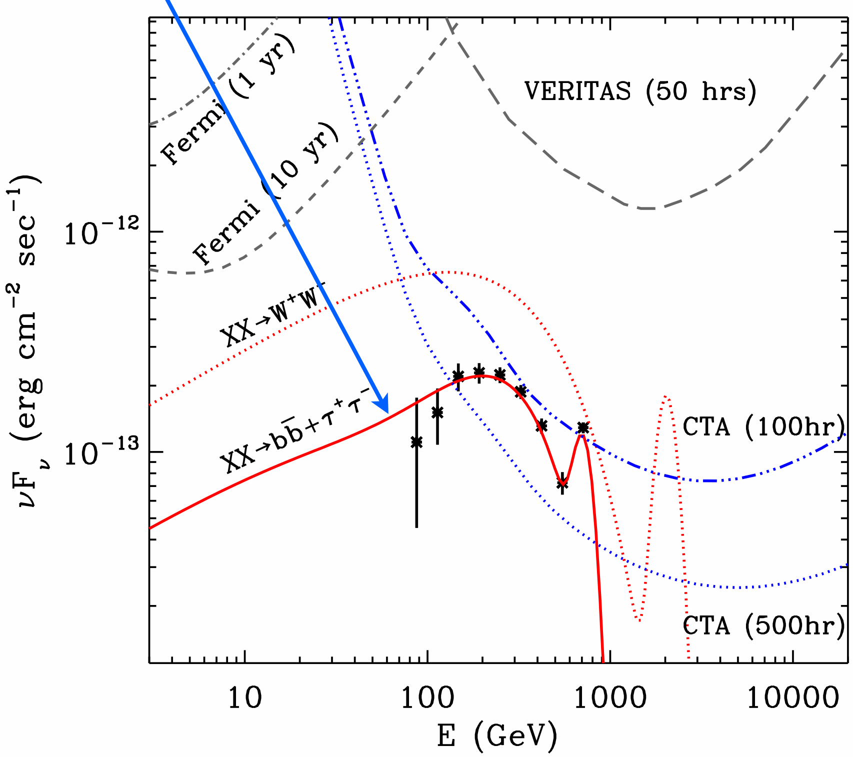

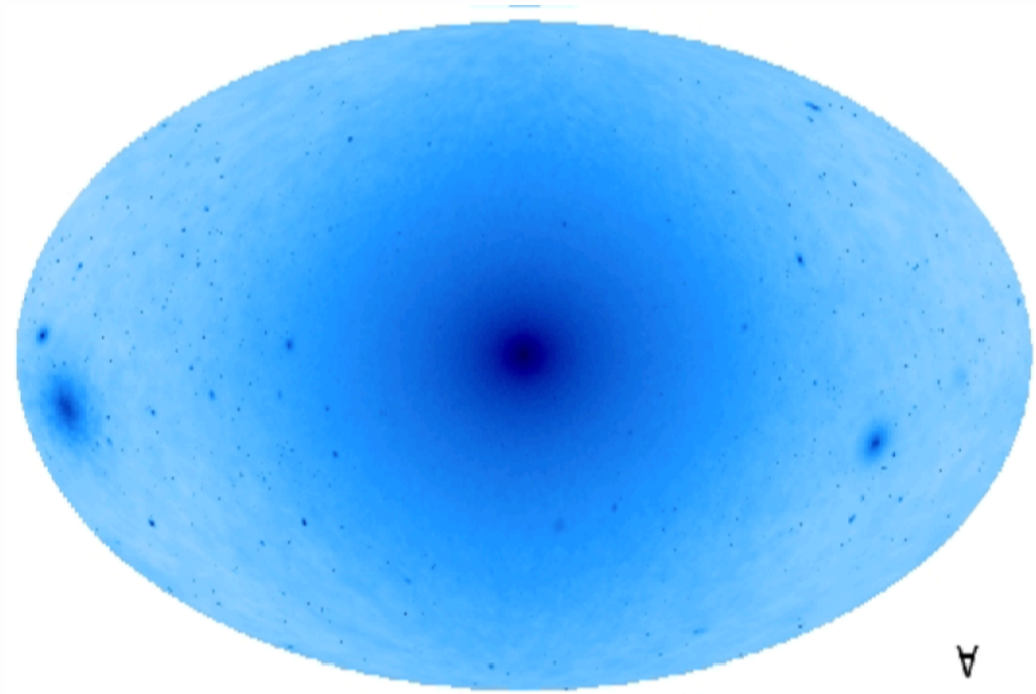

Line-of-sight integral of ρ^2 for a Milky-Way-like halo in the VL Lactea II ΛCDM N-body simulations (Kuhlen et al.)

Gamma-rays from DM

$$E_\gamma \Phi_\gamma(\theta) \approx 10^{-10} \underbrace{\left(E_{\gamma,\mathrm{TeV}} \frac{dN}{dE_{\gamma,\mathrm{TeV}}}\right) \left(\frac{\langle\sigma v\rangle}{10^{-26}\mathrm{cm}^{-3}\mathrm{s}^{-1}}\right) \left(\frac{100\,\mathrm{GeV}}{M_\chi}\right)^2}_{\text{Particle Physics Input}} \underbrace{J(\theta)} \;\mathrm{erg\,cm^{-2}s^{-1}sr^{-1}}$$

$$J(\theta) = \underbrace{\frac{1}{8.5\,\mathrm{kpc}} \left(\frac{1}{0.3\,\mathrm{GeV/cm^3}}\right)^2 \int_{\text{line of sight}} \rho^2(l)\,dl(\theta)}_{\text{Astrophysics/Cosmology Input}}$$

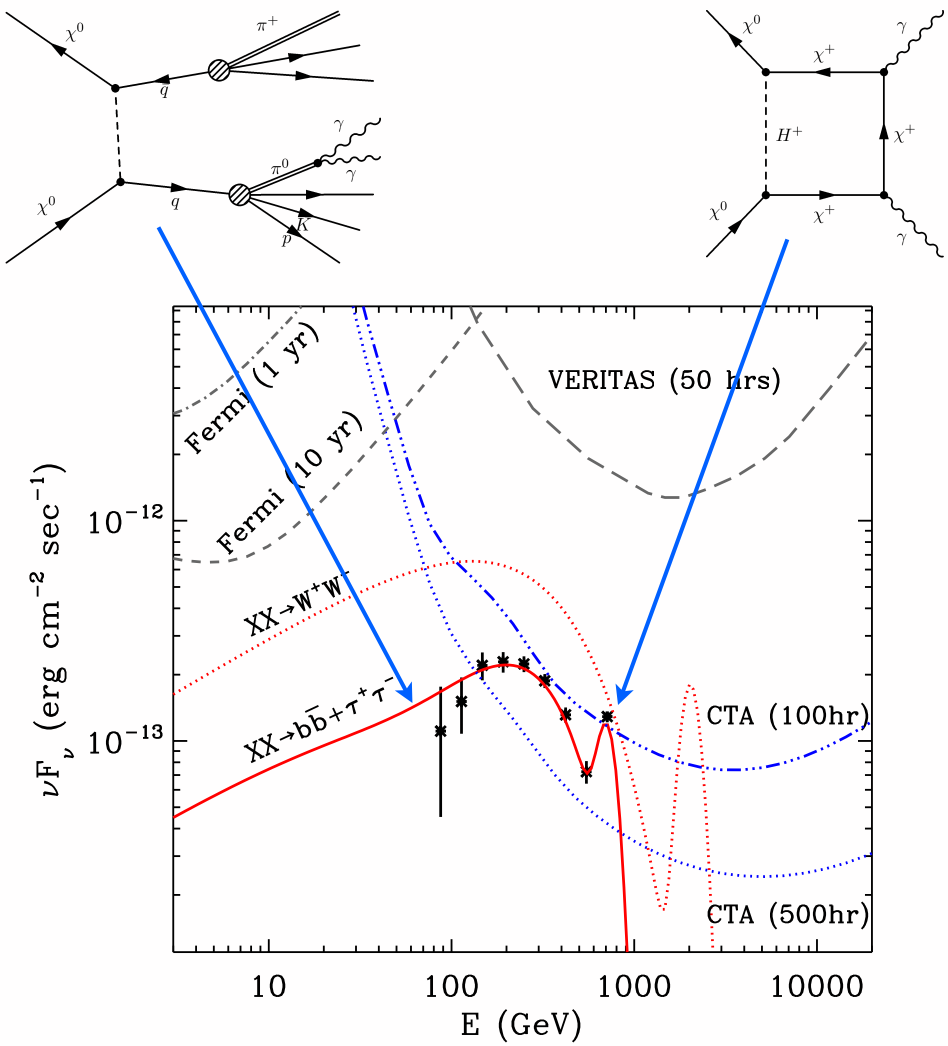

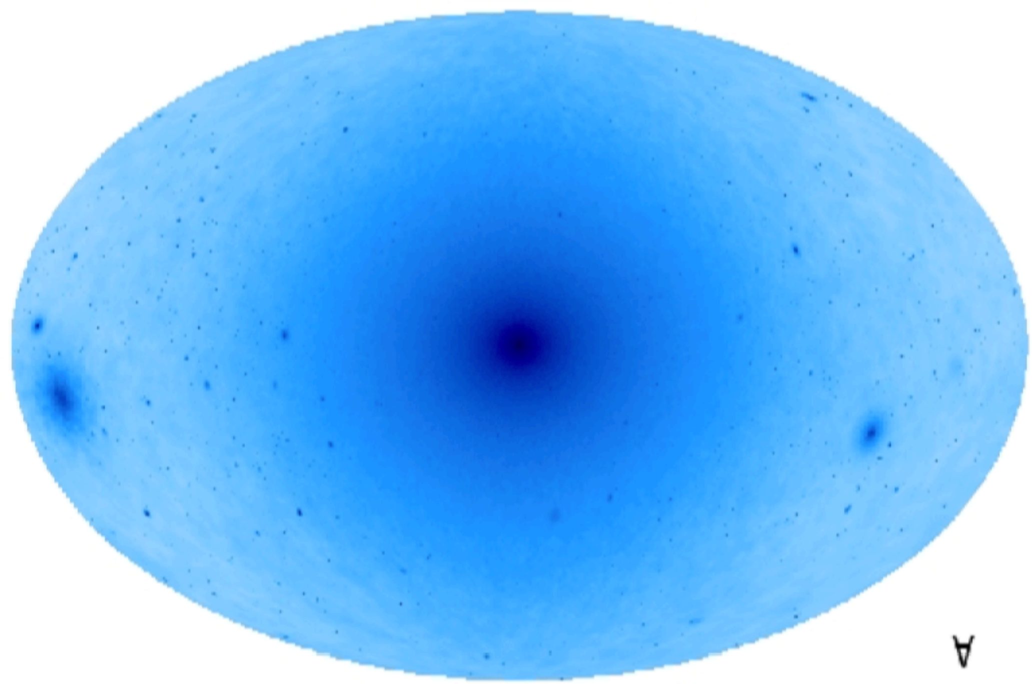

Line-of-sight integral of ρ^2 for a Milky-Way-like halo in the VL Lactea II ΛCDM N-body simulations (Kuhlen et al.)

Gamma-rays from DM

$$E_\gamma \Phi_\gamma(\theta) \approx 10^{-10} \underbrace{\left(E_{\gamma,\mathrm{TeV}} \frac{dN}{dE_{\gamma,\mathrm{TeV}}}\right) \left(\frac{\langle \sigma v \rangle}{10^{-26}\mathrm{cm}^{-3}\mathrm{s}^{-1}}\right) \left(\frac{100\,\mathrm{GeV}}{M_\chi}\right)^2}_{\text{Particle Physics Input}} \underbrace{J(\theta)} \ \mathrm{erg\,cm^{-2}s^{-1}sr^{-1}}$$

$$J(\theta) = \underbrace{\frac{1}{8.5\,\mathrm{kpc}} \left(\frac{1}{0.3\,\mathrm{GeV/cm^3}}\right)^2 \int_{\text{line of sight}} \rho^2(l)\,dl(\theta)}_{\text{Astrophysics/Cosmology Input}}$$

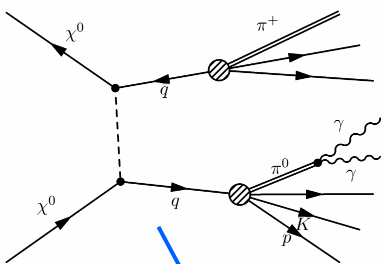

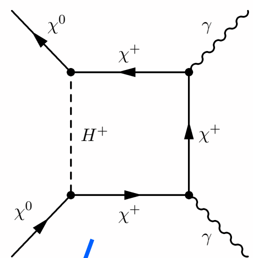

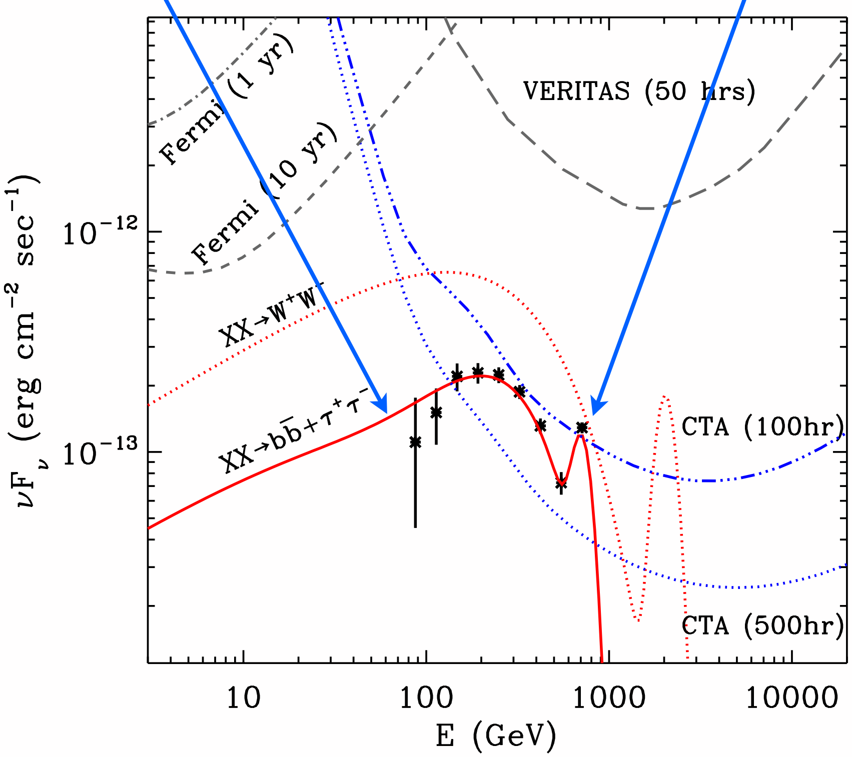

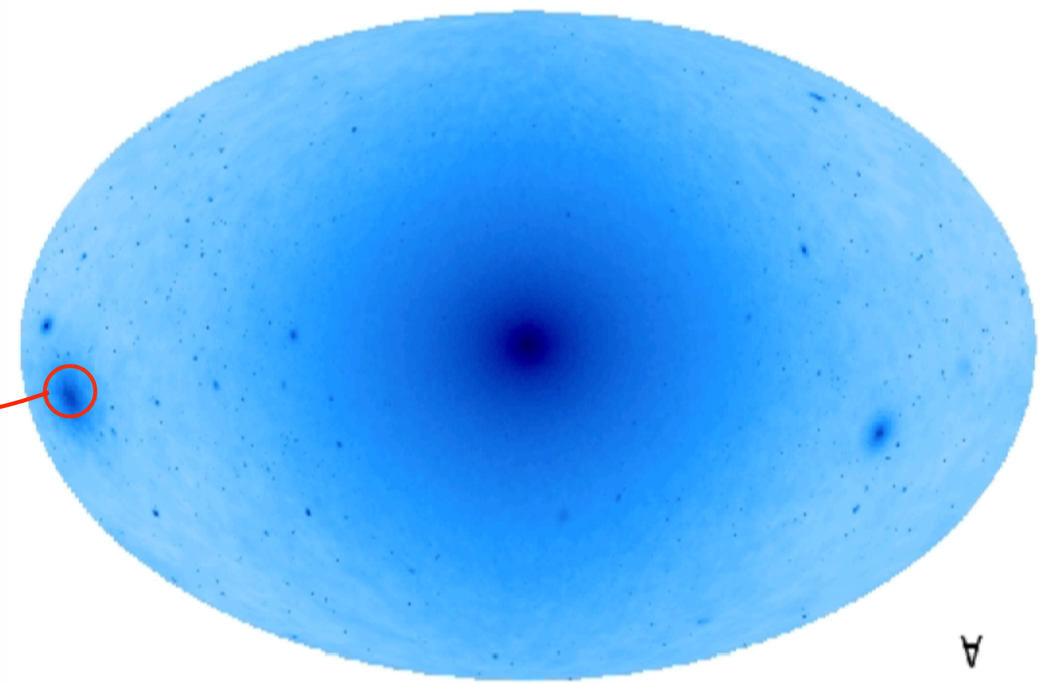

Line-of-sight integral of ρ^2 for a Milky-Way-like halo in the VL Lactea II ΛCDM N-body simulations (Kuhlen et al.)

Gamma-rays from DM

$$E_\gamma \Phi_\gamma(\theta) \approx 10^{-10} \underbrace{\left(E_{\gamma,\mathrm{TeV}} \frac{dN}{dE_{\gamma,\mathrm{TeV}}}\right) \left(\frac{\langle \sigma v \rangle}{10^{-26}\mathrm{cm}^{-3}\mathrm{s}^{-1}}\right) \left(\frac{100\,\mathrm{GeV}}{M_\chi}\right)^2}_{\text{Particle Physics Input}} \underbrace{J(\theta)} \ \mathrm{erg\,cm^{-2}s^{-1}sr^{-1}}$$

$$J(\theta) = \underbrace{\frac{1}{8.5\,\mathrm{kpc}} \left(\frac{1}{0.3\,\mathrm{GeV/cm^3}}\right)^2 \int_{\text{line of sight}} \rho^2(l)\,dl(\theta)}_{\text{Astrophysics/Cosmology Input}}$$

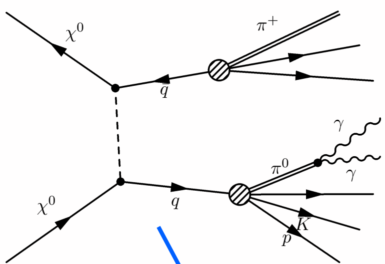

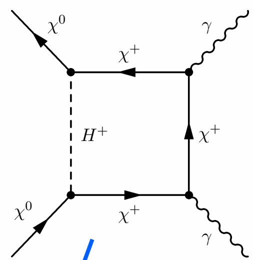

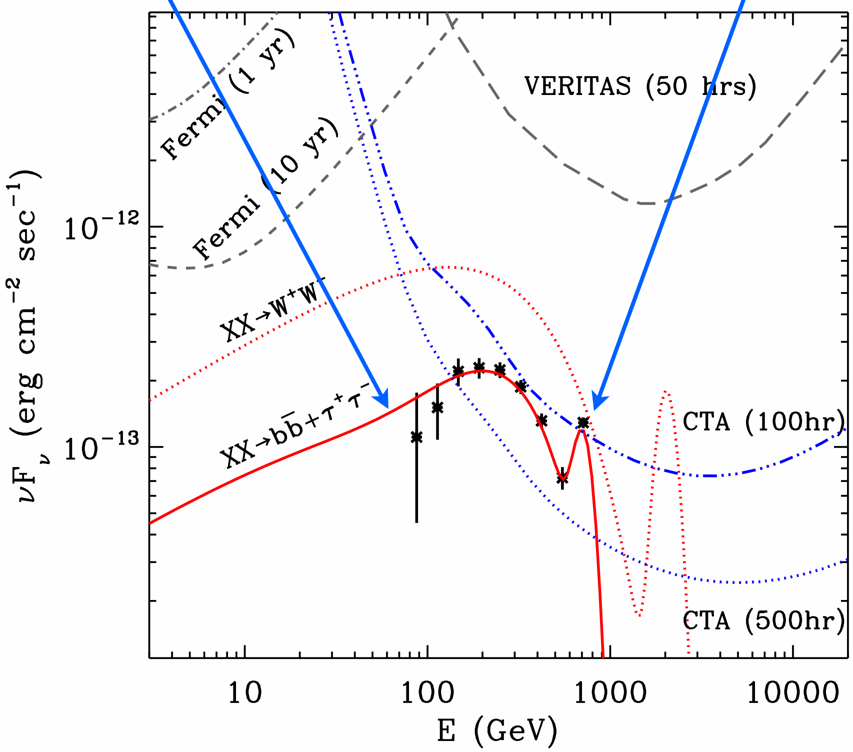

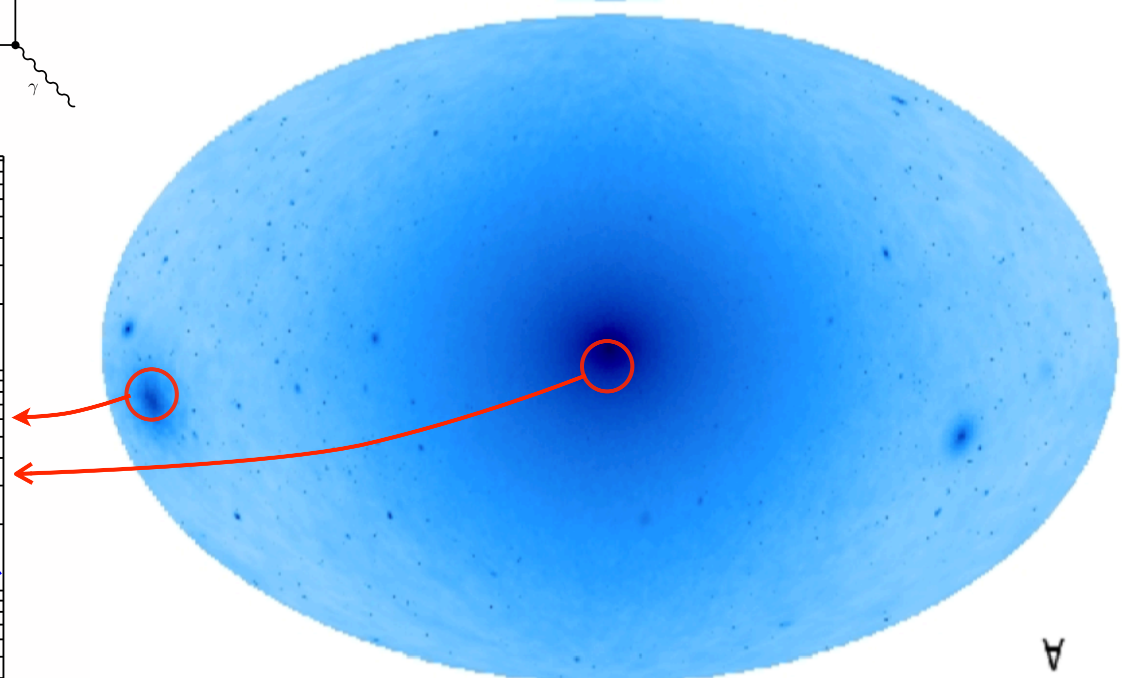

Line-of-sight integral of ρ^2 for a Milky-Way-like halo in the VL Lactea II ΛCDM N-body simulations (Kuhlen et al.)

Gamma-rays from DM

$$E_\gamma \Phi_\gamma(\theta) \approx 10^{-10} \underbrace{\left(E_{\gamma,\mathrm{TeV}} \frac{dN}{dE_{\gamma,\mathrm{TeV}}}\right) \left(\frac{\langle \sigma v \rangle}{10^{-26}\mathrm{cm^{-3}s^{-1}}}\right) \left(\frac{100\,\mathrm{GeV}}{M_\chi}\right)^2}_{\text{Particle Physics Input}} \underbrace{J(\theta)} \; \mathrm{erg\,cm^{-2}s^{-1}sr^{-1}}$$

$$J(\theta) = \underbrace{\frac{1}{8.5\,\mathrm{kpc}} \left(\frac{1}{0.3\,\mathrm{GeV/cm^3}}\right)^2 \int_{\text{line of sight}} \rho^2(l)\,dl(\theta)}_{\text{Astrophysics/Cosmology Input}}$$

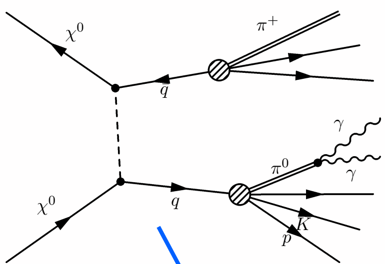

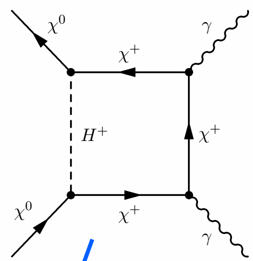

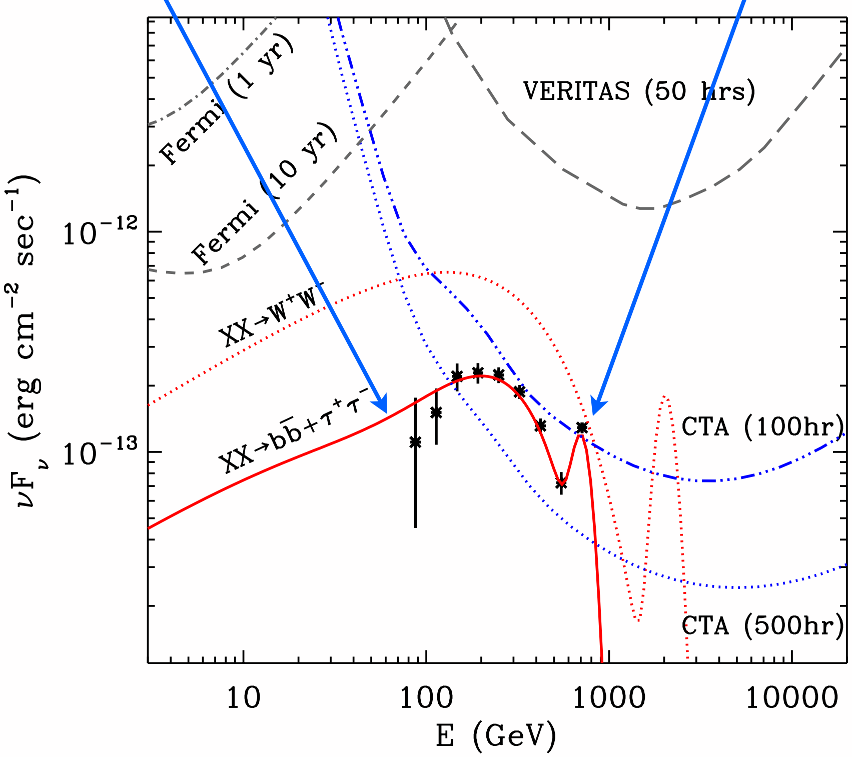

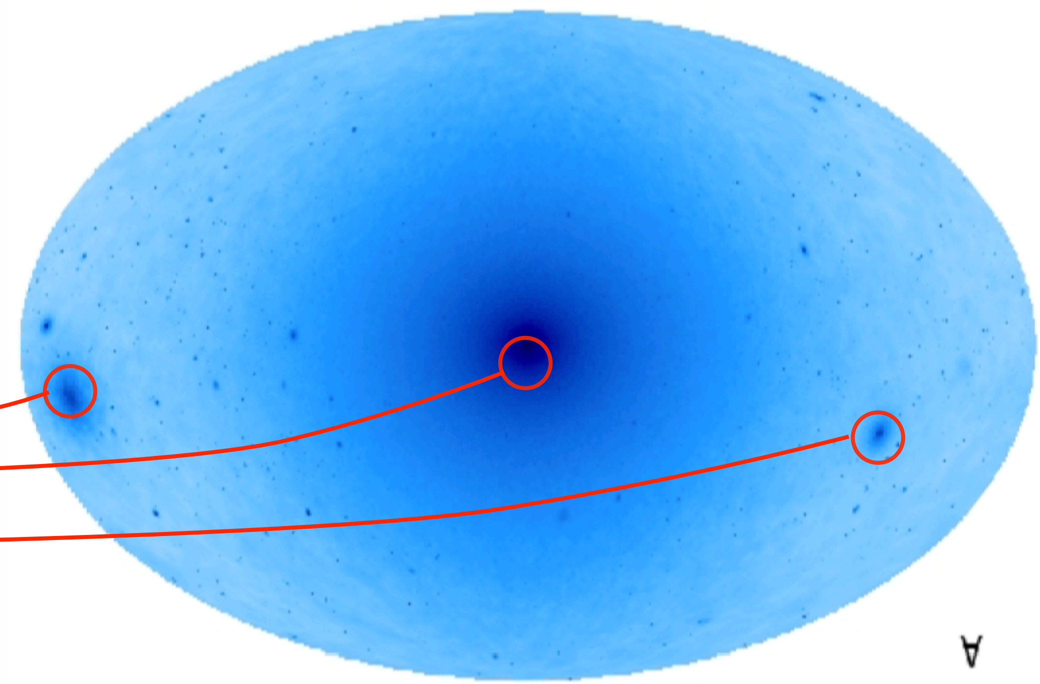

Line-of-sight integral of ρ^2 for a Milky-Way-like halo in the VL Lactea II ΛCDM N-body simulations (Kuhlen et al.)

DM and Gamma-Rays

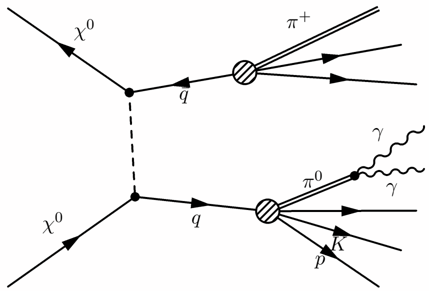

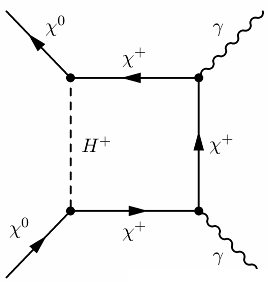

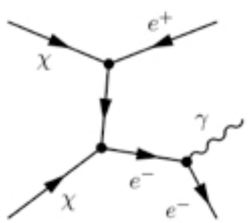

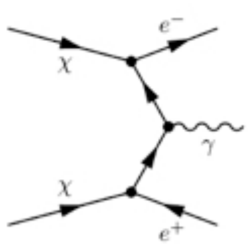

Annihilation Channel	Secondary Processes	Signals	Notes
$\chi\chi \rightarrow q\bar{q},\ gg$	$p, \bar{p}, \pi^{\pm}, \pi^0$	p, e, ν, γ	
$\chi\chi \rightarrow W^+W^-$	$W^{\pm} \rightarrow l^{\pm}\nu_l,\ W^{\pm} \rightarrow u\bar{d} \rightarrow \pi^{\pm},\ \pi^0$	p, e, ν, γ	
$\chi\chi \rightarrow Z^0Z^0$	$Z^0 \rightarrow l\bar{l},\ \nu\bar{\nu},\ q\bar{q} \rightarrow$ pions	p, e, γ, ν	
$\chi\chi \rightarrow \tau^{\pm}$	$\tau^{\pm} \rightarrow \nu_{\tau}e^{\pm}\nu_e,\ \tau \rightarrow \nu_{\tau}W^{\pm} \rightarrow p, \bar{p},$ pions	p, e, γ, ν	
$\chi\chi \rightarrow \mu^+\mu^-$		e, γ	Rapid energy loss of μs in sun before decay results in sub-threshold νs
$\chi\chi \rightarrow \gamma\gamma$ $\chi\chi \rightarrow Z^0\gamma$	 Z^0 decay	γ γ	Loop suppressed Loop suppressed
$\chi\chi \rightarrow e^+e^-$		e, γ	Helicity suppressed
$\chi\chi \rightarrow \nu\bar{\nu}$		ν	Helicity suppressed (important for non-Majorana WIMPs?)
$\chi\chi \rightarrow \phi\bar{\phi}$	$\phi \rightarrow e^+e^-$	$e^{\pm}$	New scalar field with $m_{\chi} < m_q$ to explain large electron signal and avoid overproduction of p, γ

DM and Gamma-Rays

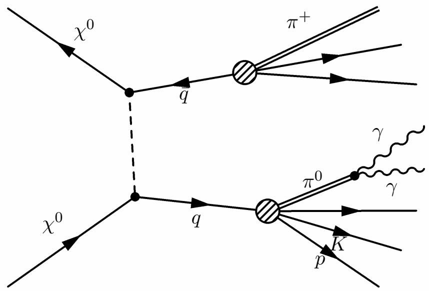

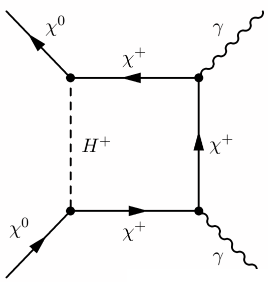

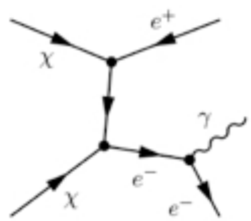

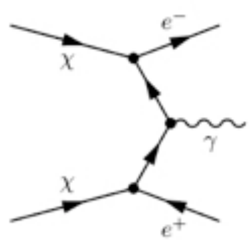

Annihilation Channel	Secondary Processes	Signals	Notes
$\chi\chi \to q\bar{q},\ gg$	$p, \bar{p}, \pi^\pm, \pi^0$	p, e, ν, γ	
$\chi\chi \to W^+W^-$	$W^\pm \to l^\pm\nu_l,\ W^\pm \to u\bar{d} \to \pi^\pm,\ \pi^0$	p, e, ν, γ	
$\chi\chi \to Z^0Z^0$	$Z^0 \to l\bar{l},\ \nu\bar{\nu},\ q\bar{q} \to$ pions	p, e, γ, ν	
$\chi\chi \to \tau^\pm$	$\tau^\pm \to \nu_\tau e^\pm \nu_e,\ \tau \to \nu_\tau W^\pm \to p, \bar{p}$, pions	p, e, γ, ν	
$\chi\chi \to \mu^+\mu^-$		e, γ	Rapid energy loss of μs in sun before decay results in sub-threshold νs
$\chi\chi \to \gamma\gamma$ $\chi\chi \to Z^0\gamma$	 Z^0 decay	γ γ	Loop suppressed Loop suppressed
$\chi\chi \to e^+e^-$		e, γ	Helicity suppressed
$\chi\chi \to \nu\bar{\nu}$		ν	Helicity suppressed (important for non-Majorana WIMPs?)
$\chi\chi \to \phi\phi$	$\phi \to e^+e^-$	$e^\pm$	New scalar field with $m_\chi < m_q$ to explain large electron signal and avoid overproduction of p, γ

internal/final state bremms
inverse Compton γ's

DM and Gamma-Rays

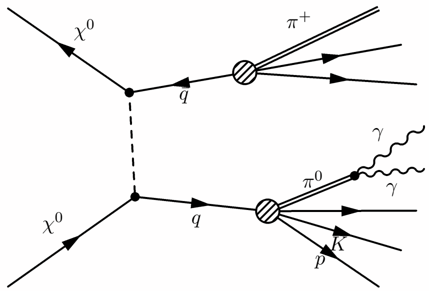

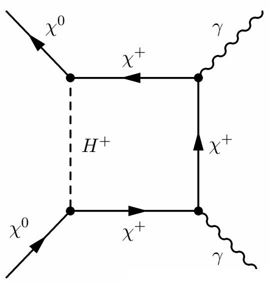

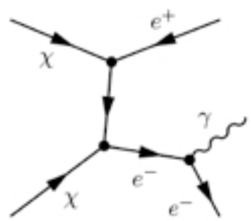

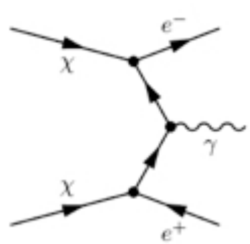

Annihilation Channel	Secondary Processes	Signals	Notes
$\chi\chi \to q\bar{q},\ gg$	$p, \bar{p}, \pi^{\pm}, \pi^0$	p, e, ν, γ	
$\chi\chi \to W^+W^-$	$W^{\pm} \to l^{\pm}\nu_l,\ W^{\pm} \to u\bar{d} \to \pi^{\pm},\ \pi^0$	p, e, ν, γ	
$\chi\chi \to Z^0Z^0$	$Z^0 \to l\bar{l},\ \nu\bar{\nu},\ q\bar{q} \to$ pions	p, e, γ, ν	
$\chi\chi \to \tau^{\pm}$	$\tau^{\pm} \to \nu_\tau e^{\pm}\nu_e,\ \tau \to \nu_\tau W^{\pm} \to p, \bar{p}$, pions	p, e, γ, ν	
$\chi\chi \to \mu^+\mu^-$		e, γ	Rapid energy loss of μs in sun before decay results in sub-threshold νs
$\chi\chi \to \gamma\gamma$ $\chi\chi \to Z^0\gamma$	Z^0 decay	γ γ	Loop suppressed Loop suppressed
$\chi\chi \to e^+e^-$		e, γ	Helicity suppressed
$\chi\chi \to \nu\bar{\nu}$		ν	Helicity suppressed (important for non-Majorana WIMPs?)
$\chi\chi \to \phi\phi$	$\phi \to e^+e^-$	$e^{\pm}$	New scalar field with $m_\chi < m_q$ to explain large electron signal and avoid overproduction of p, γ

internal/final state bremms
inverse Compton γ's

All channels lead to γ-rays. Cross section for γ-ray production is closely tied to total annihilation cross section in the early universe.

A Brief History…

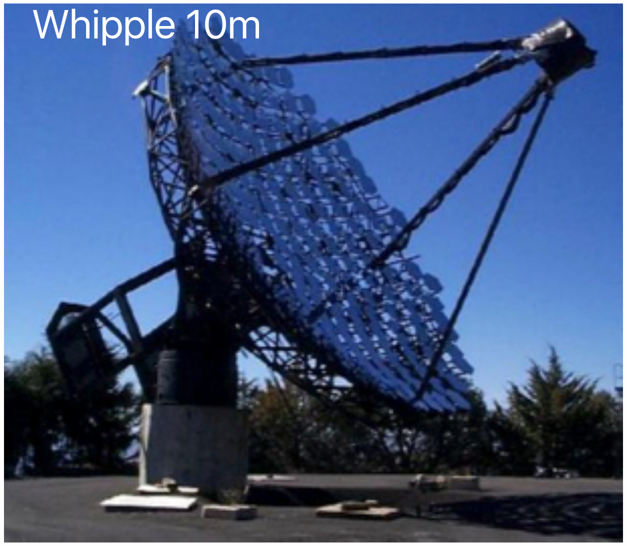

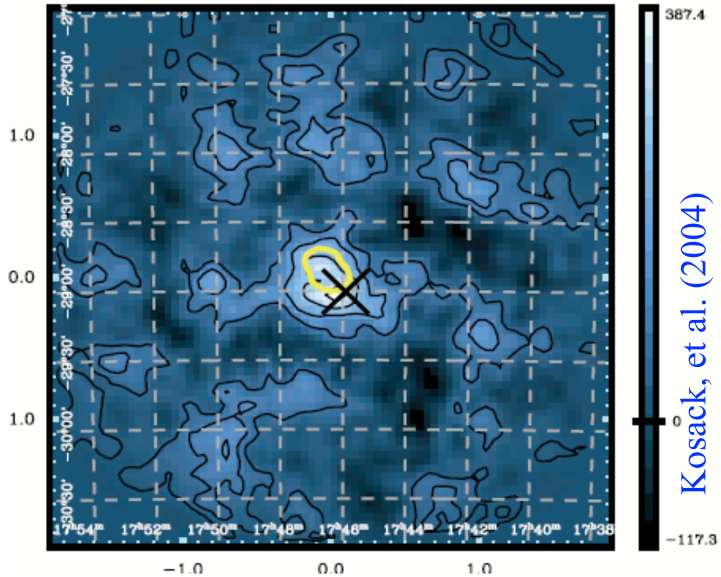

- EGRET detected GC source 3EG J1746-2851 (Hartman et al. 1999). Whipple 10m observed GC for ~ ten years (1995-2003) resulting in ~4 sigma evidence for emission from GC. HESS definitively detected the GC, followed by Fermi, VERITAS and MAGIC

A Brief History...

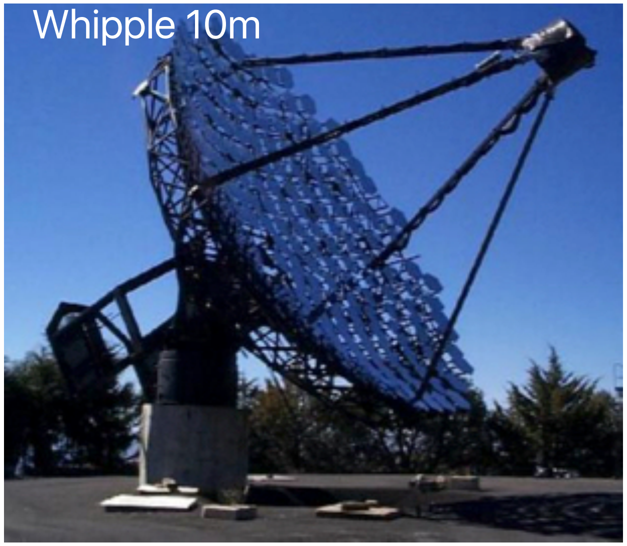

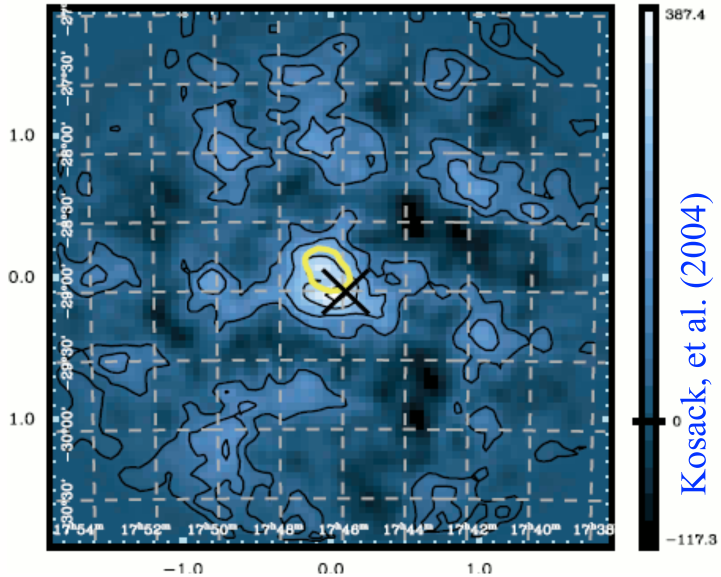

Kosack, et al. (2004)

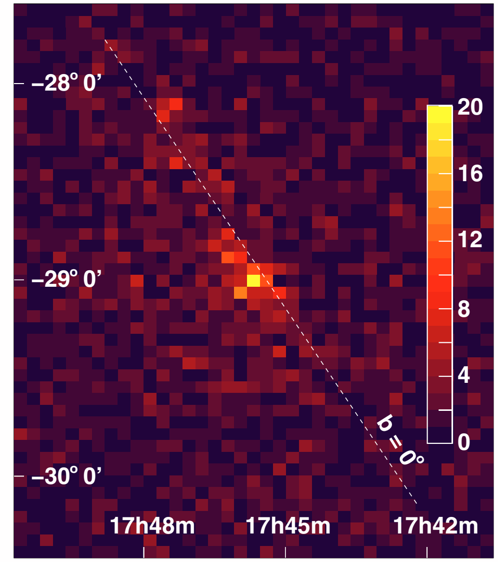

Aharonian et al., A&A 425, L13 (2004)

- EGRET detected GC source 3EG J1746-2851 (Hartman et al. 1999). Whipple 10m observed GC for ~ ten years (1995-2003) resulting in ~4 sigma evidence for emission from GC. HESS definitively detected the GC, followed by Fermi, VERITAS and MAGIC

A Brief History...

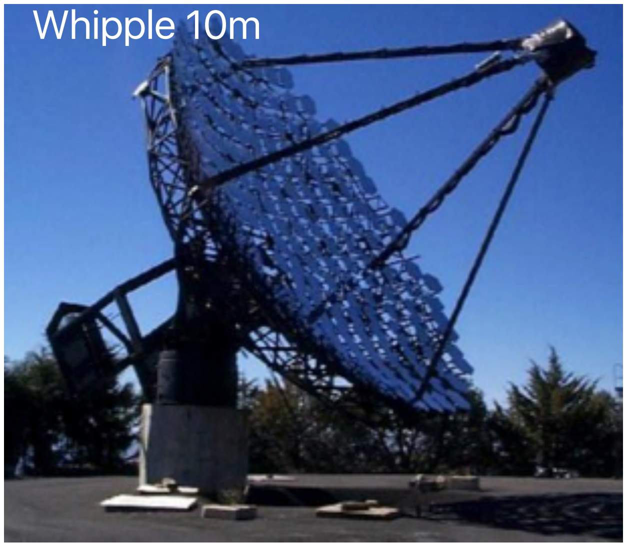

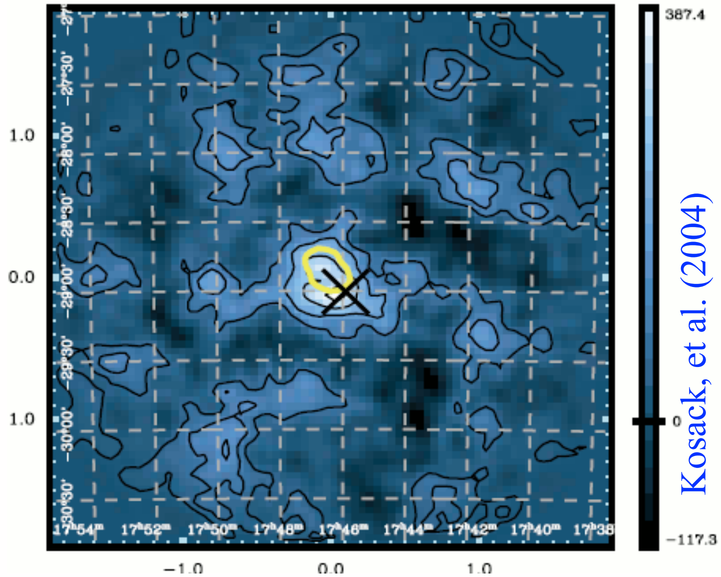

Kosack, et al. (2004)

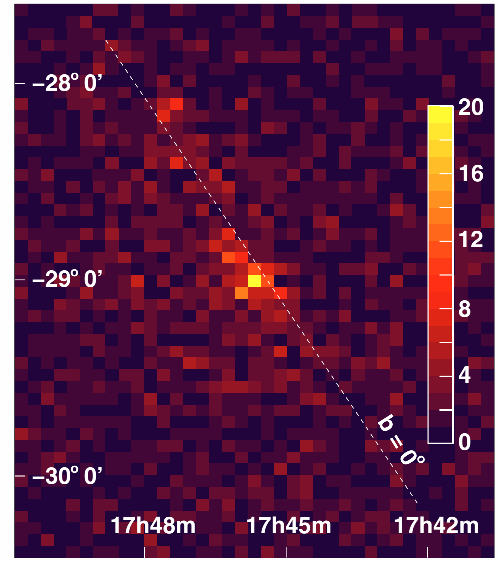

Aharonian et al., A&A 425, L13 (2004)

- EGRET detected GC source 3EG J1746-2851 (Hartman et al. 1999). Whipple 10m observed GC for ~ ten years (1995-2003) resulting in ~4 sigma evidence for emission from GC. HESS definitively detected the GC, followed by Fermi, VERITAS and MAGIC

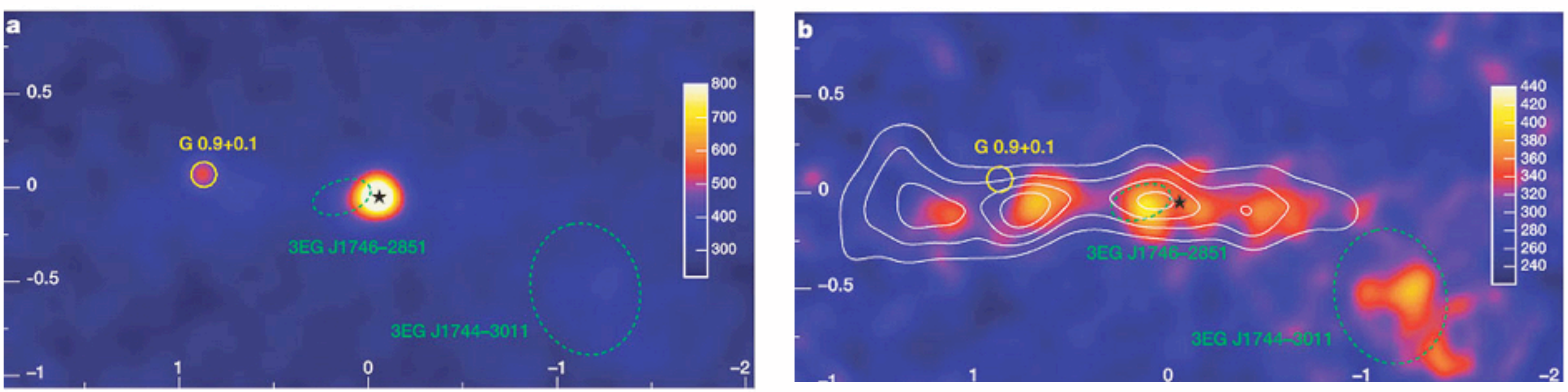

HESS GC region (Aharonian et al., 2006, Nature 439, 695)

Large Zenith Angle

GC transits at ~30 deg Elevation

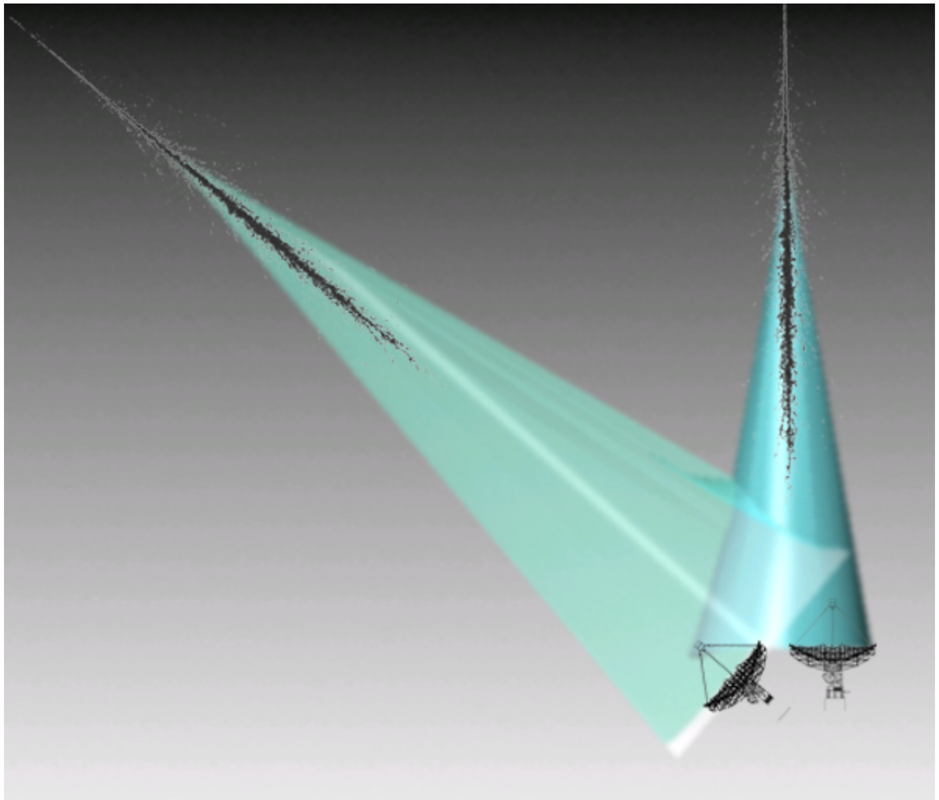

- While it is more sensible to build a telescope in the southern hemisphere to look for DM from the Galactic Center, LZA observations provide an enormous effective area at high energies - especially important for annihilation channels that result in gamma-ray emission near the kinematic maximum.

VERITAS GC Data

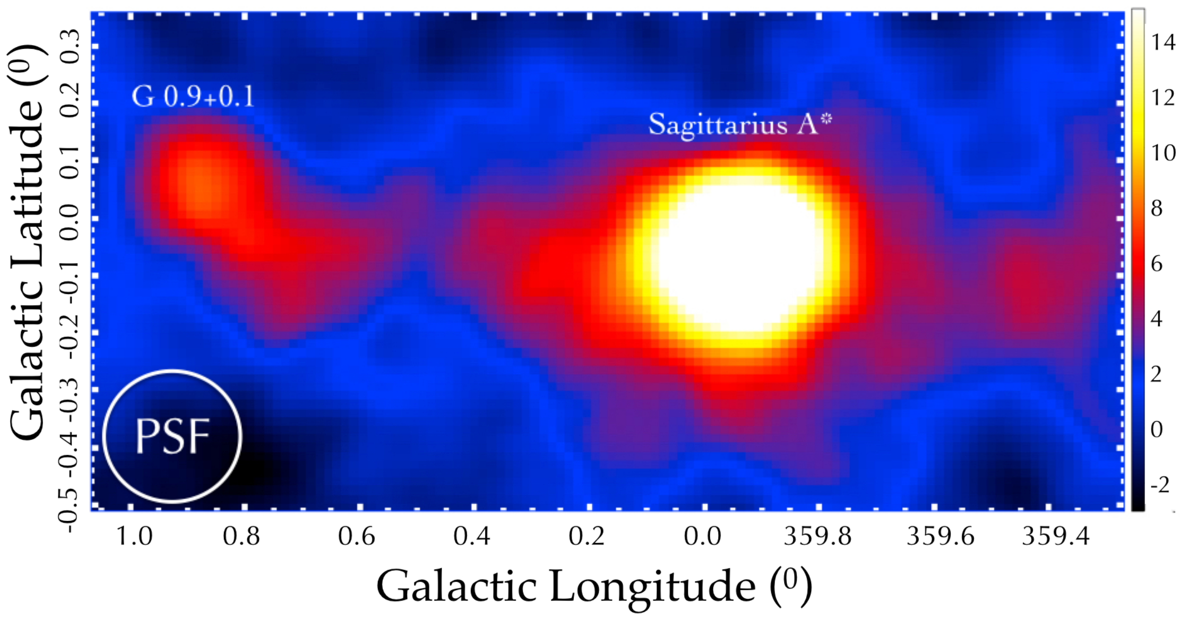

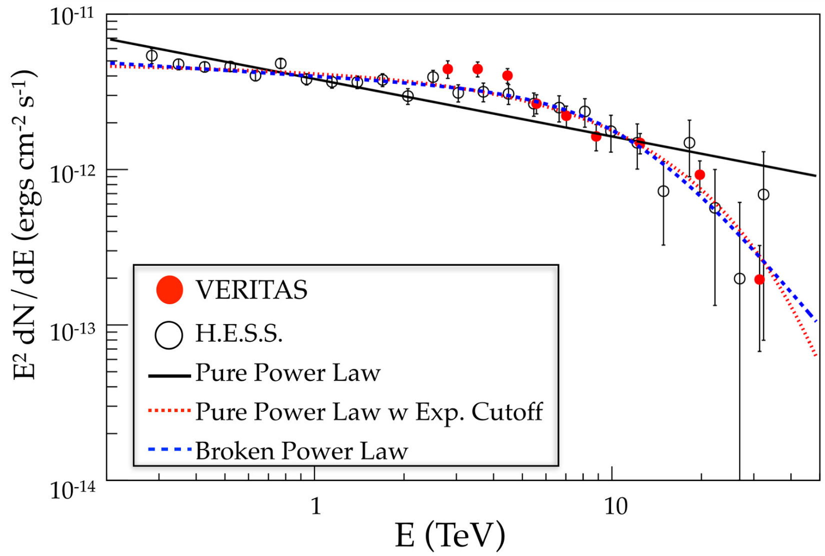

VERITAS GC Data

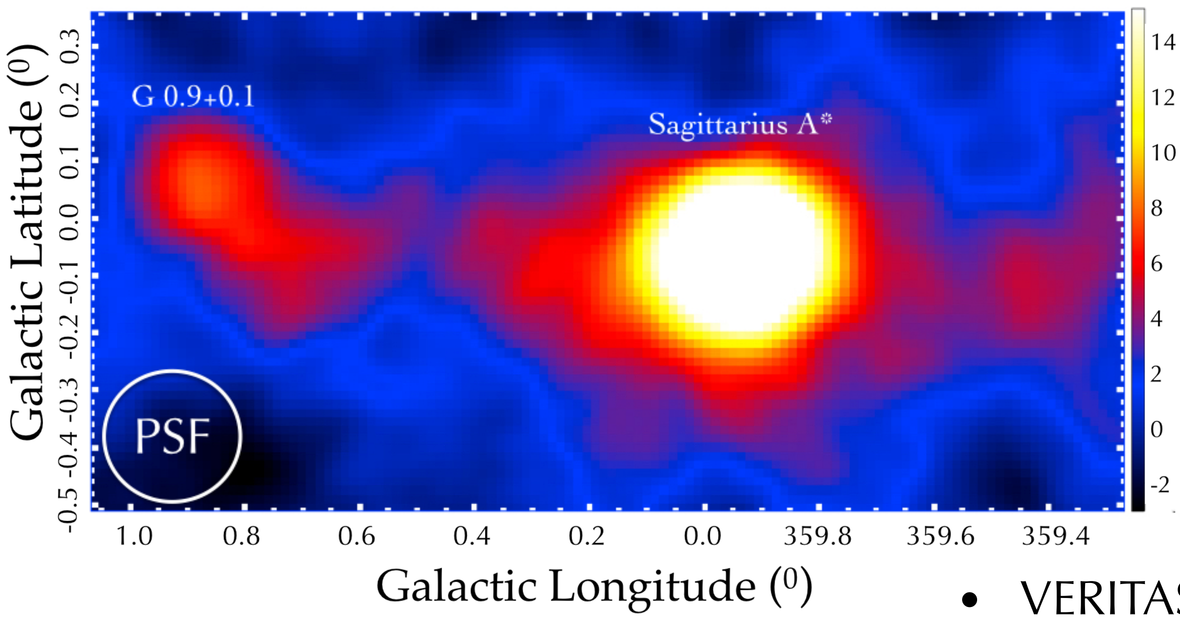

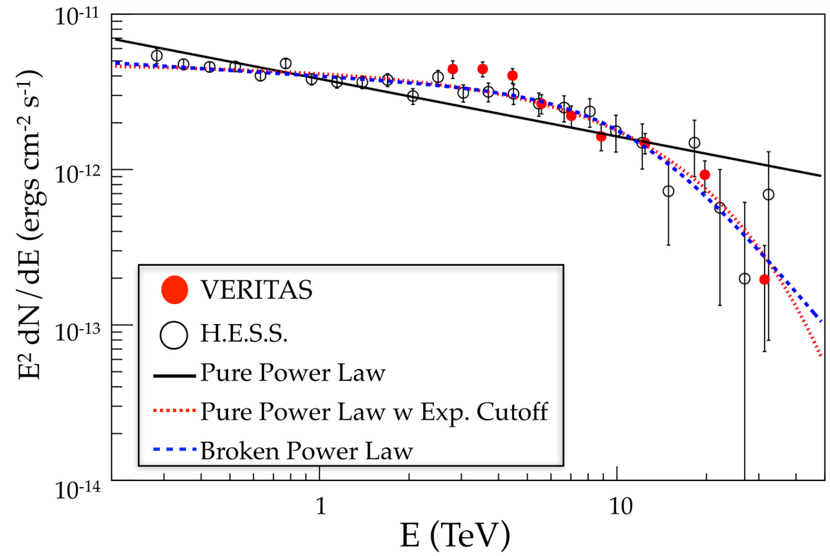

- VERITAS data from Archer et al., 2016, ApJ, 821, 129 ``TeV *Gamma-Ray observations of the GC Ridge by VERITAS''*
- 85 hours of Large Zenith Angle (~30deg elevation at transit) from 2010-2014.

VERITAS GC Data

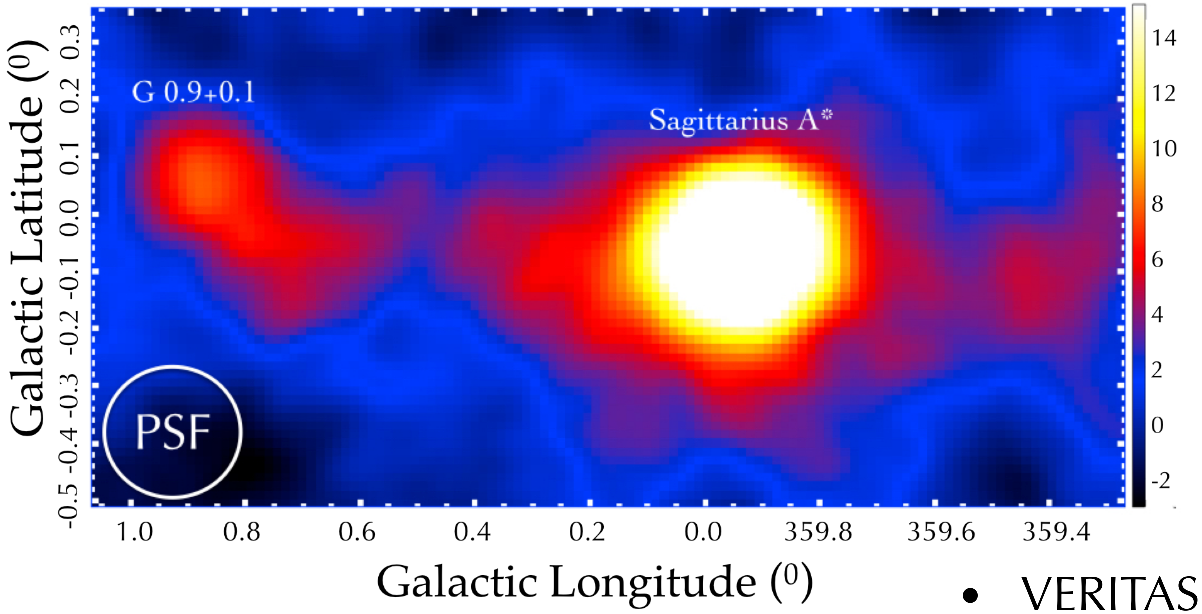

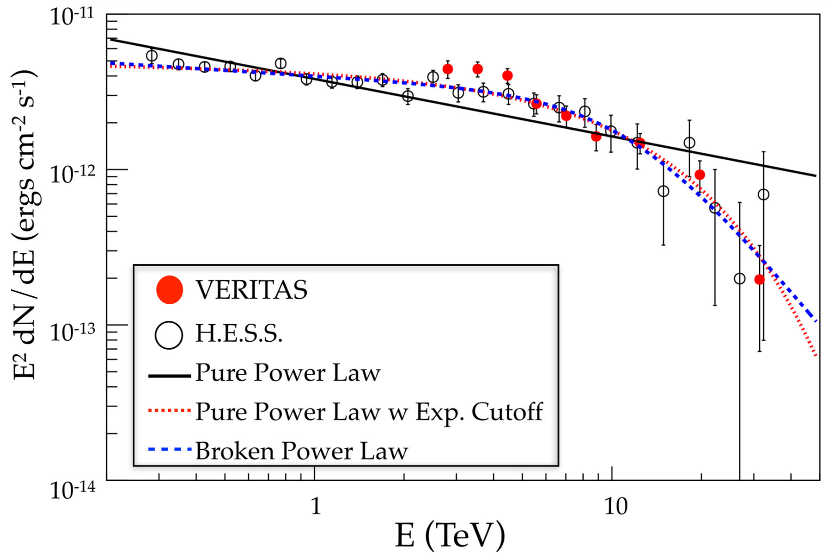

- VERITAS data from Archer et al., 2016, ApJ, 821, 129 ``Te*V Gamma-Ray observations of the GC Ridge by VERITAS''*
- 85 hours of Large Zenith Angle (~30deg elevation at transit) from 2010-2014.
- GC seen at 25 sigma using LZA analysis method. Spectrum in good agreement with HESS.

VERITAS GC Data

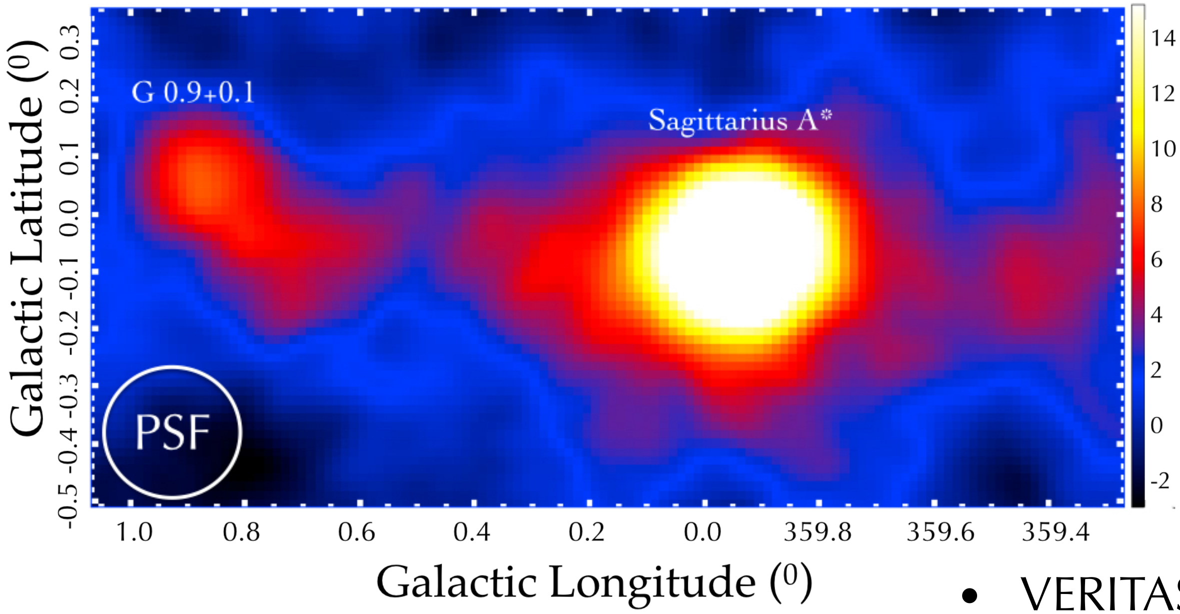

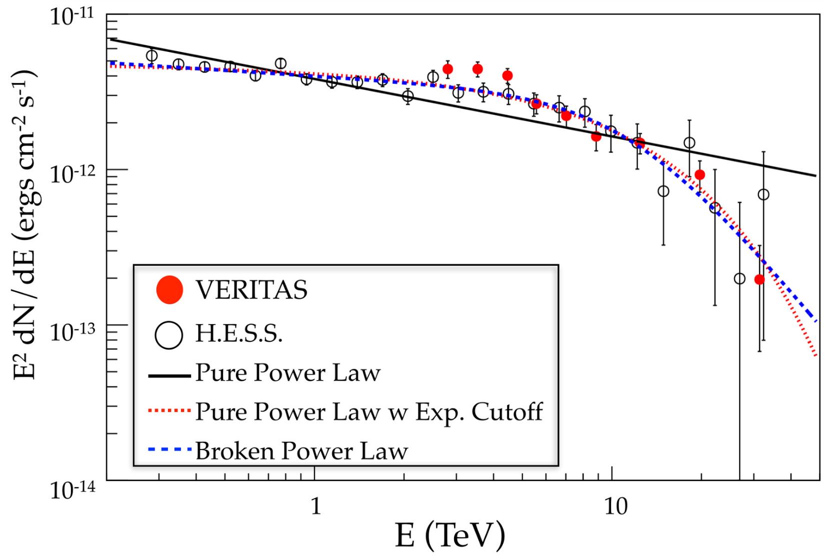

- VERITAS data from Archer et al., 2016, ApJ, 821, 129 ``TeV *Gamma-Ray observations of the GC Ridge by VERITAS''*
- 85 hours of Large Zenith Angle (~30deg elevation at transit) from 2010-2014.
- GC seen at 25 sigma using LZA analysis method. Spectrum in good agreement with HESS.
- Lots of other sources in GC region!

VERITAS GC Data

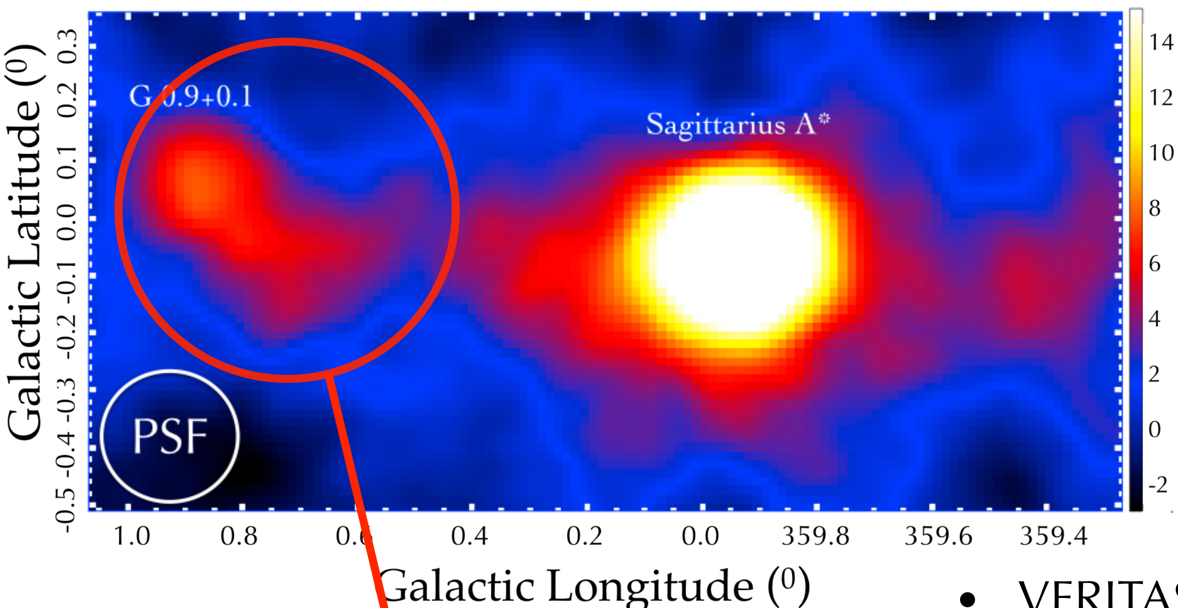

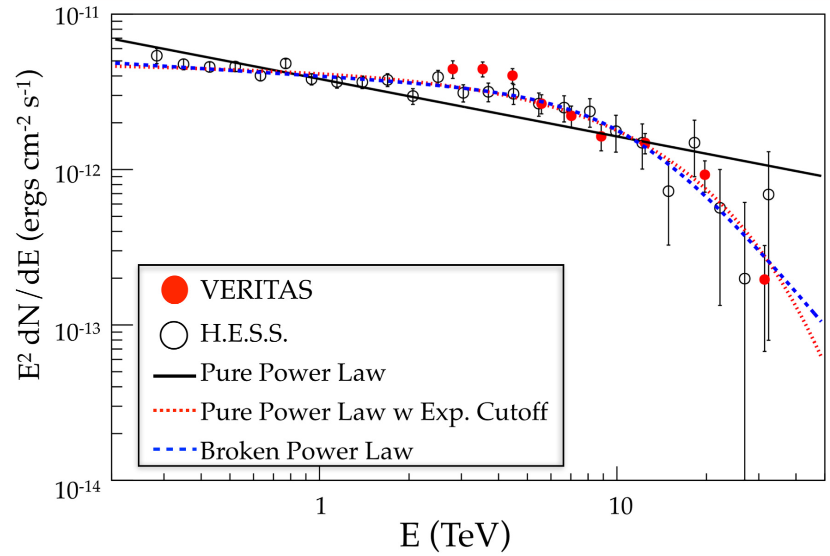

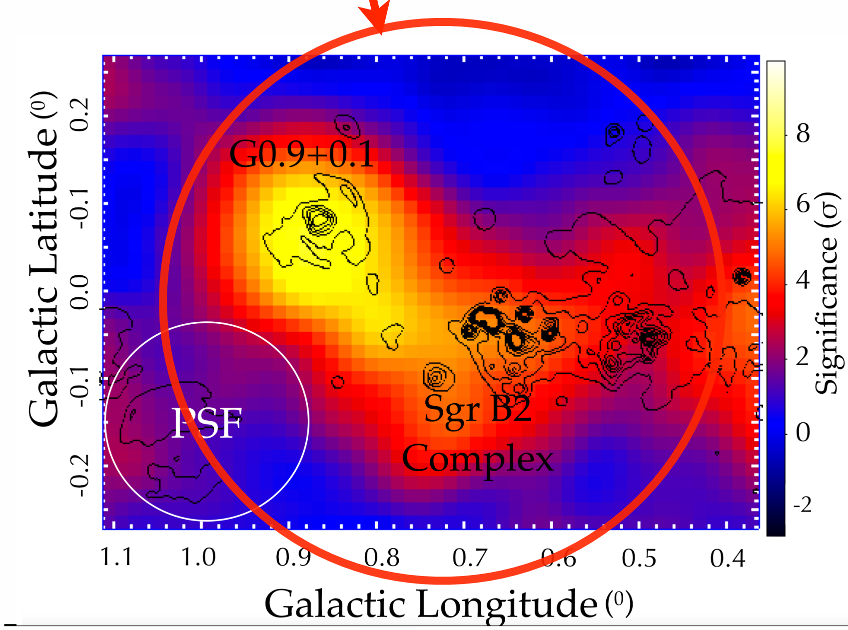

- VERITAS data from Archer et al., 2016, ApJ, 821, 129 ``*TeV Gamma-Ray observations of the GC Ridge by VERITAS''*
- 85 hours of Large Zenith Angle (~30deg elevation at transit) from 2010-2014.
- GC seen at 25 sigma using LZA analysis method. Spectrum in good agreement with HESS.
- Lots of other sources in GC region!

Where to Look for DM

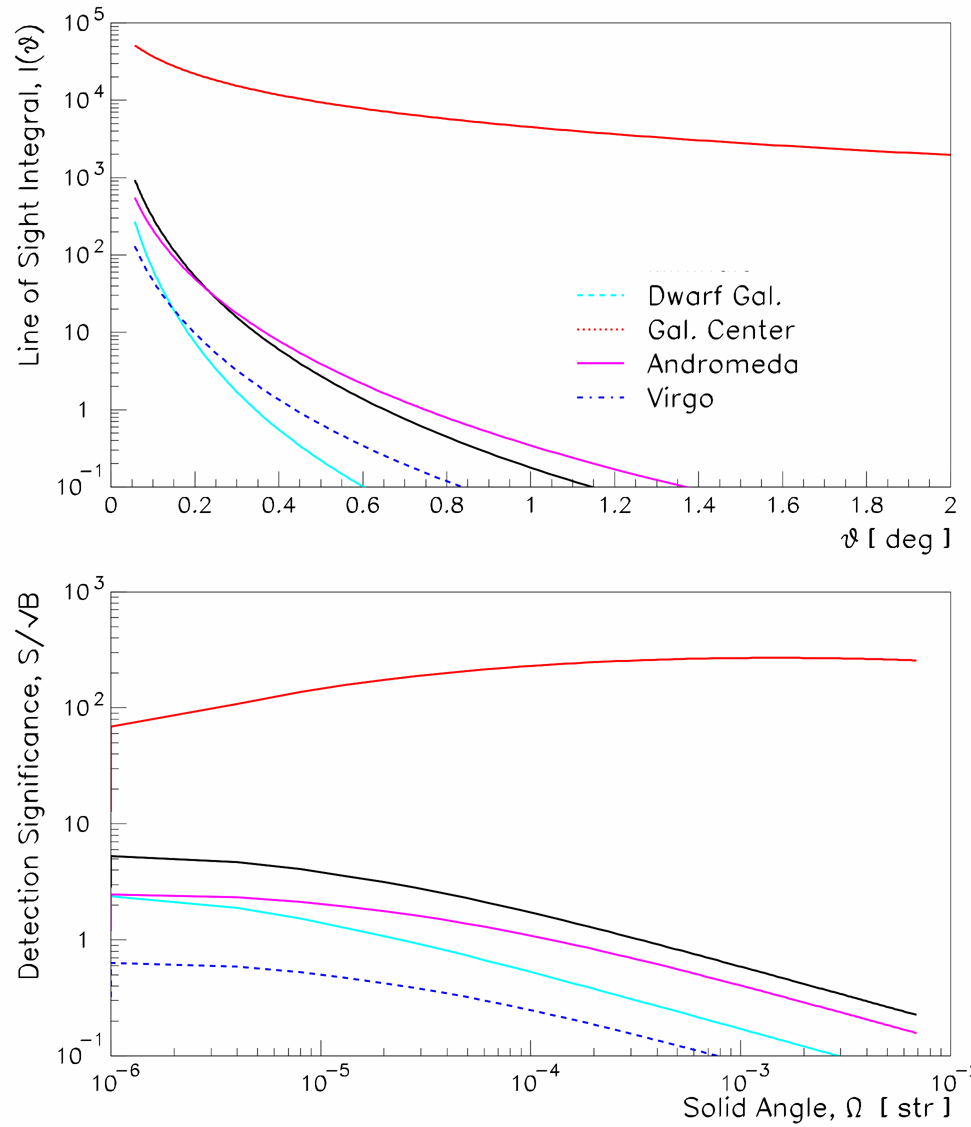

JB 2002

Where to Look for DM

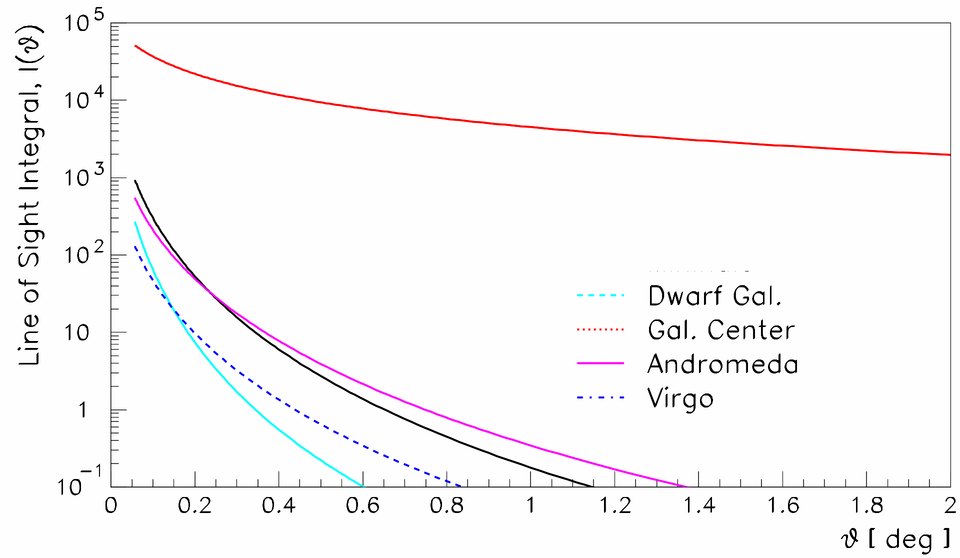

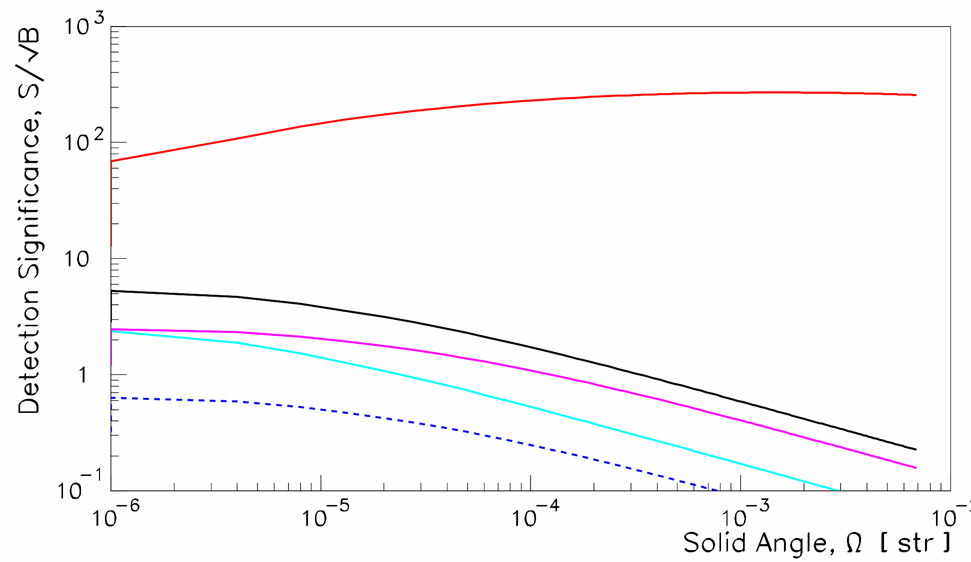

JB 2002

Where to Look for DM

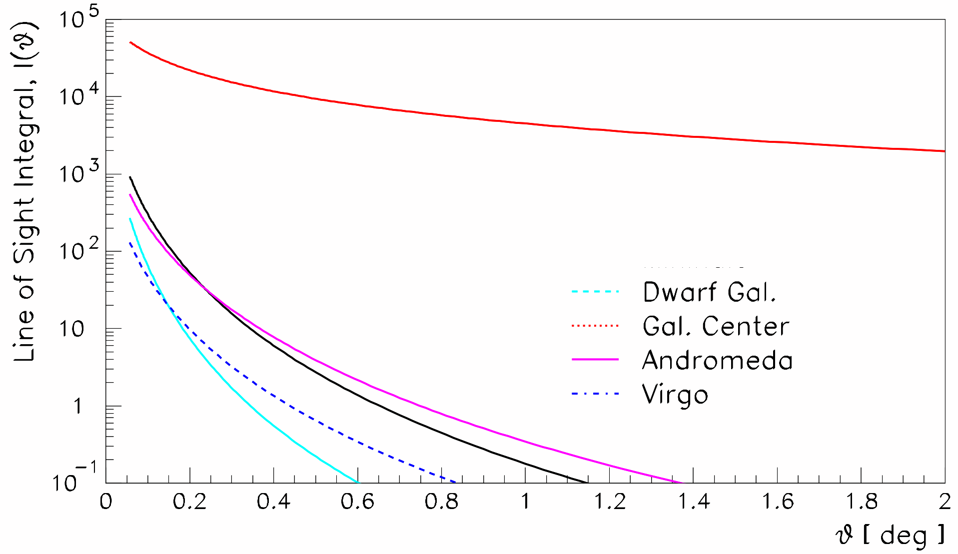

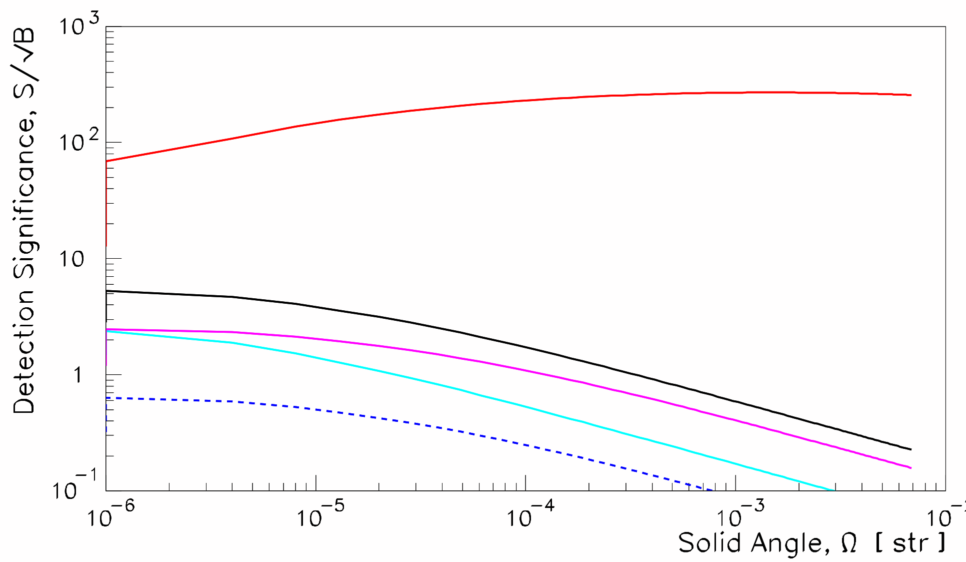

JB 2002

Where to Look for DM

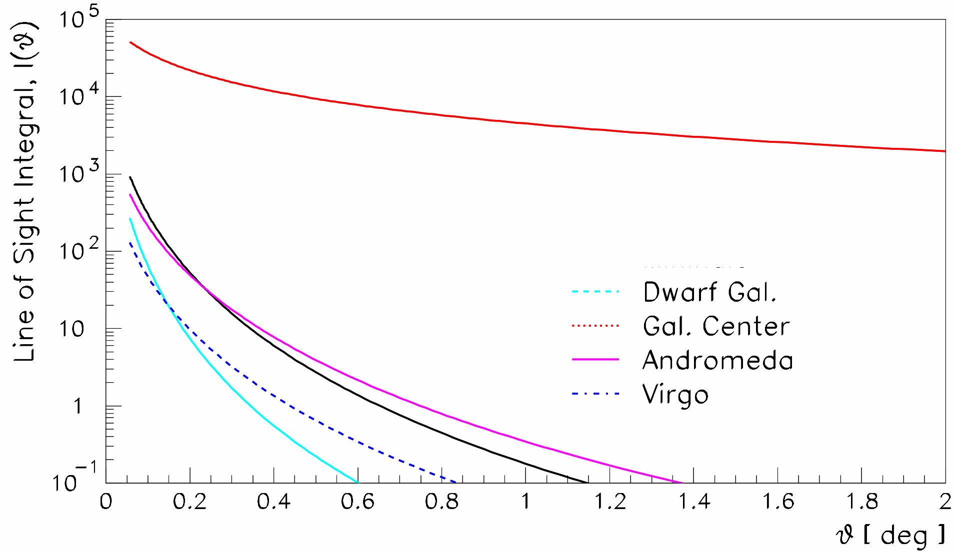

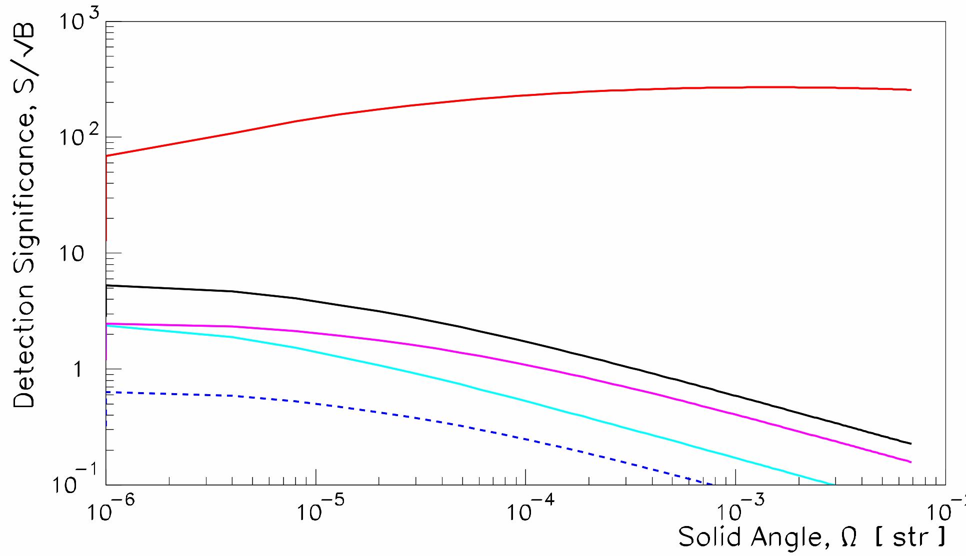

JB 2002

Ten Years of Dwarf Galaxy

Stellar velocity dispersion of stars in Dwarf galaxies giving density profiles, and J-factors (the figure of merit for detectibility). VERITAS conducted a 10 year program of Dwarf observing.

Dwarf	$\log_{10} J_1(0.5^\circ)$ [GeV^2 cm^{-5}]	$\log_{10} J_2(0.5^\circ)$ [GeV^2 cm^{-5}]	$\log_{10} D_1(0.5^\circ)$ [GeV cm^{-2}]	Exposure v4 [min]	Exposure v5 [min]	Exposure v6 [min]	Total Expos [min]
Segue 1	$19.4^{+0.3}_{-0.4}$	$17.0^{+2.1}_{-2.2}$	$18.0^{+0.2}_{-0.3}$	0	6121	4921	11042
Ursa Major II	$19.4^{+0.4}_{-0.4}$	$19.9^{+0.7}_{-0.5}$	$18.4^{+0.3}_{-0.3}$	0	0	10869	10869
Ursa Minor	$18.9^{+0.3}_{-0.2}$	$19.0^{+0.1}_{-0.1}$	$18.0^{+0.2}_{-0.1}$	711	2209	6844	9724
Draco	$18.8^{+0.1}_{-0.1}$	$19.1^{+0.4}_{-0.2}$	$18.5^{+0.1}_{-0.1}$	1169	2170	3435	6813
Coma Berencies	$19.0^{+0.4}_{-0.4}$	$19.6^{+0.8}_{-0.7}$	$18.0^{+0.2}_{-0.3}$	0	0	2204	2204
Segue II	$16.2^{+1.1}_{-1.0}$	$18.9^{+1.1}_{-1.1}$	$15.9^{+0.4}_{-0.4}$	0	0	1128	1128
Boötes 1	$18.2^{+0.4}_{-0.4}$	$18.5^{+0.6}_{-0.4}$	$17.9^{+0.2}_{-0.3}$	960	0	0	960
Leo II	$18.0^{+0.2}_{-0.2}$	$17.8^{+0.2}_{-0.2}$	$17.2^{+0.4}_{-0.5}$	0	0	946	946
Willman 1	N/A	N/A	N/A	931	0	0	931
Triangulum II	N/A	N/A	N/A	0	0	909	909
Canes Ver. II	$17.7^{+0.5}_{-0.4}$	$18.5^{+1.2}_{-0.9}$	$17.0^{+0.2}_{-0.2}$	0	0	864	864
Canes Ver. I	$17.4^{+0.4}_{-0.3}$	$17.5^{+0.4}_{-0.2}$	$17.6^{+0.4}_{-0.7}$	0	0	850	850
Hercules I	$16.9^{+0.7}_{-0.7}$	$17.5^{+0.7}_{-0.7}$	$16.7^{+0.4}_{-0.4}$	0	0	794	794
Sextans I	$18.0^{+0.2}_{-0.2}$	$17.6^{+0.2}_{-0.2}$	$17.9^{+0.1}_{-0.2}$	0	0	783	783
Draco II	N/A	N/A	N/A	0	0	598	598
Ursa Major I	$17.9^{+0.6}_{-0.3}$	$18.7^{+0.6}_{-0.5}$	$17.6^{+0.2}_{-0.4}$	0	0	482	482
Leo I	$17.8^{+0.2}_{-0.2}$	$17.8^{+0.5}_{-0.2}$	$17.9^{+0.2}_{-0.2}$	0	0	409	409
Leo V	$16.4^{+0.9}_{-0.9}$	$16.1^{+1.2}_{-1.0}$	$15.9^{+0.5}_{-0.5}$	0	0	167	167
Leo IV	$16.3^{+1.1}_{-1.7}$	$16.2^{+1.5}_{-1.6}$	$16.1^{+0.7}_{-1.1}$	0	0	151	151

VERITAS Combined Dwarf Limits

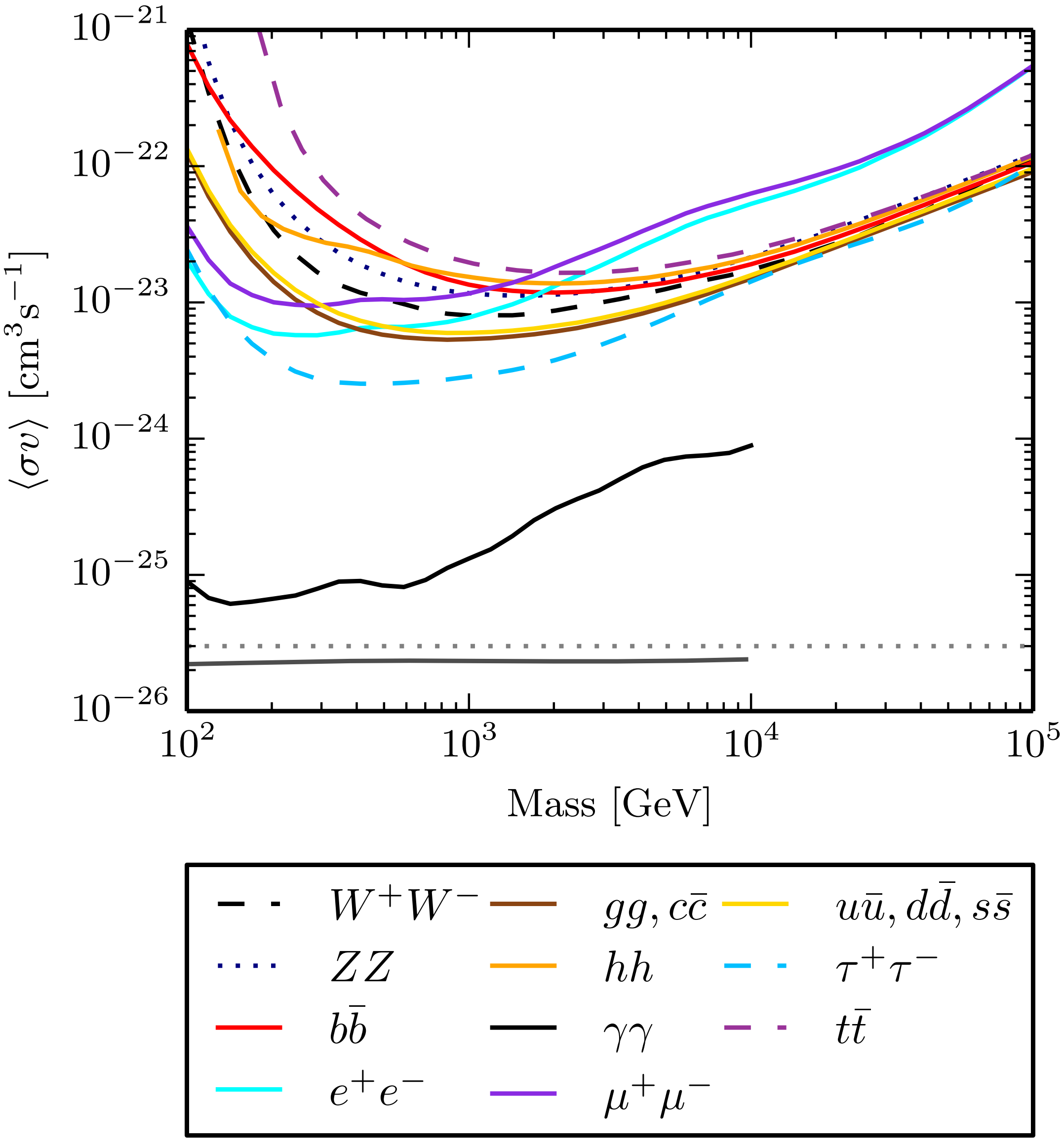

"Dark matter constraints from a joint analysis of dwarf Spheroidal galaxy observations with VERITAS", Archambaldt et al. (for VERITAS), PRD, 95, 082001 (2017)

VERITAS Combined Dwarf Limits

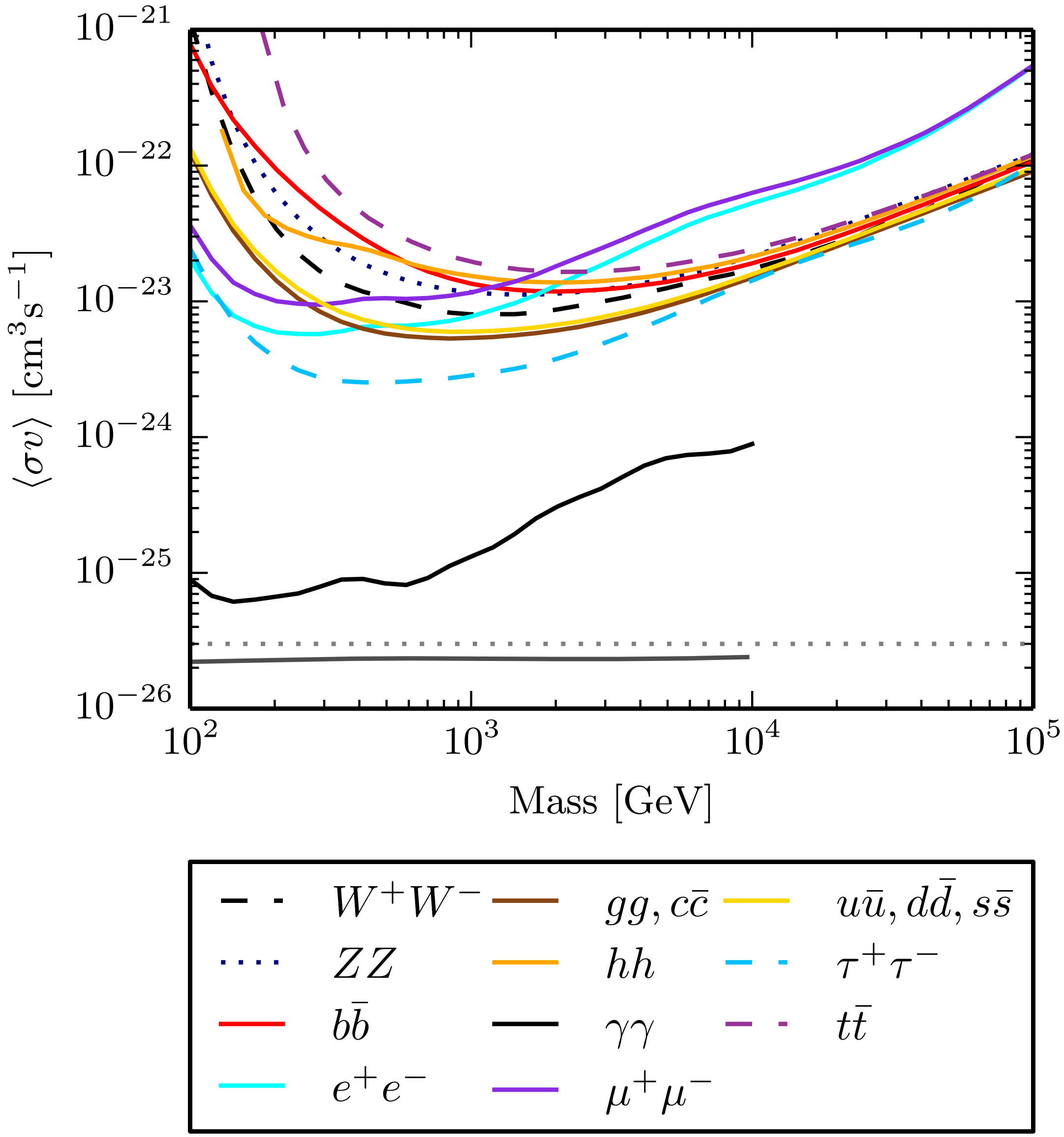

- VERITAS 95% CL velocity-averaged cross section as a function of DM mass for stacked dwarf galaxy observations for different Annihilation channels.

"Dark matter constraints from a joint analysis of dwarf Spheroidal galaxy observations with VERITAS", Archambaldt et al. (for VERITAS), PRD, 95, 082001 (2017)

VERITAS Combined Dwarf Limits

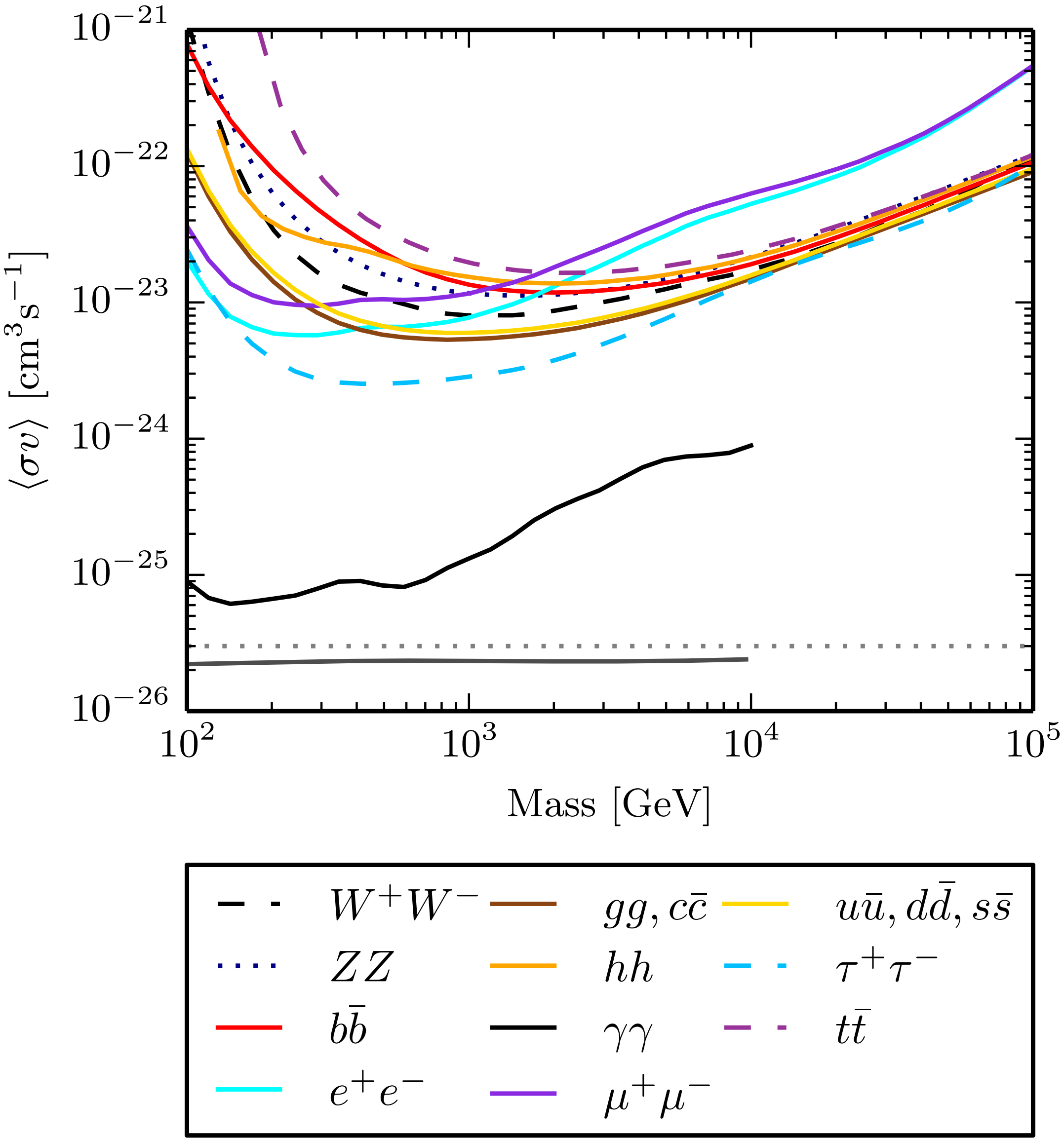

- VERITAS 95% CL velocity-averaged cross section as a function of DM mass for stacked dwarf galaxy observations for different Annihilation channels.
- Results depend on Dwarf galaxies with the highest J-factor. New measurements (e.g., DES) are revealing more, and perhaps better Dwarfs.

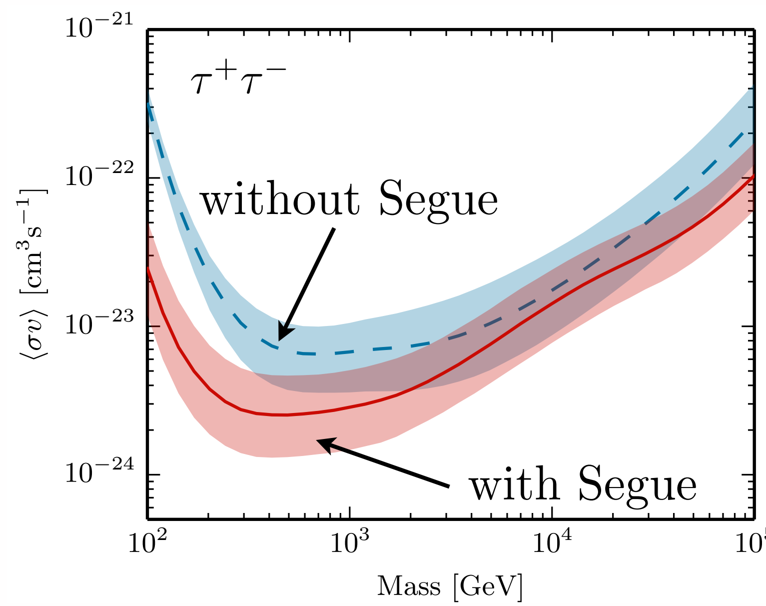

"Dark matter constraints from a joint analysis of dwarf Spheroidal galaxy observations with VERITAS", Archambaldt et al. (for VERITAS), PRD, 95, 082001 (2017)

W/Z Sommerfeld Enhancement

At sufficiently high neutralino masses, the W and Z can act as carriers of a long-range (Yukawa-like) force, resulting in a velocity dependent enhancement in cross section.

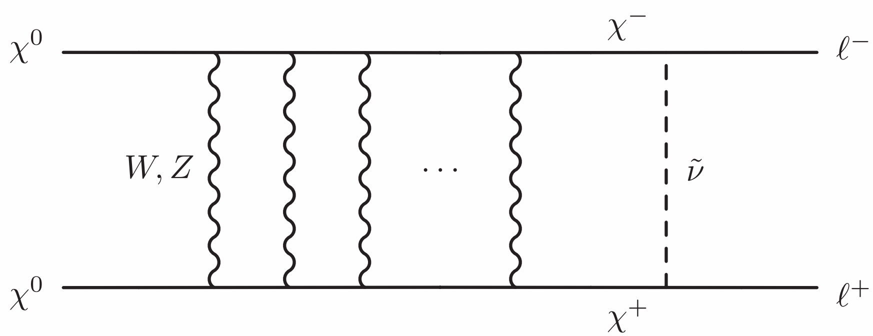

Lattanzi and Silk, PRD 79, 083523 (2009), Profumo (2005)

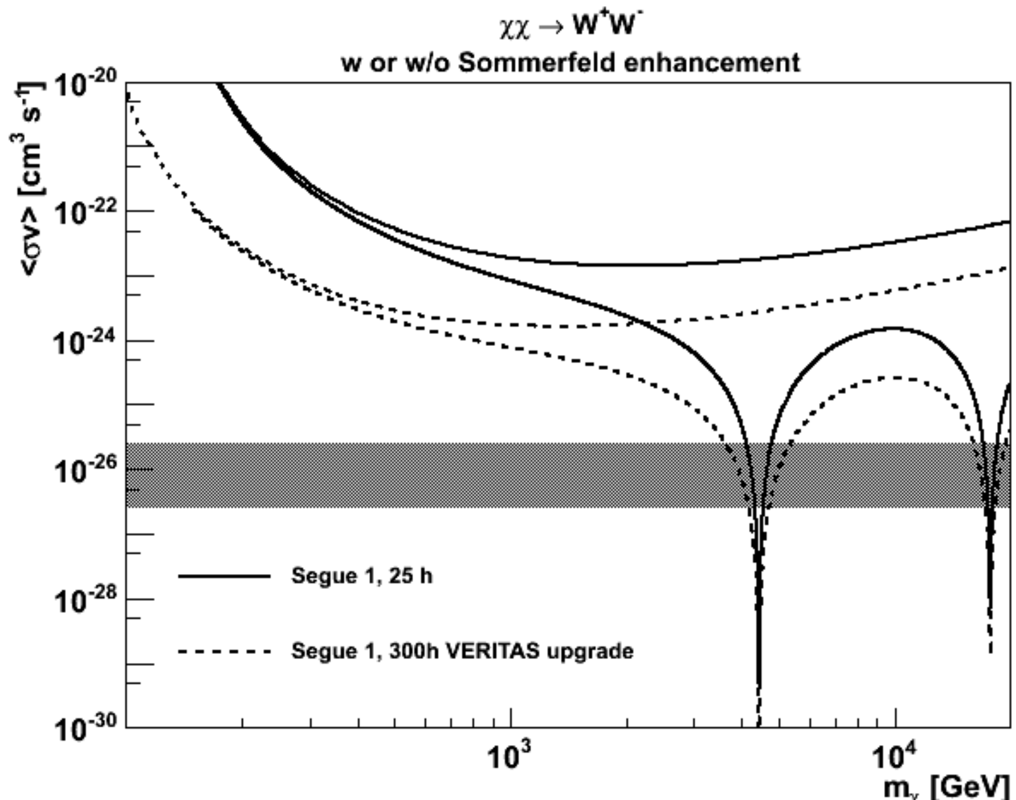

(Matthieu Vivier et al. for the VERITAS Collaboration)

W/Z Sommerfeld Enhancement

At sufficiently high neutralino masses, the W and Z can act as carriers of a long-range (Yukawa-like) force, resulting in a velocity dependent enhancement in cross section.

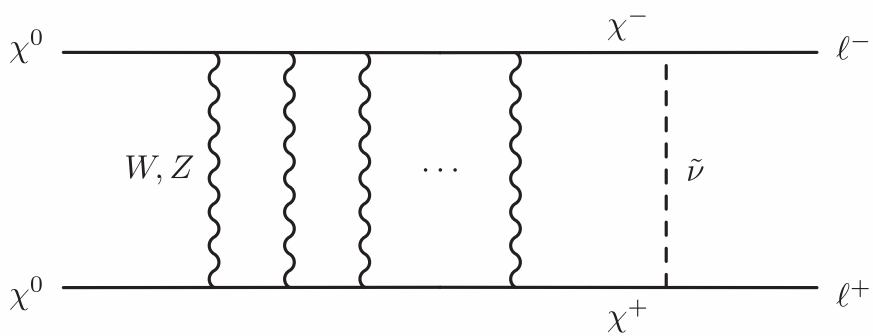

Lattanzi and Silk, PRD 79, 083523 (2009), Profumo (2005)

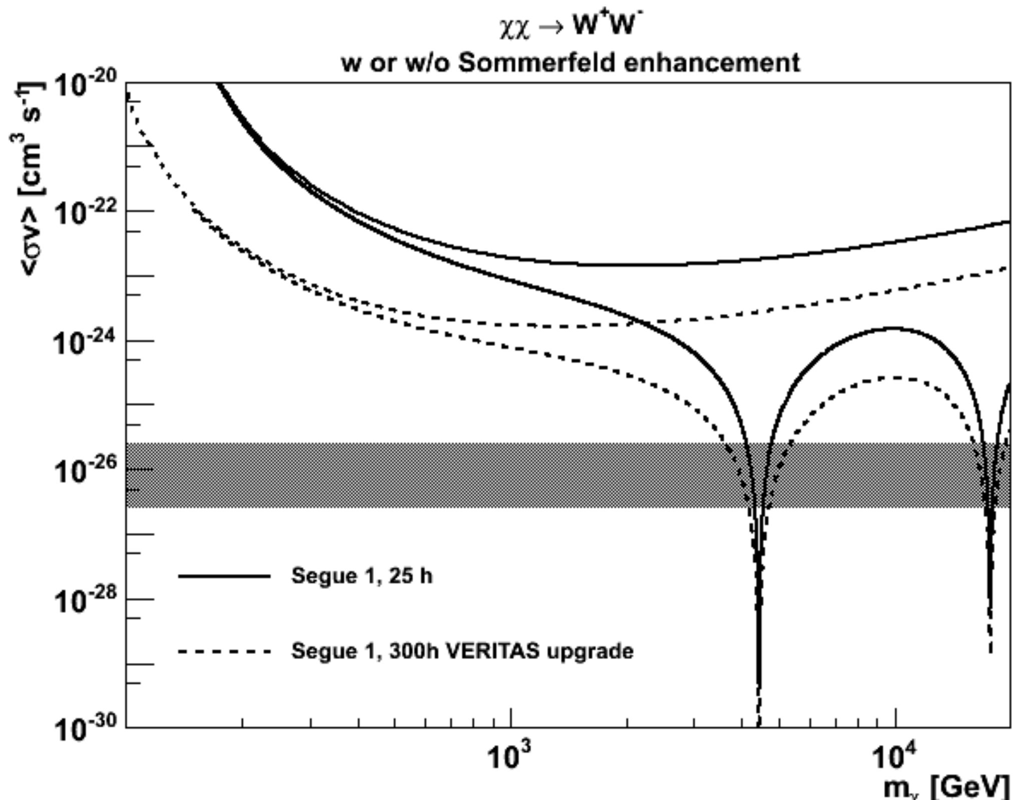

(Matthieu Vivier et al. for the VERITAS Collaboration)

- At high mass, we generically expect Sommerfeld enhancement from W, Z exchange for standard neutralinos can give large enhancement in cross section,

HAWC Dwarf Limits

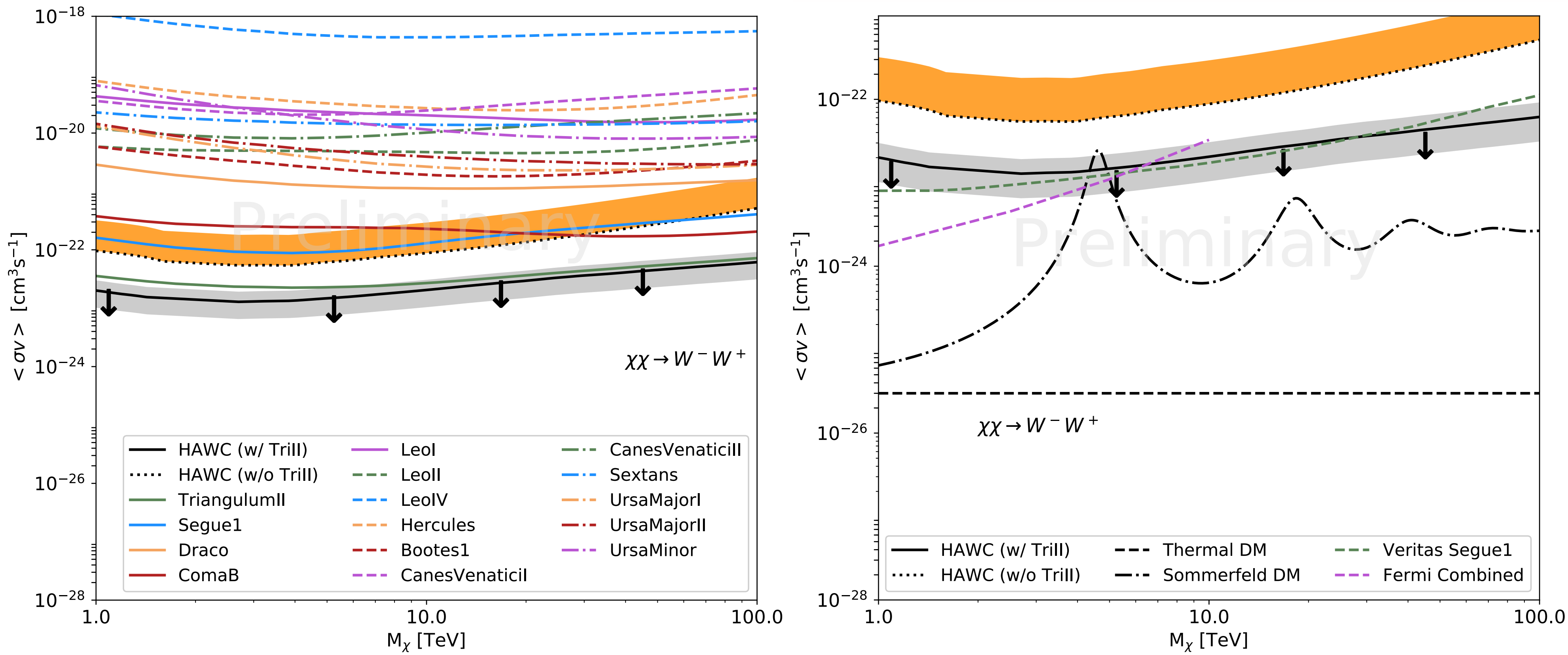

"Dark Matter Limits from Dwarf Spheroidal Galaxies with the HAWC Gamma-Ray Observatory", A. Albert et al. (for the HAWC Collaboration), 2017, ApJ, 853,154

GC Upper Limits

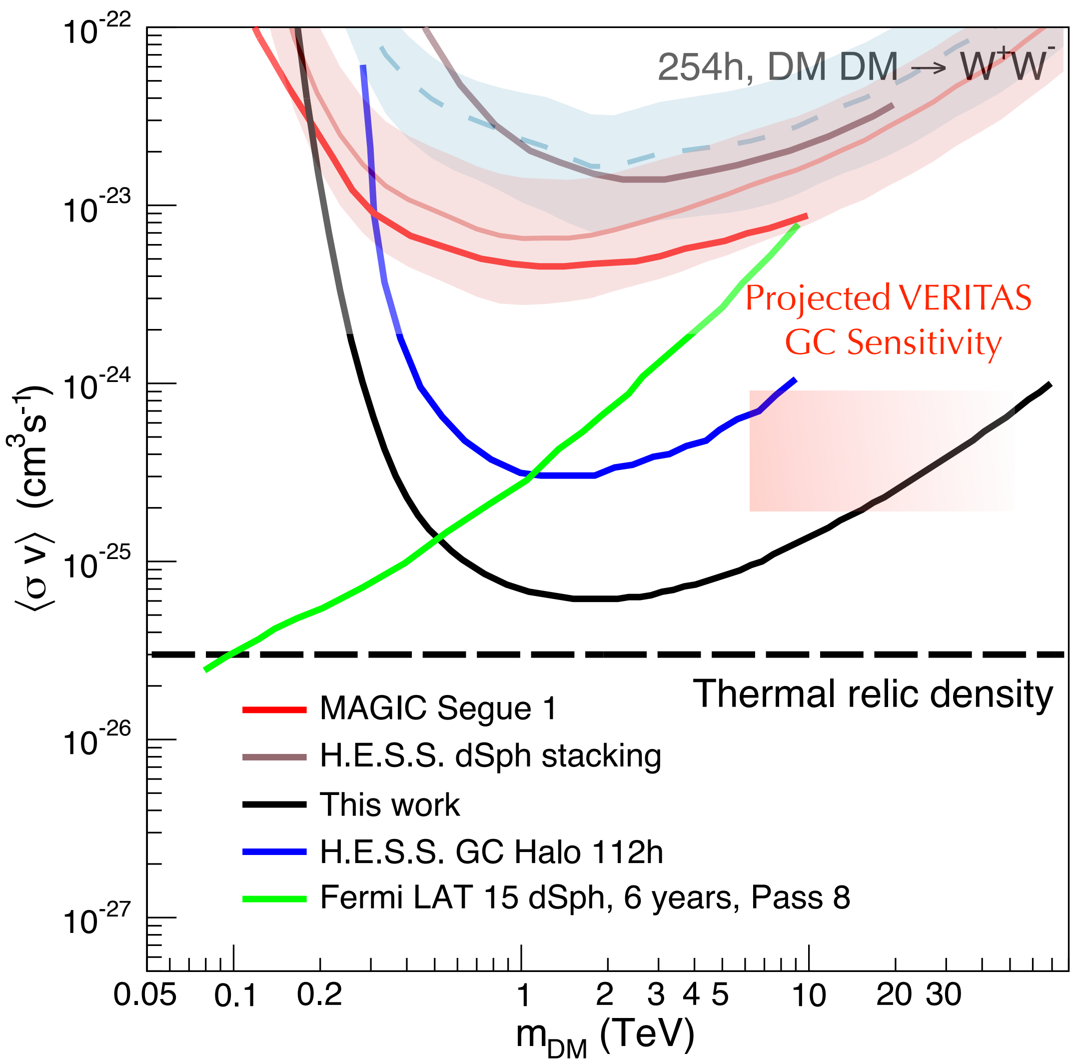

``Search for dark matter annihilations towards the inner Galactic halo from 10 years of observations with H.E.S.S.” , Abdallah et al. (for the HESS collaboration), 2016, PRL, 117, 1301)

GC Upper Limits

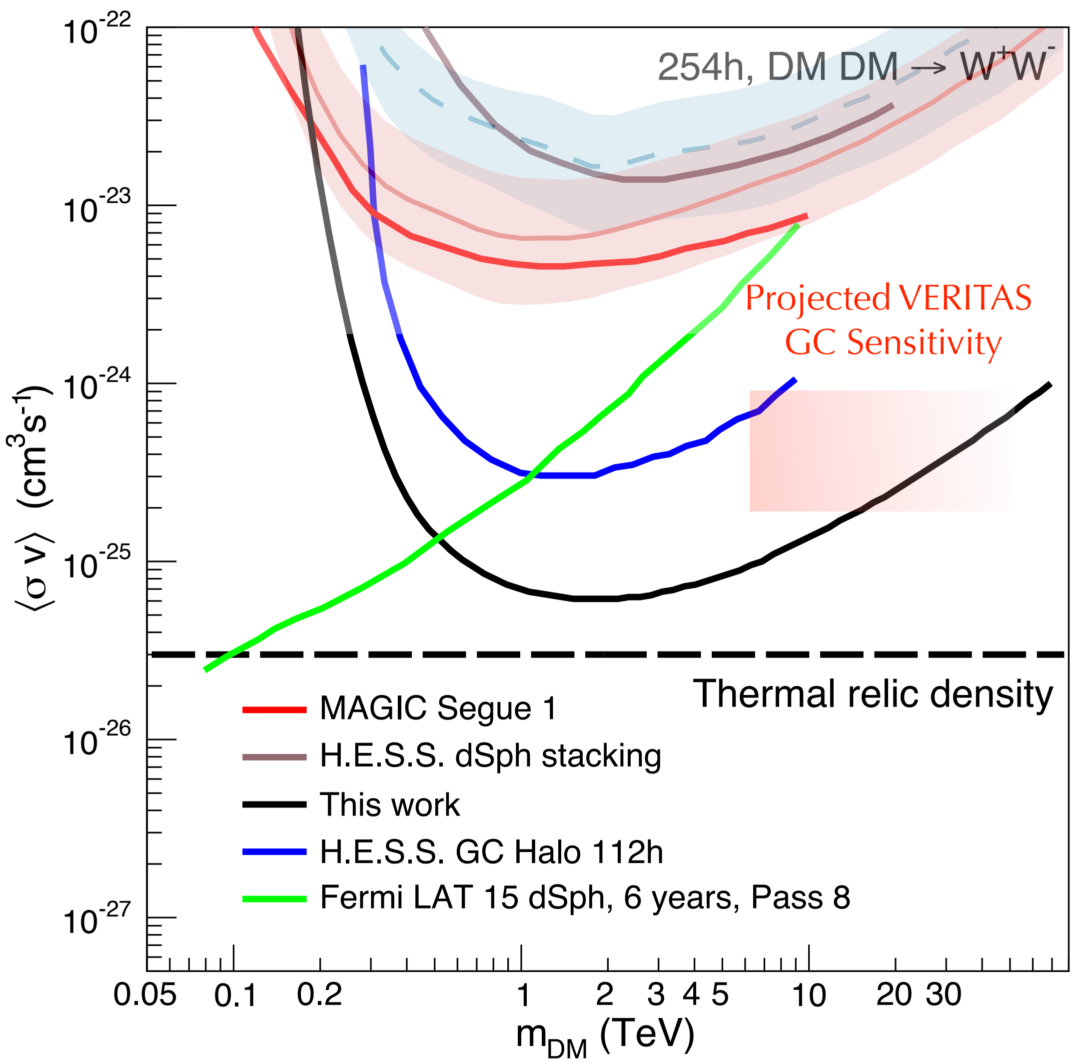

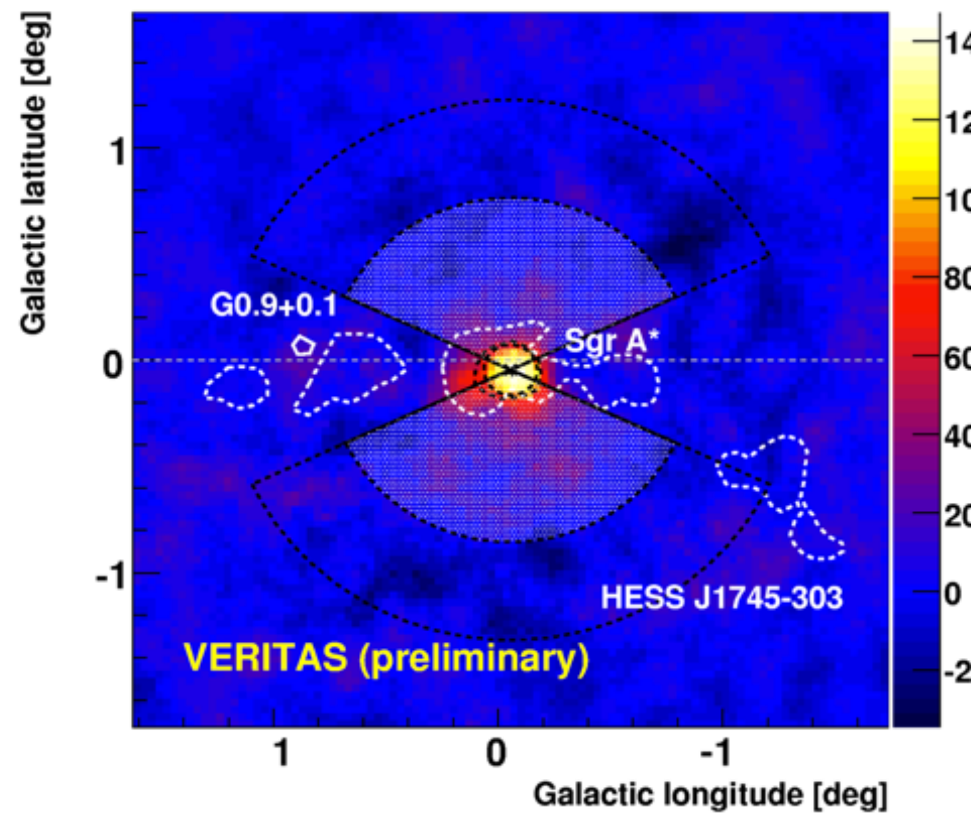

``Search for dark matter annihilations towards the inner Galactic halo from 10 years of observations with H.E.S.S." , Abdallah et al. (for the HESS collaboration), 2016, PRL, 117, 1301)

CTA

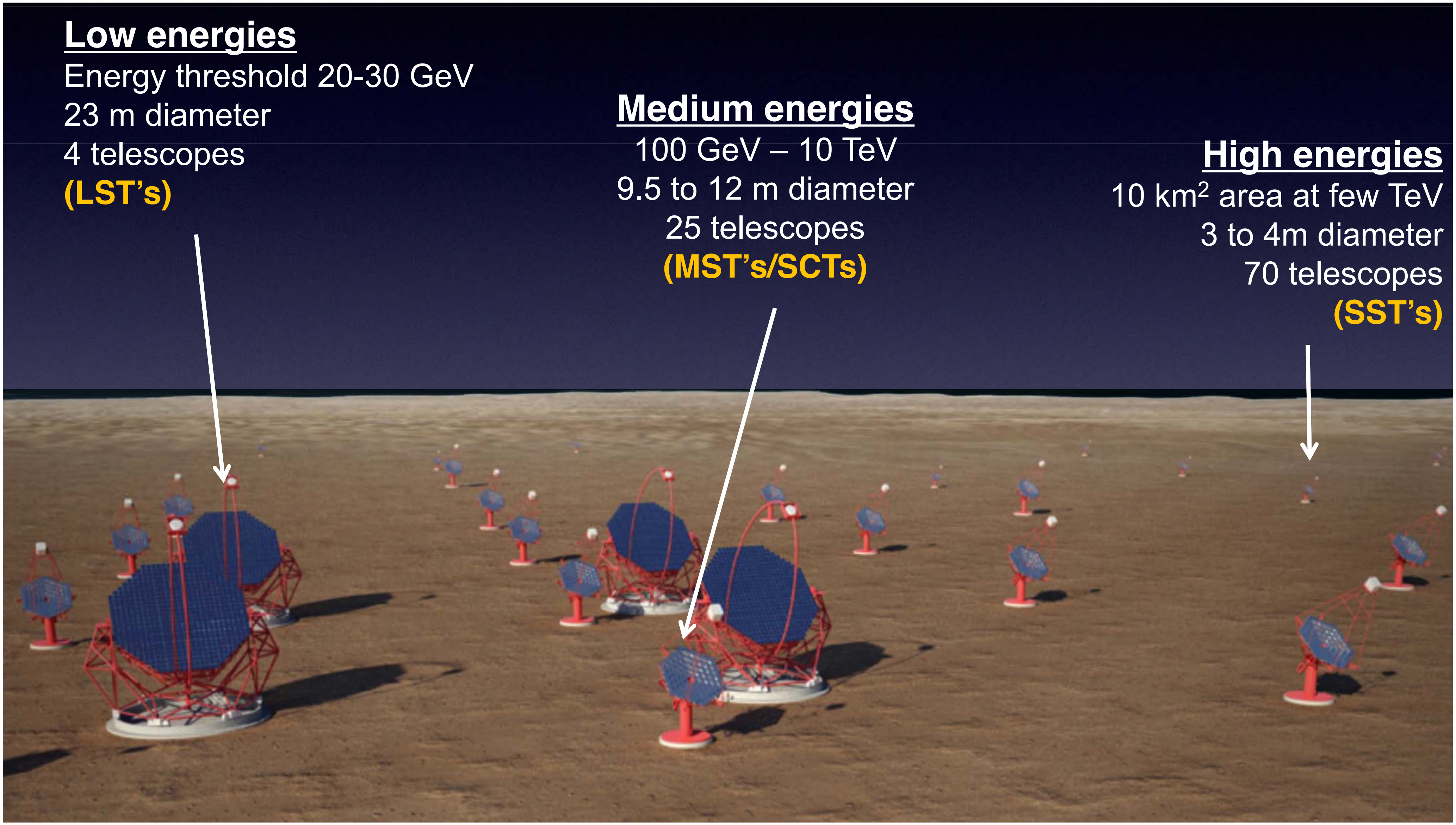
Low energies
Energy threshold 20-30 GeV
23 m diameter
4 telescopes
(LST's)
Medium energies
100 GeV – 10 TeV
9.5 to 12 m diameter
25 telescopes
(MST's/SCTs)
High energies
10 km² area at few TeV
3 to 4m diameter
70 telescopes
(SST's)

Flux Sensitivity

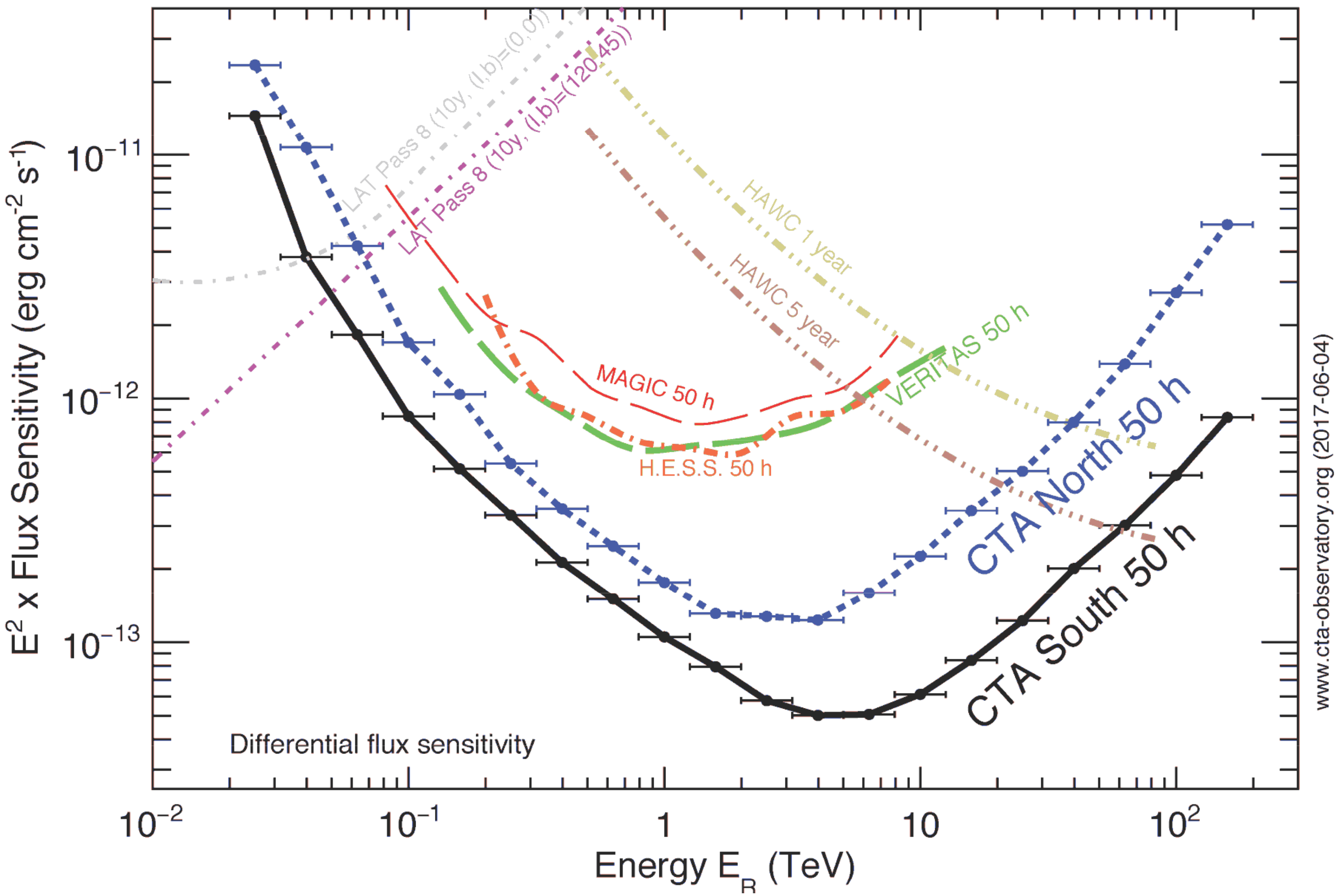

Major sensitivity improvement & wider energy range

→ Factor of >10 increase in source population

(credit: Rene Ong)

CTA GC Sensitivity

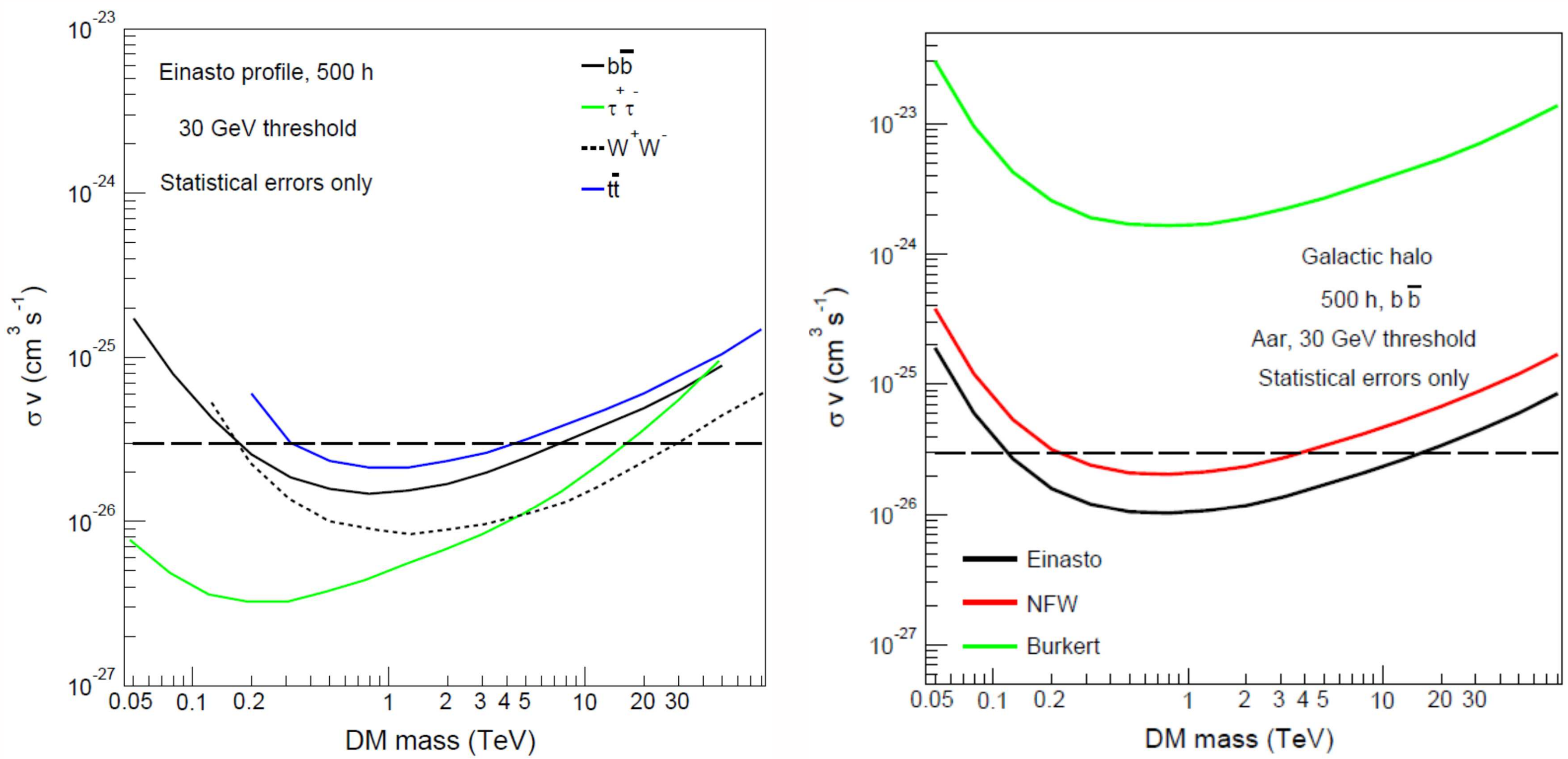

Figure1. Left: Sensitivity for σ v from observation on the Galactic Halo with Einsasto dark matter profile and for different annihilation modes as indicated. **Right**: for cuspy (NFW, Einasto) and cored (Burkert) dark matter halo profiles. For both plots only statistical errors are taken into account. The dashed horizontal lines indicate the level of the thermal cross-section of 3×10^{-26} cm^3 s^{-1}.

`Prospects for Indirect Dark Matter Searches with the Cherenkov Telescope Array (CTA)'' , J. Carr et al. (for the CTA Consortium), 2015 in Proc. of the 34th ICRC conference,

If the US Funded CTA…

- If NSF and DOE had the budget to follow through on the advice of the NWNH decadal survey, Snowmass and P5 this is what we could have achieved…

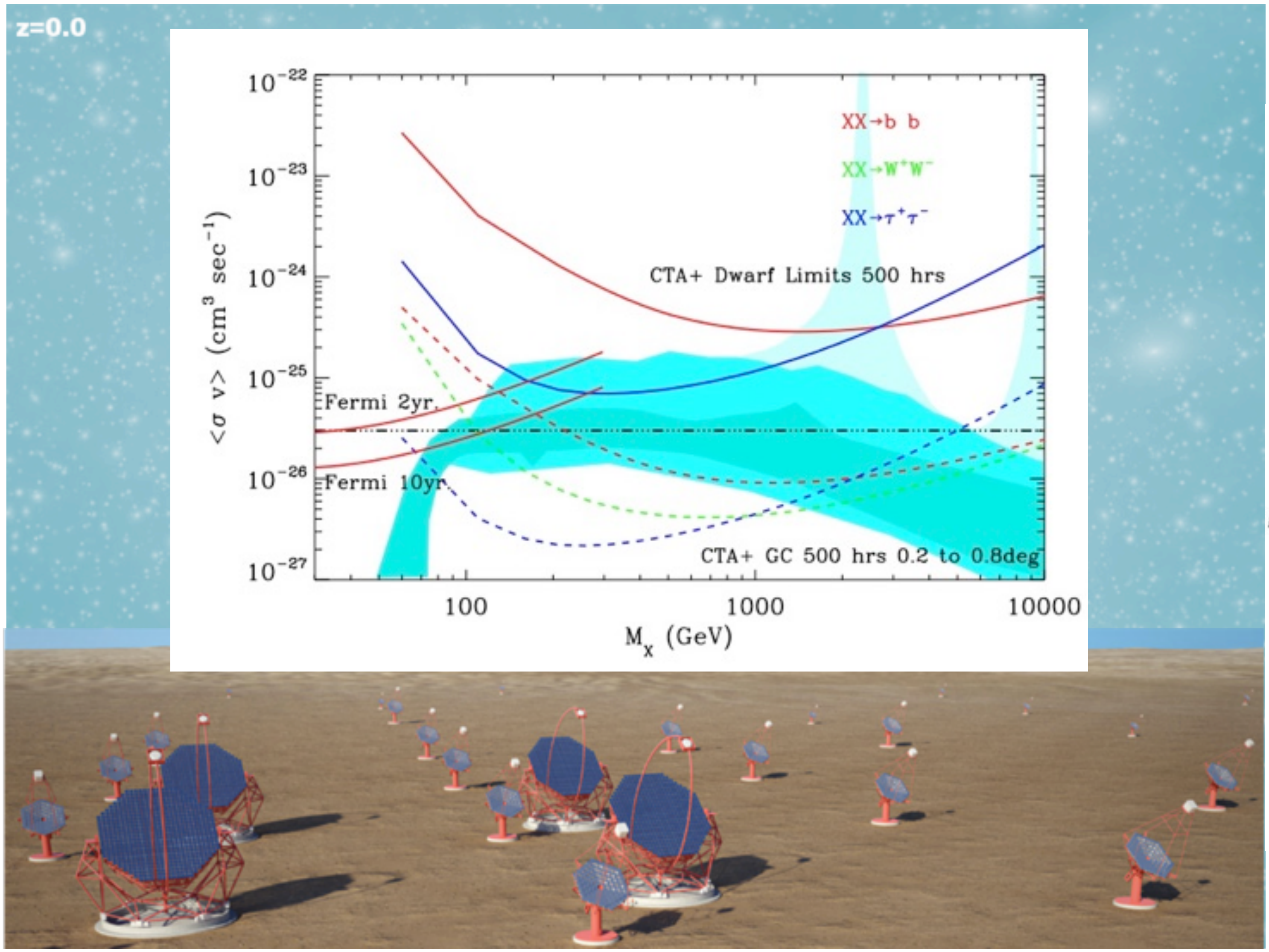

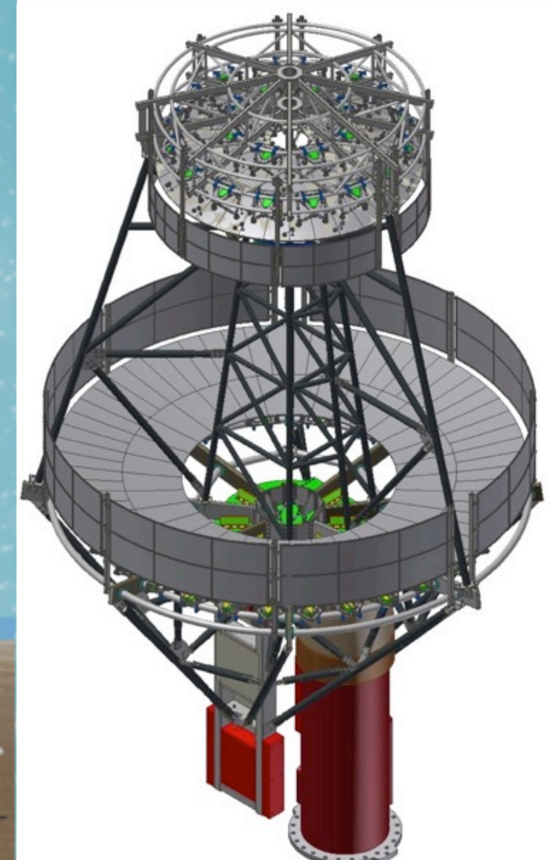

II. Gamma-Ray Searches for Axion-Like-Particles

Axions and ALPs

One expects CP violating term in QCD Lagrangian:

$$\mathcal{L}_{\rm QCD} = \frac{1}{4} G_a^{\mu\nu} G_{a\mu\nu} + g\phi\, G_a^{\mu\nu} \tilde{G}_{a\mu\nu} + \text{interactions.}$$

$$Note: F_{\mu\nu}\tilde{F}^{\mu\nu} = \vec{B}\cdot\vec{E} \leftrightarrow G_{\mu\nu}\tilde{G}^{\mu\nu} = \vec{B}_a \cdot \vec{E}_a \text{ which is odd under } T \Rightarrow \text{odd under } CP$$

Peccei-Quinn solution: introduce new field (with MH potential). At $T < f_a$ symmetry broken, and axial mode of field settles at some angle $\theta = a$.

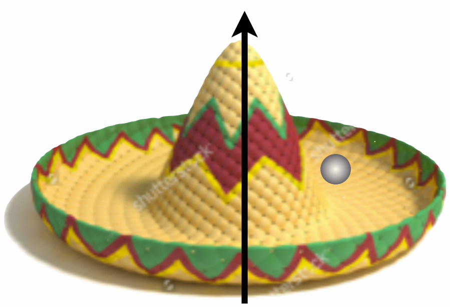

Axions and ALPs

One expects CP violating term in QCD Lagrangian:

$$\mathcal{L}_{\rm QCD} = \frac{1}{4} G_a^{\mu\nu} G_{a\mu\nu} + g\phi\, G_a^{\mu\nu} \tilde{G}_{a\mu\nu} + \text{interactions.}$$

$$Note: F_{\mu\nu}\tilde{F}^{\mu\nu} = \vec{B}\cdot\vec{E} \leftrightarrow G_{\mu\nu}\tilde{G}^{\mu\nu} = \vec{B}_a \cdot \vec{E}_a \text{ which is odd under } T \Rightarrow \text{odd under } CP$$

Peccei-Quinn solution: introduce new field (with MH potential). At $T < f_a$ symmetry broken, and axial mode of field settles at some angle $\theta = a$.

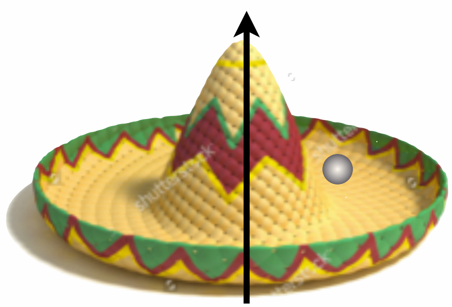

When $T \sim \Lambda_{\rm QCD}$ tilting of hat gives axion field a VEV $\langle a \rangle = 0$ that cancels the CP violating term. The a field oscillates about its VEV with a mass given by the curvature of the potential.

Axions and ALPs

One expects CP violating term in QCD Lagrangian:

$$\mathcal{L}_{\rm QCD} = \frac{1}{4} G_a^{\mu\nu} G_{a\mu\nu} + g\phi\, G_a^{\mu\nu} \tilde{G}_{a\mu\nu} + \text{interactions.}$$

$$Note: F_{\mu\nu}\tilde{F}^{\mu\nu} = \vec{B}\cdot\vec{E} \leftrightarrow G_{\mu\nu}\tilde{G}^{\mu\nu} = \vec{B}_a\cdot\vec{E}_a \text{ which is odd under } T \Rightarrow \text{odd under } CP$$

Peccei-Quinn solution: introduce new field (with MH potential). At $T < f_a$ symmetry broken, and axial mode of field settles at some angle $\theta = a$.

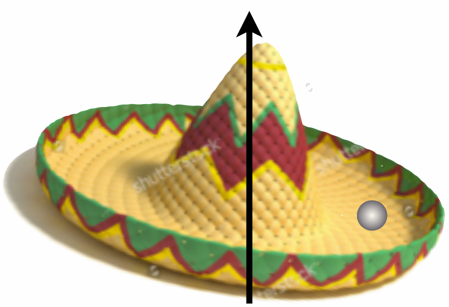

When $T \sim \Lambda_{\rm QCD}$ tilting of hat gives axion field a VEV $\langle a \rangle = 0$ that cancels the CP violating term. The a field oscillates about its VEV with a mass given by the curvature of the potential.

Axions and ALPs

One expects CP violating term in QCD Lagrangian:

$$\mathcal{L}_{\rm QCD} = \frac{1}{4} G_a^{\mu\nu} G_{a\mu\nu} + g\phi\, G_a^{\mu\nu} \tilde{G}_{a\mu\nu} + \text{interactions.}$$

$$Note: F_{\mu\nu}\tilde{F}^{\mu\nu} = \vec{B}\cdot\vec{E} \leftrightarrow G_{\mu\nu}\tilde{G}^{\mu\nu} = \vec{B}_a\cdot\vec{E}_a \text{ which is odd under } T \Rightarrow \text{odd under } CP$$

Peccei-Quinn solution: introduce new field (with MH potential). At $T < f_a$ symmetry broken, and axial mode of field settles at some angle $\theta = a$.

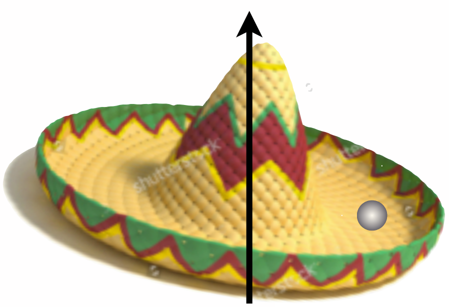

When $T \sim \Lambda_{\rm QCD}$ tilting of hat gives axion field a VEV $\langle a \rangle = 0$ that cancels the CP violating term. The a field oscillates about its VEV with a mass given by the curvature of the potential.

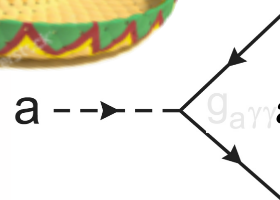

axion coupling to gluons $\Rightarrow$

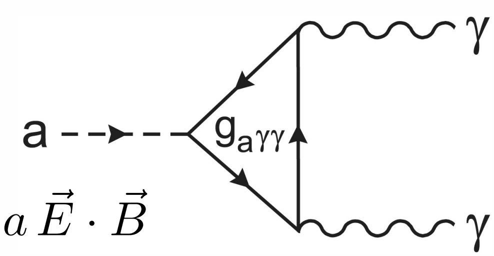

$$\mathcal{L}_{\rm EM} \mathrel{+}= g_{a\gamma\gamma} a F^{\mu\nu}\tilde{F}_{\mu\nu} = g_{a\gamma\gamma} a\, \vec{E}\cdot\vec{B}$$

Axions and ALPs

One expects CP violating term in QCD Lagrangian:

$$\mathcal{L}_{\rm QCD} = \frac{1}{4} G_a^{\mu\nu} G_{a\mu\nu} + g\phi\, G_a^{\mu\nu} \tilde{G}_{a\mu\nu} + \text{interactions.}$$

$Note : F_{\mu\nu}\tilde{F}^{\mu\nu} = \vec{B}\cdot\vec{E} \leftrightarrow G_{\mu\nu}\tilde{G}^{\mu\nu} = \vec{B}_a \cdot \vec{E}_a$ which is odd under $T \Rightarrow$ odd under CP

Peccei-Quinn solution: introduce new field (with MH potential). At $T < f_a$ symmetry broken, and axial mode of field settles at some angle $\theta = a$.

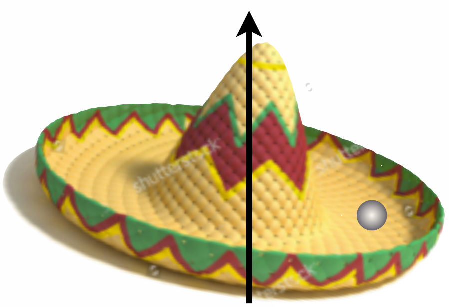

When $T \sim \Lambda_{\rm QCD}$ tilting of hat gives axion field a VEV $\langle a \rangle = 0$ that cancels the CP violating term. The a field oscillates about its VEV with a mass given by the curvature of the potential.

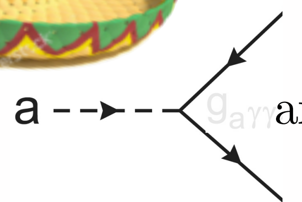

axion coupling to gluons $\Rightarrow$

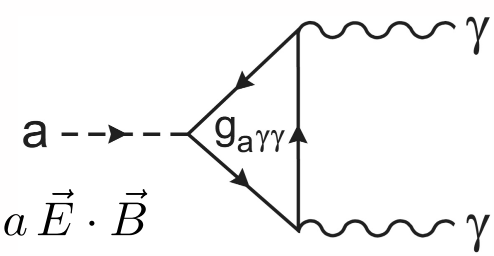

$$\mathcal{L}_{\rm EM} \mathrel{+}= g_{a\gamma\gamma} a F^{\mu\nu}\tilde{F}_{\mu\nu} = g_{a\gamma\gamma} a\, \vec{E}\cdot\vec{B}$$

The single parameter f_a determines axion mass, coupling constant and relic density. Axion-Like Particles (ALPs) are pseudoscalars with similar coupling to photons, but are less constrained/motivated. Axions and ALPs can be detected with Haloscopes like ADMX (via the Primakoff process), cooling curves of stars and compact objects, or light-through-wall experiments.

Axion-Photon Mixing

From the total Lagrangian $\mathcal{L}_{\rm EM} + g_{a\gamma\gamma} a F^{\mu\nu}\tilde{F}_{\mu\nu}$ one can find the equations of motion for the two components of the vector potential A_x and A_y and for the axion field a. Grouping these into a single 3 component wave function, one obtains the Schrödinger like equation:

$$\left(i\frac{d}{dz} + E + \mathcal{M}\right)\Psi(z) = 0 \qquad \Psi(z) = \begin{pmatrix} A_y \\ A_x \\ a \end{pmatrix}$$

$$\mathcal{M} = \begin{pmatrix} \Delta_{\rm pl} & 0 & \Delta_{a\gamma}\sin\psi \\ 0 & \Delta_{\rm pl} & \Delta_{a\gamma}\cos\psi \\ \Delta_{a\gamma}\sin\psi & \Delta_{a\gamma}\cos\psi & \Delta_a \end{pmatrix}$$

Axion-Photon Mixing

From the total Lagrangian $\mathcal{L}_{\rm EM} + g_{a\gamma\gamma} a F^{\mu\nu}\tilde{F}_{\mu\nu}$ one can find the equations of motion for the two components of the vector potential A_x and A_y and for the axion field a. Grouping these into a single 3 component wave function, one obtains the Schrödinger like equation:

$$\left(i\frac{d}{dz} + E + \mathcal{M}\right)\Psi(z) = 0 \qquad \Psi(z) = \begin{pmatrix} A_y \\ A_x \\ a \end{pmatrix}$$

$$\mathcal{M} = \begin{pmatrix} \Delta_{\rm pl} & 0 & \Delta_{a\gamma}\sin\psi \\ 0 & \Delta_{\rm pl} & \Delta_{a\gamma}\cos\psi \\ \Delta_{a\gamma}\sin\psi & \Delta_{a\gamma}\cos\psi & \Delta_a \end{pmatrix}$$

$$\Delta_{\rm pl} = -\omega_{\rm pl}^2/(2E_\gamma) \qquad \Delta_a = -m_a^2/(2E_\gamma) \qquad \Delta_{a\gamma} = B\, g_{a\gamma\gamma}/2$$

Axion-Photon Mixing

From the total Lagrangian $\mathcal{L}_{\rm EM} + g_{a\gamma\gamma} a F^{\mu\nu}\tilde{F}_{\mu\nu}$ one can find the equations of motion for the two components of the vector potential A_x and A_y and for the axion field a. Grouping these into a single 3 component wave function, one obtains the Schrödinger like equation:

$$\left(i\frac{d}{dz} + E + \mathcal{M}\right)\Psi(z) = 0 \qquad \Psi(z) = \begin{pmatrix} A_y \\ A_x \\ a \end{pmatrix}$$

$$\mathcal{M} = \begin{pmatrix} \Delta_{\rm pl} & 0 & \Delta_{a\gamma}\sin\psi \\ 0 & \Delta_{\rm pl} & \Delta_{a\gamma}\cos\psi \\ \Delta_{a\gamma}\sin\psi & \Delta_{a\gamma}\cos\psi & \Delta_a \end{pmatrix}$$

$$\Delta_{\rm pl} = -\omega_{\rm pl}^2/(2E_\gamma) \qquad \Delta_a = -m_a^2/(2E_\gamma) \qquad \Delta_{a\gamma} = B\, g_{a\gamma\gamma}/2$$

$$\Delta_{\rm osc} \equiv \sqrt{(\Delta_{\rm pl} - \Delta_a)^2 + 4\Delta_{a\gamma}^2}$$

Axion-Photon Mixing

From the total Lagrangian $\mathcal{L}_{\rm EM} + g_{a\gamma\gamma} a F^{\mu\nu}\tilde{F}_{\mu\nu}$ one can find the equations of motion for the two components of the vector potential A_x and A_y and for the axion field a. Grouping these into a single 3 component wave function, one obtains the Schrödinger like equation:

$$\left(i\frac{d}{dz} + E + \mathcal{M}\right)\Psi(z) = 0 \qquad\qquad \Psi(z) = \begin{pmatrix} A_y \\ A_x \\ a \end{pmatrix}$$

$$\mathcal{M} = \begin{pmatrix} \Delta_{\rm pl} & 0 & \Delta_{a\gamma}\sin\psi \\ 0 & \Delta_{\rm pl} & \Delta_{a\gamma}\cos\psi \\ \Delta_{a\gamma}\sin\psi & \Delta_{a\gamma}\cos\psi & \Delta_a \end{pmatrix}$$

$$\Delta_{\rm pl} = -\omega_{\rm pl}^2/(2E_\gamma) \qquad \Delta_a = -m_a^2/(2E_\gamma) \qquad \Delta_{a\gamma} = B\, g_{a\gamma\gamma}/2$$

$$\Delta_{\rm osc} \equiv \sqrt{(\Delta_{\rm pl} - \Delta_a)^2 + 4\Delta_{a\gamma}^2}$$

$$P_{a\gamma}(z=\ell) = \sin^2 2\theta \sin^2\left(\frac{\Delta_{\rm osc}\ell}{2}\right) \qquad \text{where } \tan 2\theta = 2\Delta_{a\gamma}/(\Delta_{\rm pl} - \Delta_a)$$

Looks like neutrino oscillation where $\Delta m^2 = |\omega_{\rm pl}^2 - m_a^2|$. But unlike neutrino oscillations, θ depends on E_γ and there can be absorption due to $\gamma\gamma \rightarrow e^+e^-$

ALP Photon Mixing

$$P_{\alpha\gamma}(\ell) = \frac{1}{1+(E_{\rm crit}/E_\gamma)^2}\sin^2\left[\frac{B\,\ell\,g_{a\gamma\gamma}}{2}\sqrt{1+\left(\frac{E_{\rm crit}}{E_\gamma}\right)^2}\right] \qquad E_{\rm crit}({\rm GeV}) \equiv \frac{5}{2}\frac{\Delta m^2_{\mu{\rm eV}}}{B_{\rm G}\left(\frac{g_{a\gamma\gamma}}{10^{-11}\,{\rm GeV}^{-1}}\right)}$$

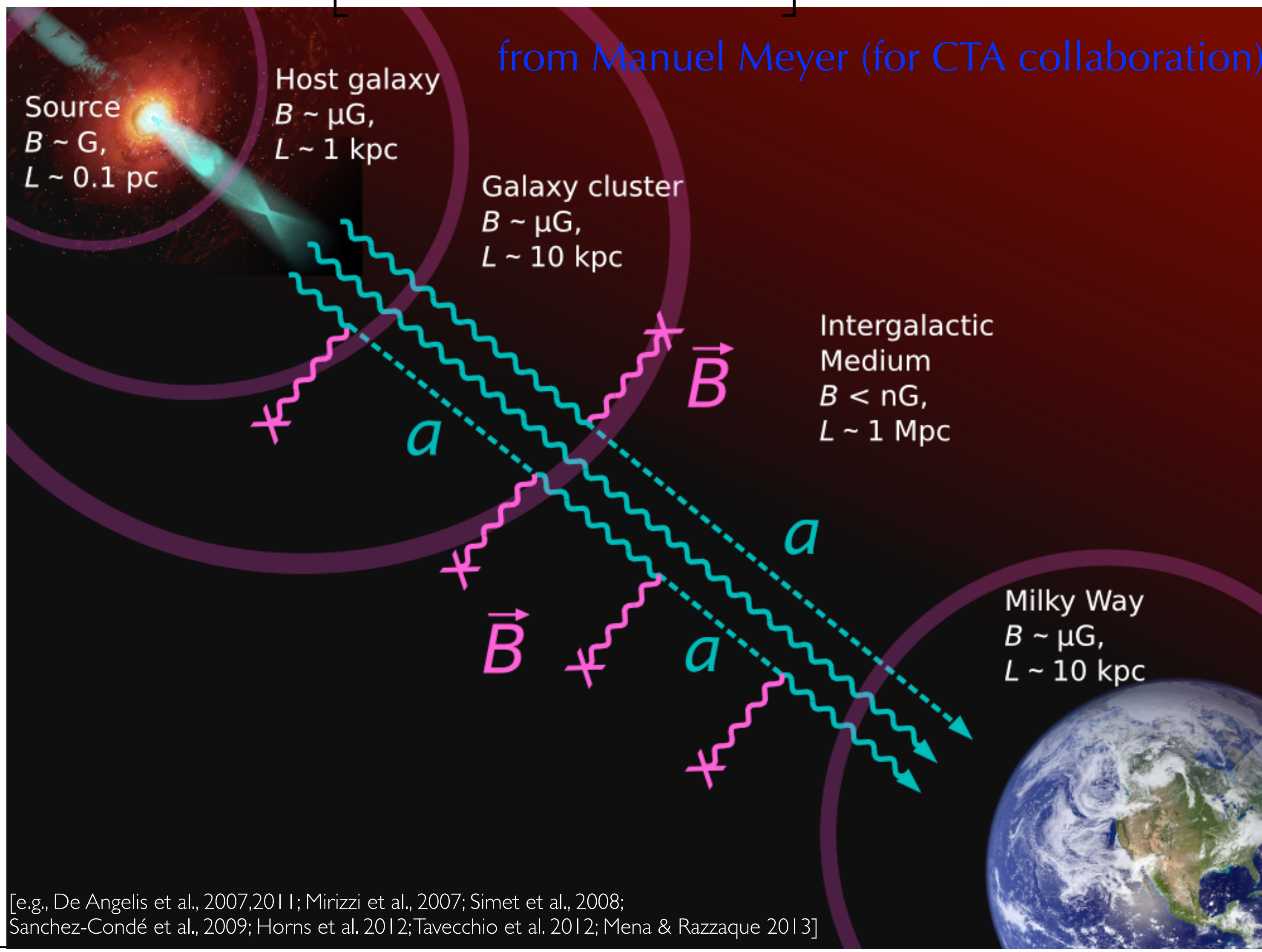

Anomalous Transparency?

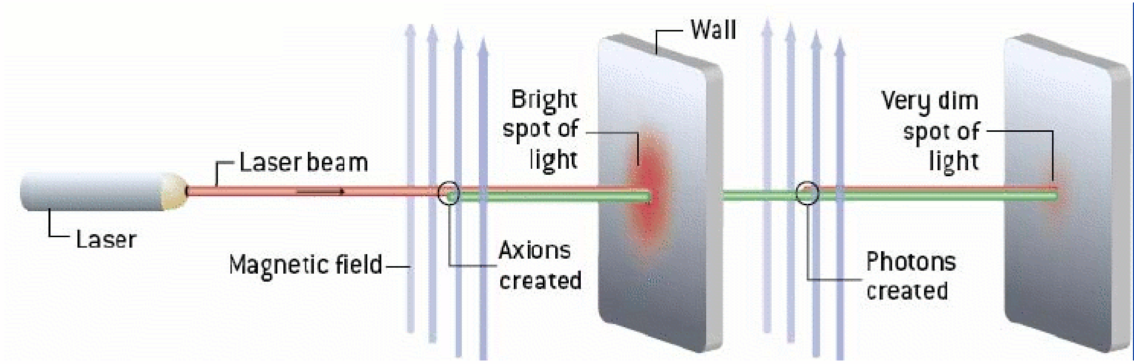

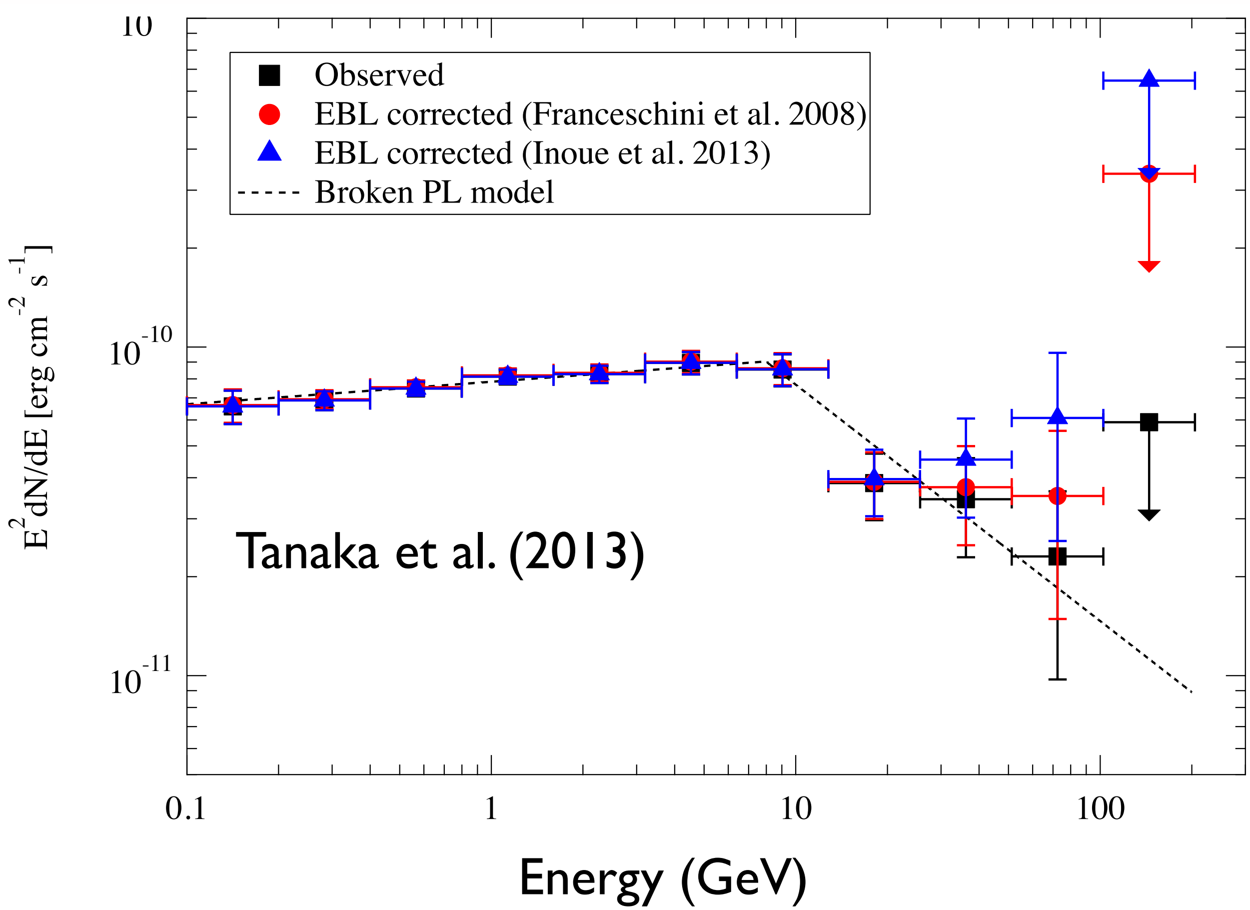

Experimental Limits on Axion DM

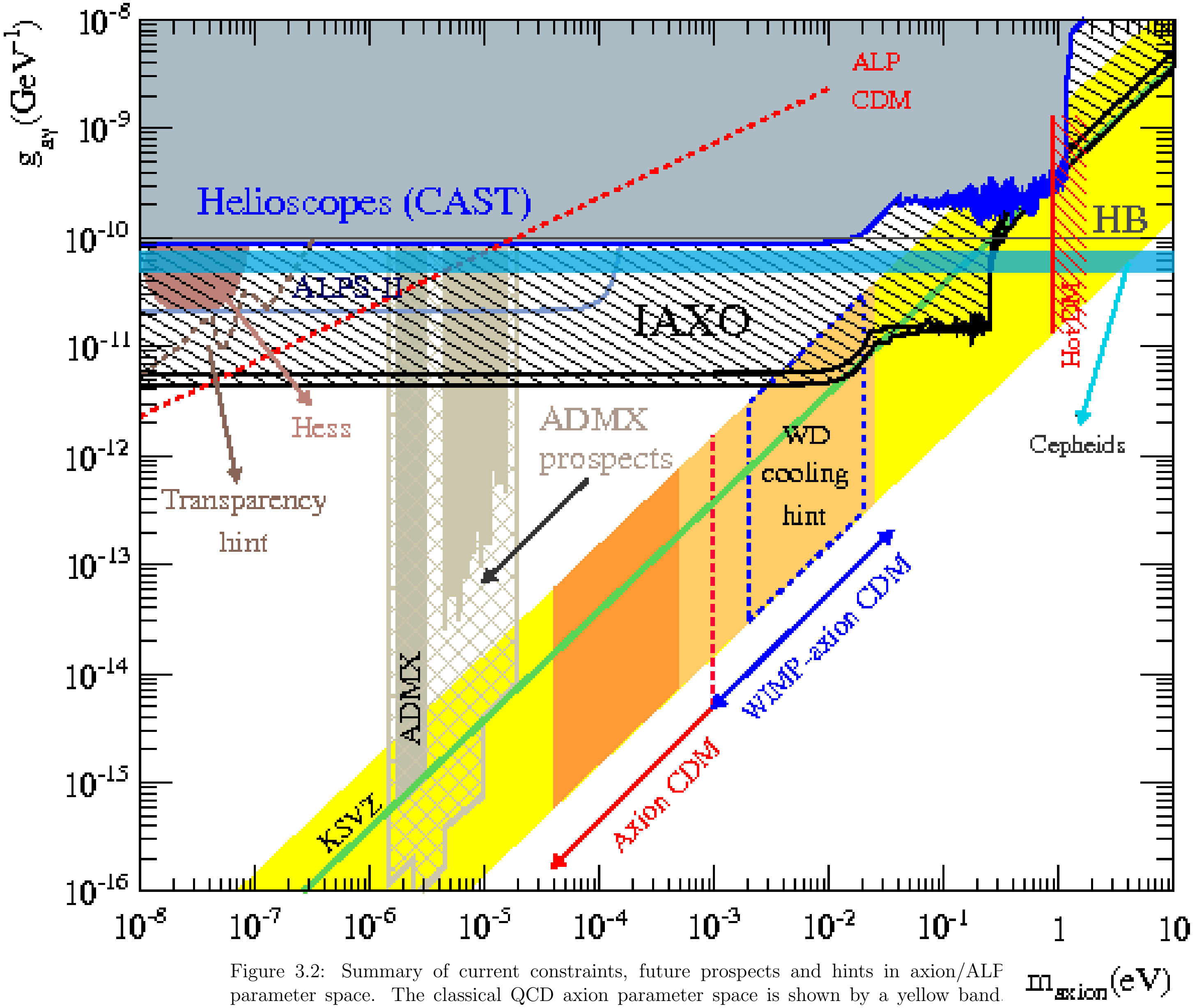

Figure 3.2: Summary of current constraints, future prospects and hints in axion/ALP parameter space. The classical QCD axion parameter space is shown by a yellow band. Axionic dark matter parameter space is shown by orange bands. In the region labeled "WIMP-axion CDM" axions would only comprise a fraction of the dark matter energy density. Prospects for IAXO and ADMX are shown by hatched regions. Figure taken from Carosi et al. (2013).

Looking Under the Lamp Post

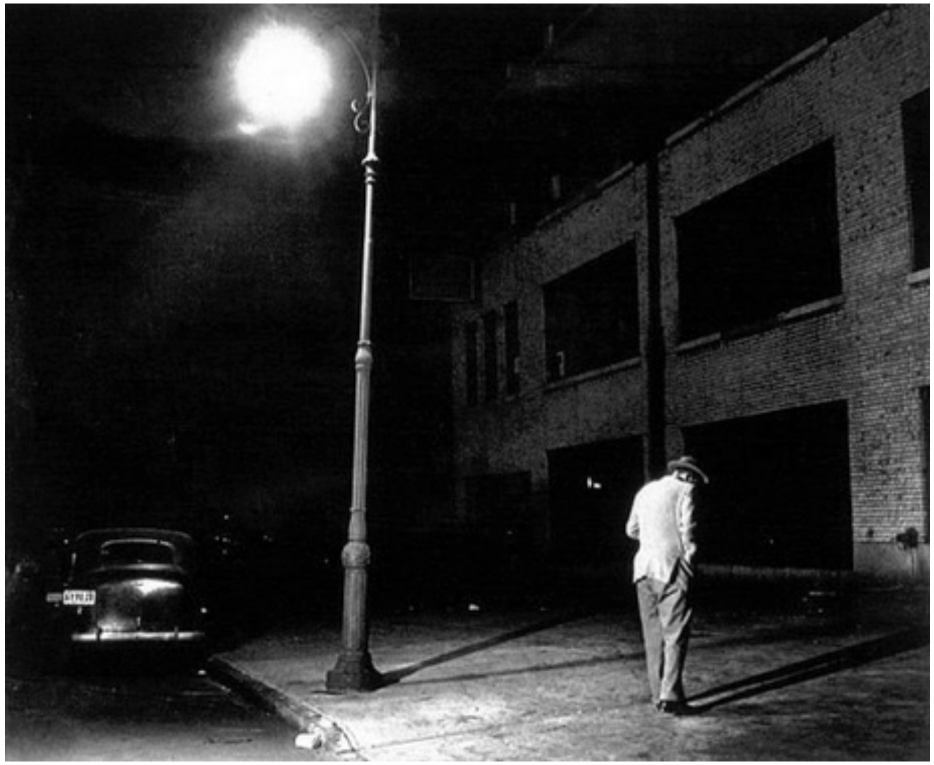

Looking Under the Lamp Post

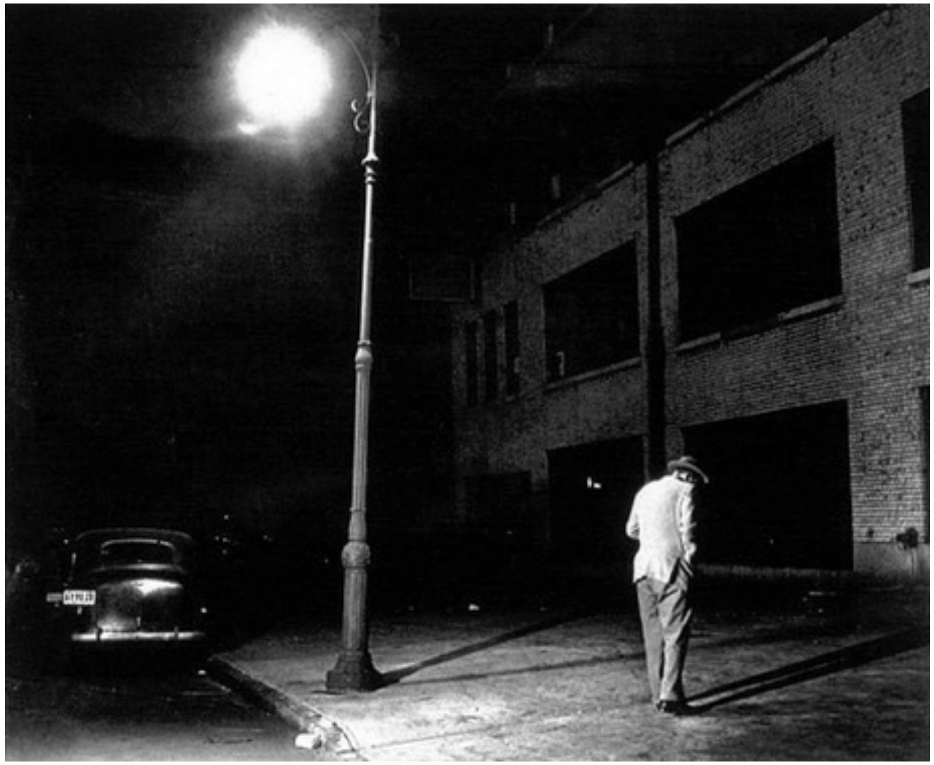

- I've heard some theorists accuse experimentalists of lacking imagination by only looking for WIMP/SUSY DM is like ``only looking for your lost keys under the lamp post''.

Looking Under the Lamp Post

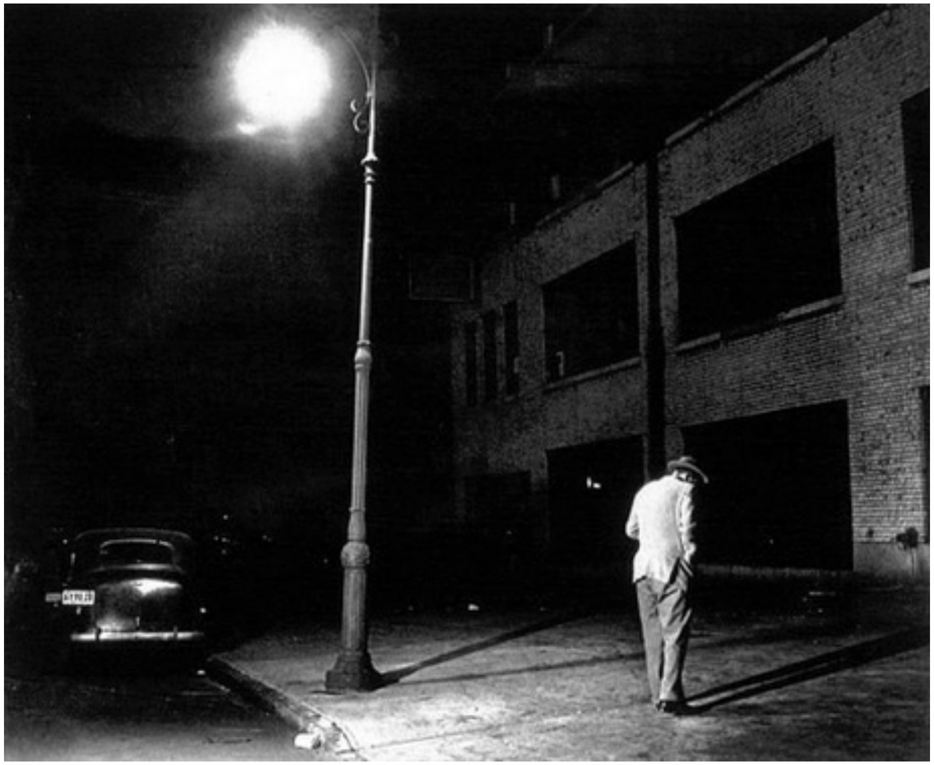

- I've heard some theorists accuse experimentalists of lacking imagination by only looking for WIMP/SUSY DM is like ``only looking for your lost keys under the lamp post''.
- Theorem: If you don't look under the lamp post where there is light, it is really hard to see anything!

Looking Under the Lamp Post

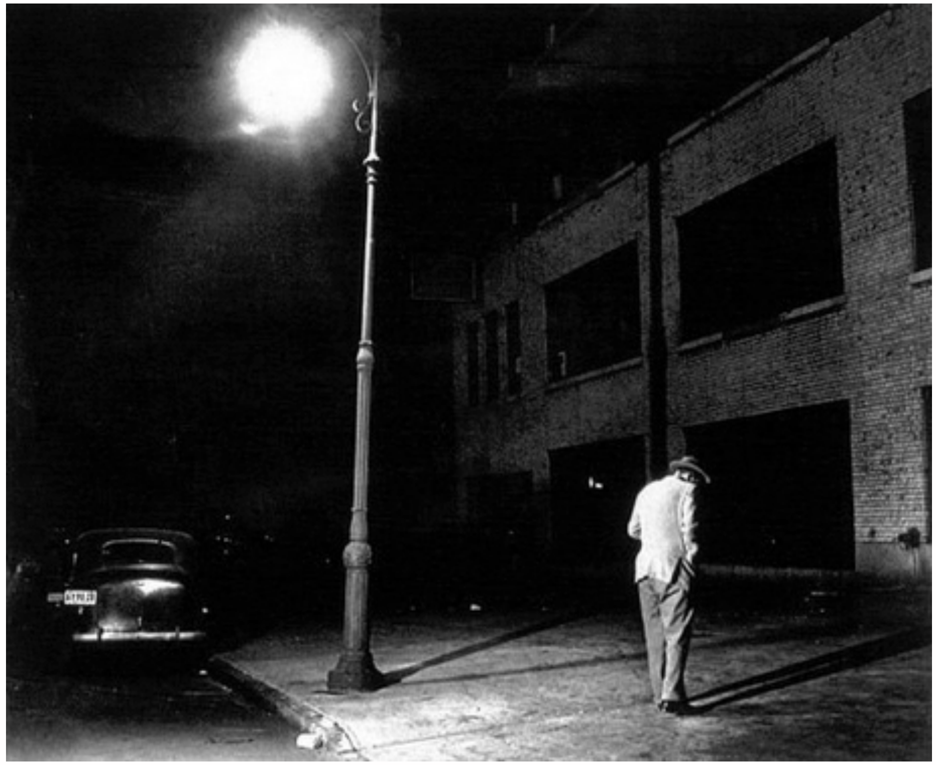

- I've heard some theorists accuse experimentalists of lacking imagination by only looking for WIMP/SUSY DM is like ``only looking for your lost keys under the lamp post''.
- Theorem: If you don't look under the lamp post where there is light, it is really hard to see anything!
  - Corollary: ``Outside of a dog a book is a man's best friend. Inside a dog it is too dark to read'' (G. Marx).

Conclusions

Conclusions

- Observations of the GC region by current generation of ACTs reveal bright GeV - TeV emission from a number of sources, including steady emission from the GC. Even with these astrophysical backgrounds, ACTs can provide powerful constraints on DM up to tens of TeV reaching within an order of magnitude of the natural cross section.

Conclusions

- **Observations of the GC region by current generation of ACTs reveal bright GeV - TeV emission from a number of sources, including steady emission from the GC. Even with these astrophysical backgrounds, ACTs can provide powerful constraints on DM up to tens of TeV reaching within an order of magnitude of the natural cross section.**

- **CTA observations of the GC could exclude much of the remaining parameter space for high mass WIMPs.**

Conclusions

- Observations of the GC region by current generation of ACTs reveal bright GeV - TeV emission from a number of sources, including steady emission from the GC. Even with these astrophysical backgrounds, ACTs can provide powerful constraints on DM up to tens of TeV reaching within an order of magnitude of the natural cross section.

- CTA observations of the GC could exclude much of the remaining parameter space for high mass WIMPs.

- Even if VERITAS, HESS, MAGIC and even CTA fail to detect dark matter, they will reveal new information about phenomena ranging from relativistic jets from supermassive black holes, a census of supernovae across the galaxy, the origin of cosmic rays, the nature of pulsar magnetospheres, the history of star formation imprinted on the primordial starlight, constraints on the primordial magnetic field, and multimessenger science through searches for electromagnetic counterparts of gravitational wave and neutrino sources - not a bad consolation prize.


III. Backup Slides

The Future

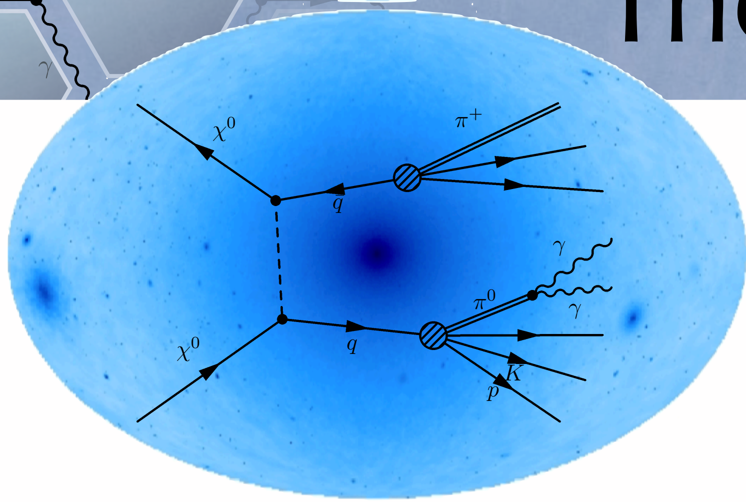

The WIMP miracle is the only reason we are looking, or know where to look. Only way to design an instrument is by starting with a hypothesis.

The Future

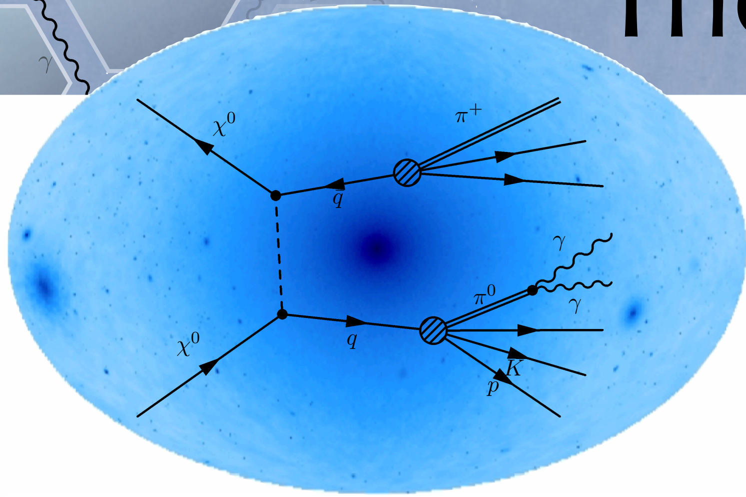

The WIMP miracle is the only reason we are looking, or know where to look. Only way to design an instrument is by starting with a hypothesis.

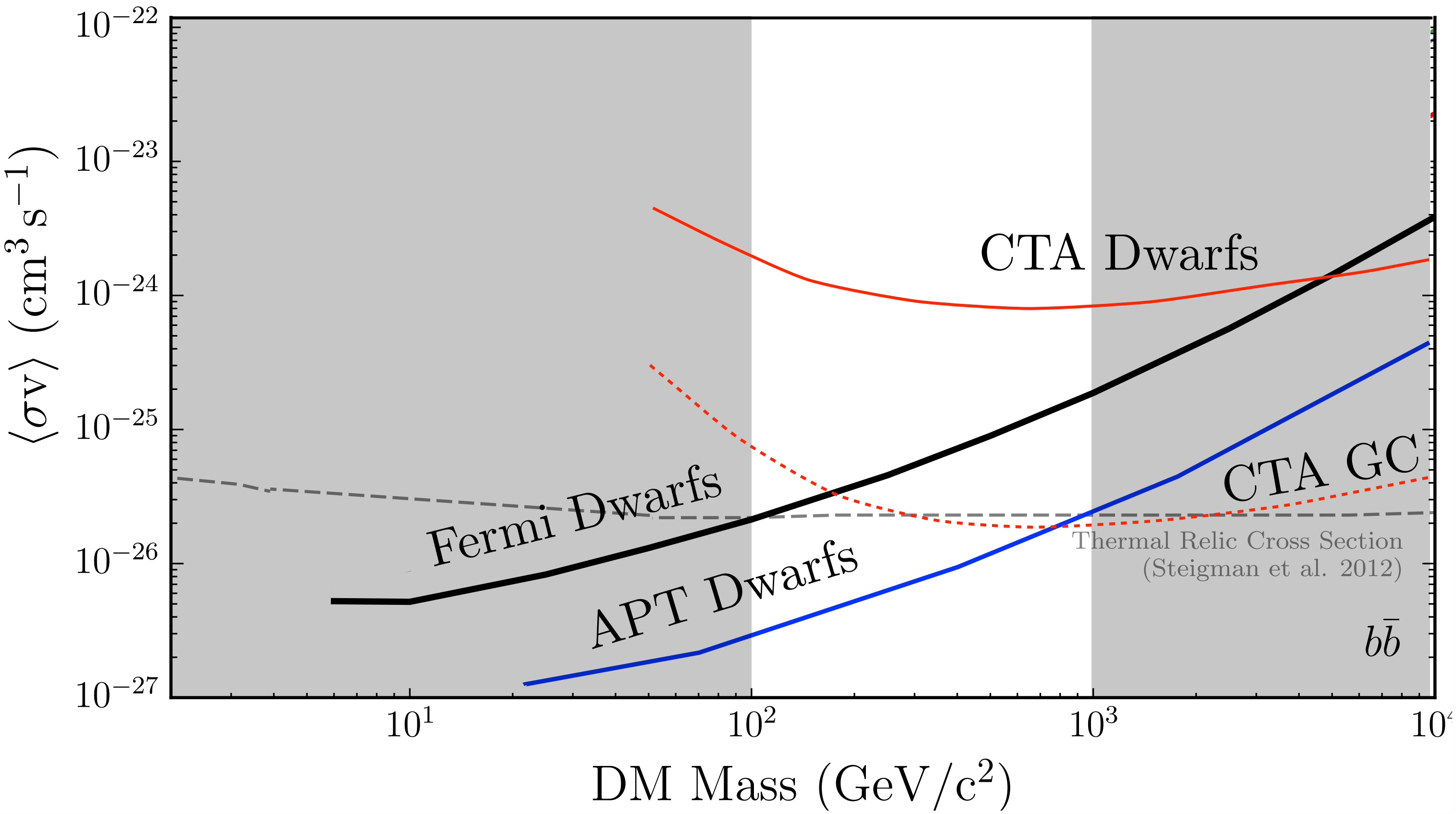

The Future

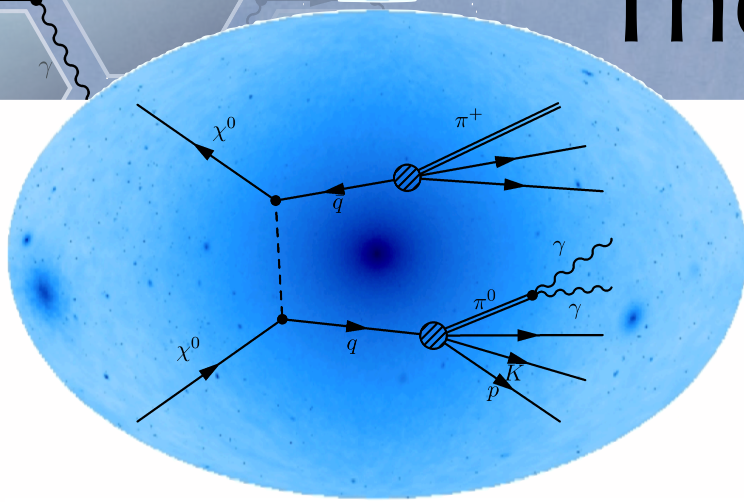

The WIMP miracle is the only reason we are looking, or know where to look. Only way to design an instrument is by starting with a hypothesis.

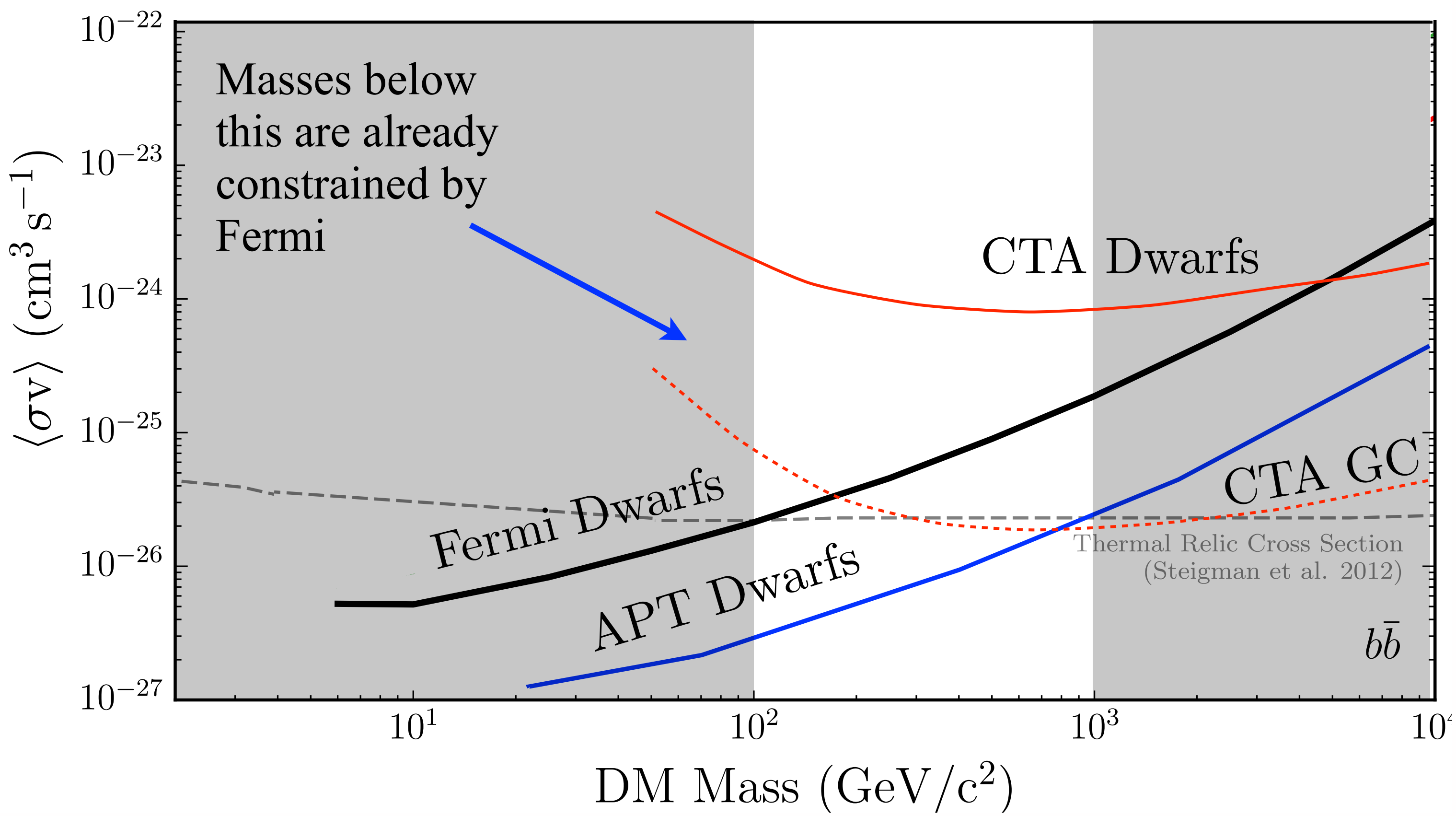

The Future

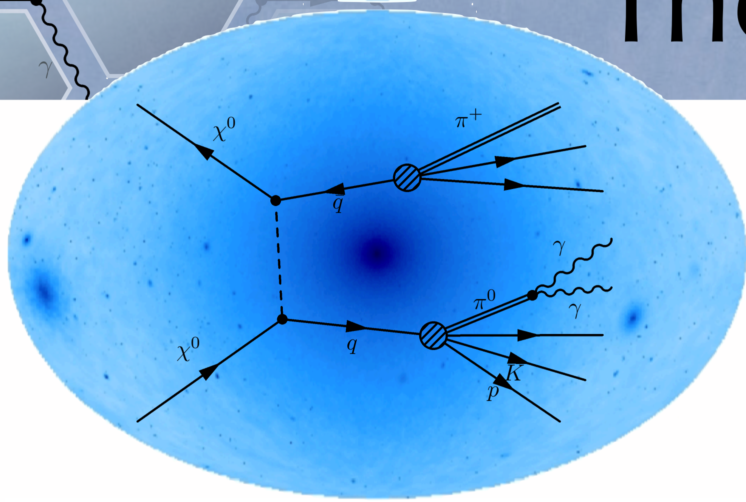

The WIMP miracle is the only reason we are looking, or know where to look. Only way to design an instrument is by starting with a hypothesis.

Masses above the natural range motivated by hierarchy problem - reason for SUSY, or exceed unitarity bound

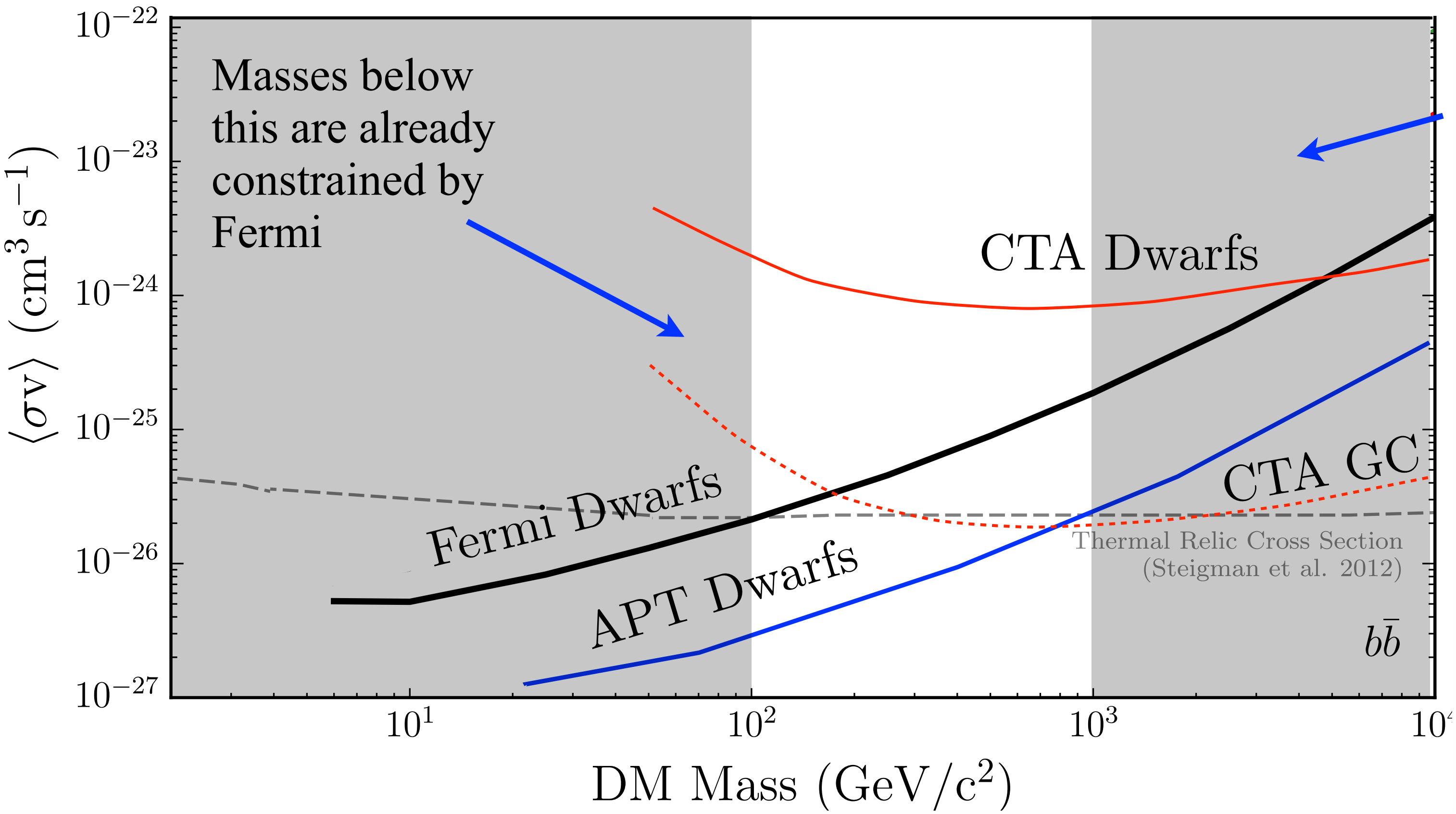

The Future

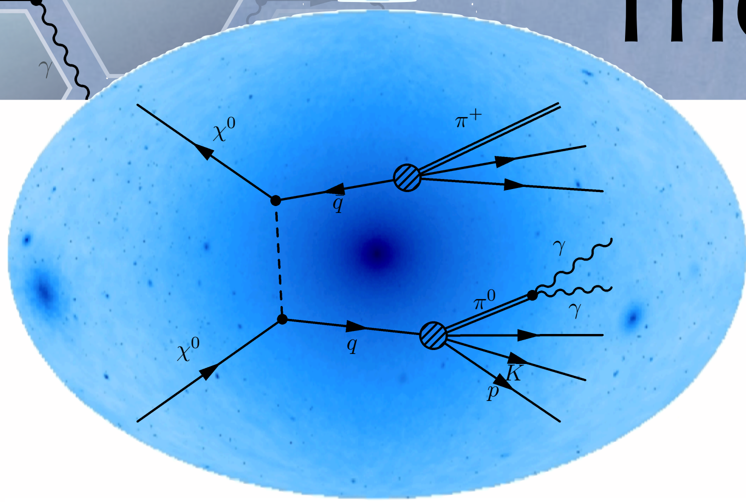

The WIMP miracle is the only reason we are looking, or know where to look. Only way to design an instrument is by starting with a hypothesis.

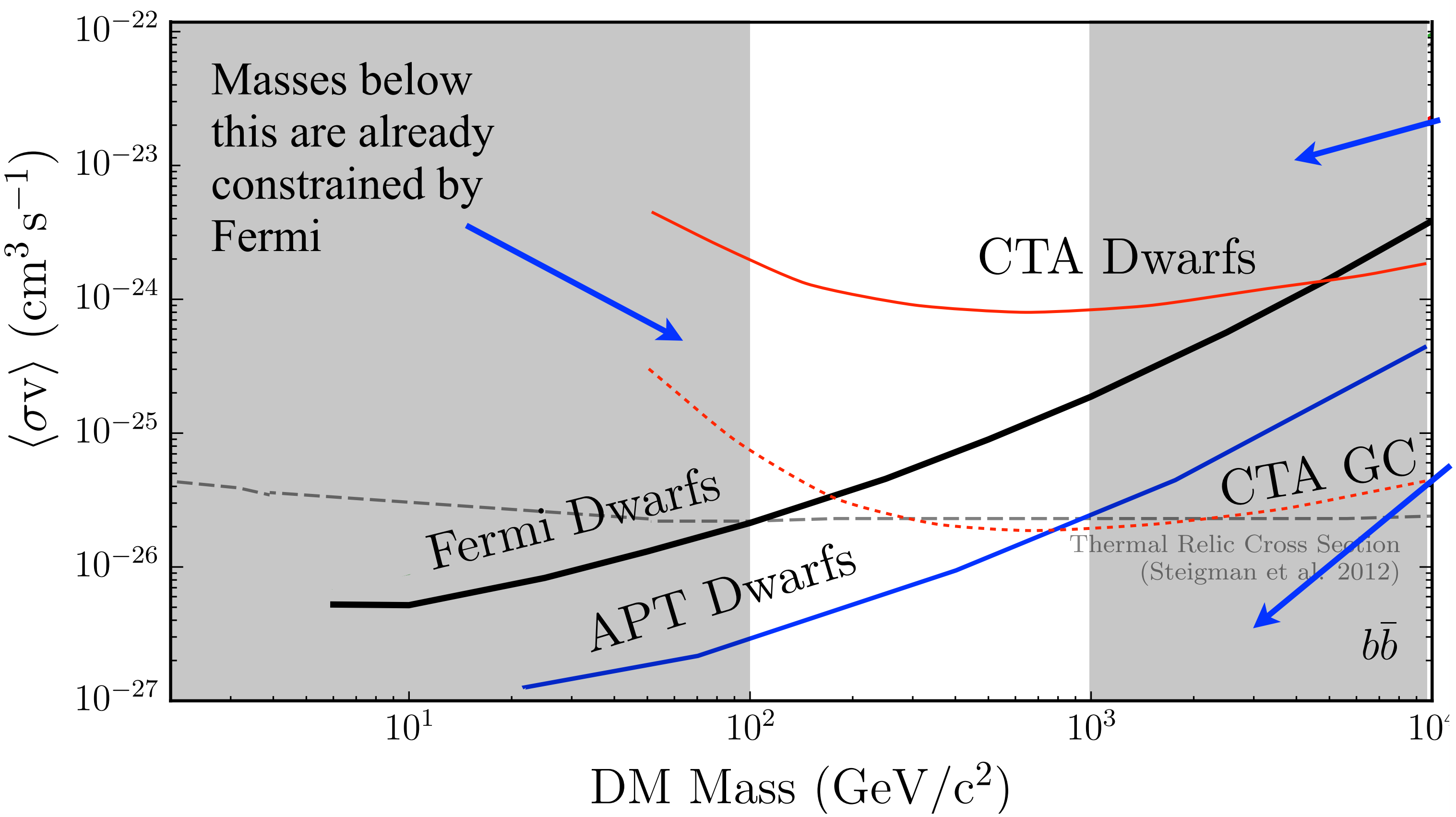

Masses above the natural range motivated by hierarchy problem - reason for SUSY, or exceed unitarity bound

Ground-based observations (CTA) of GC are better in this regime

Advanced Particle-astrophysics Telescope (APT)

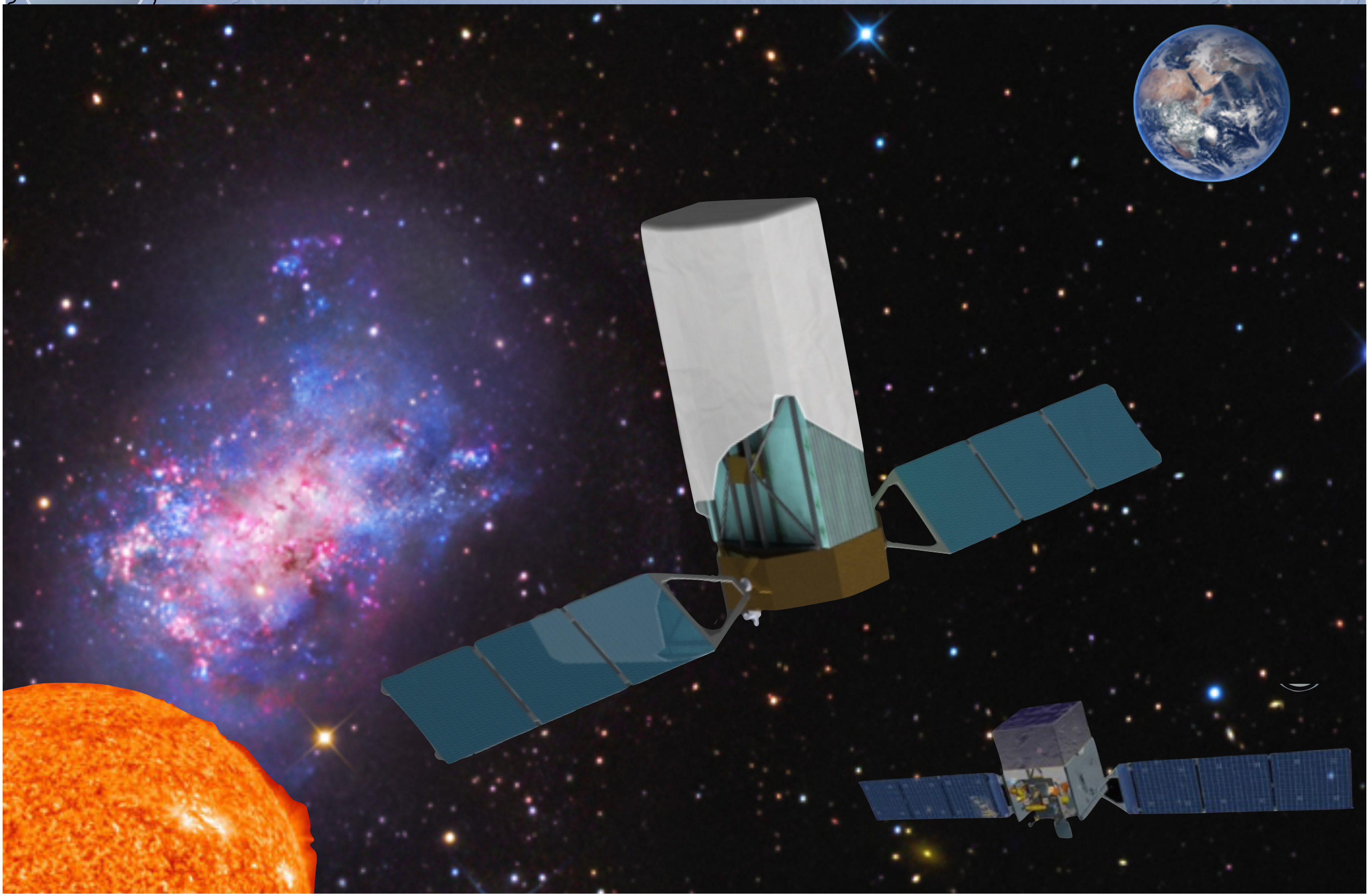

Advanced Particle-astrophysics Telescope (APT)

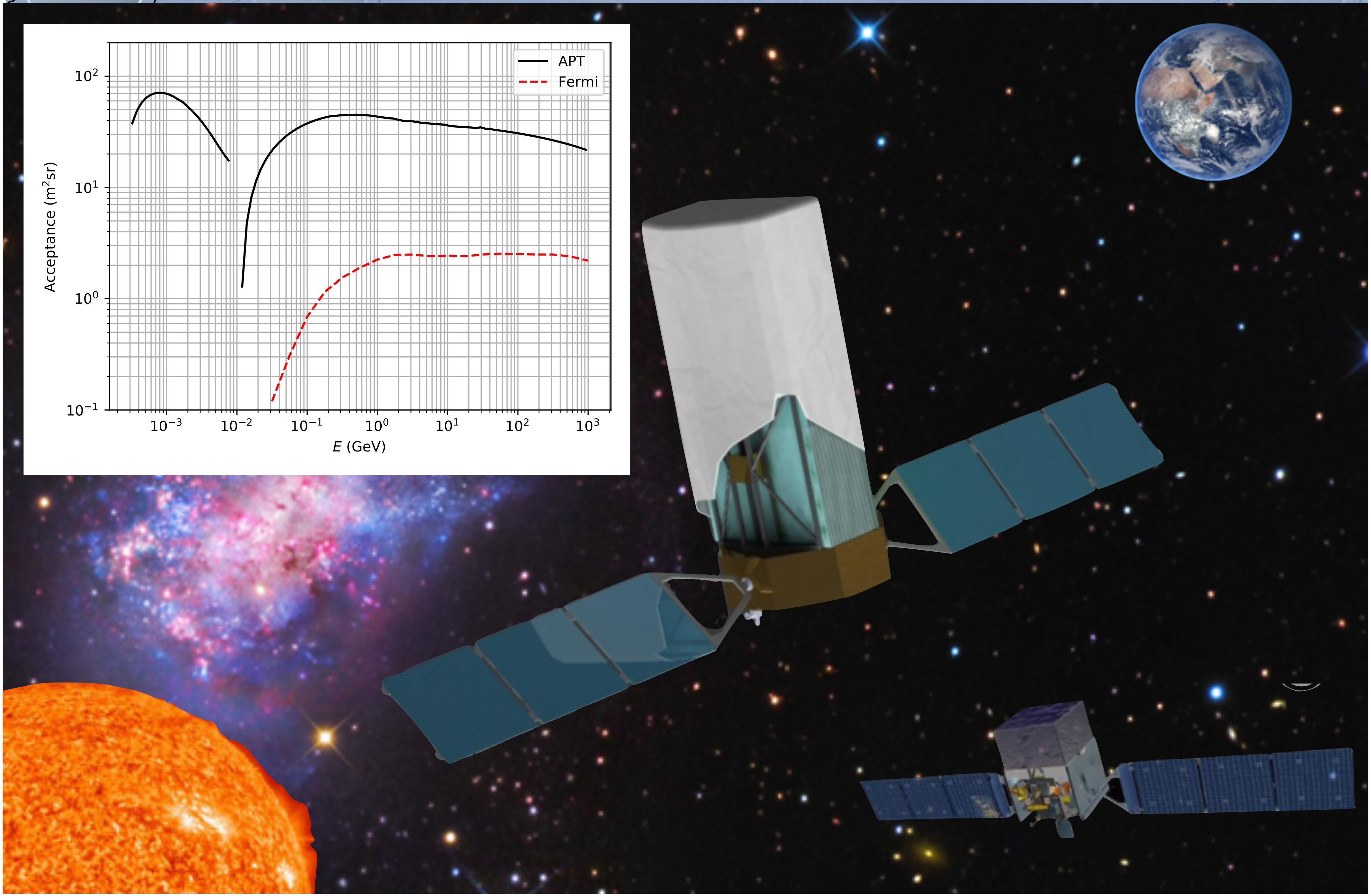

APT Instrument

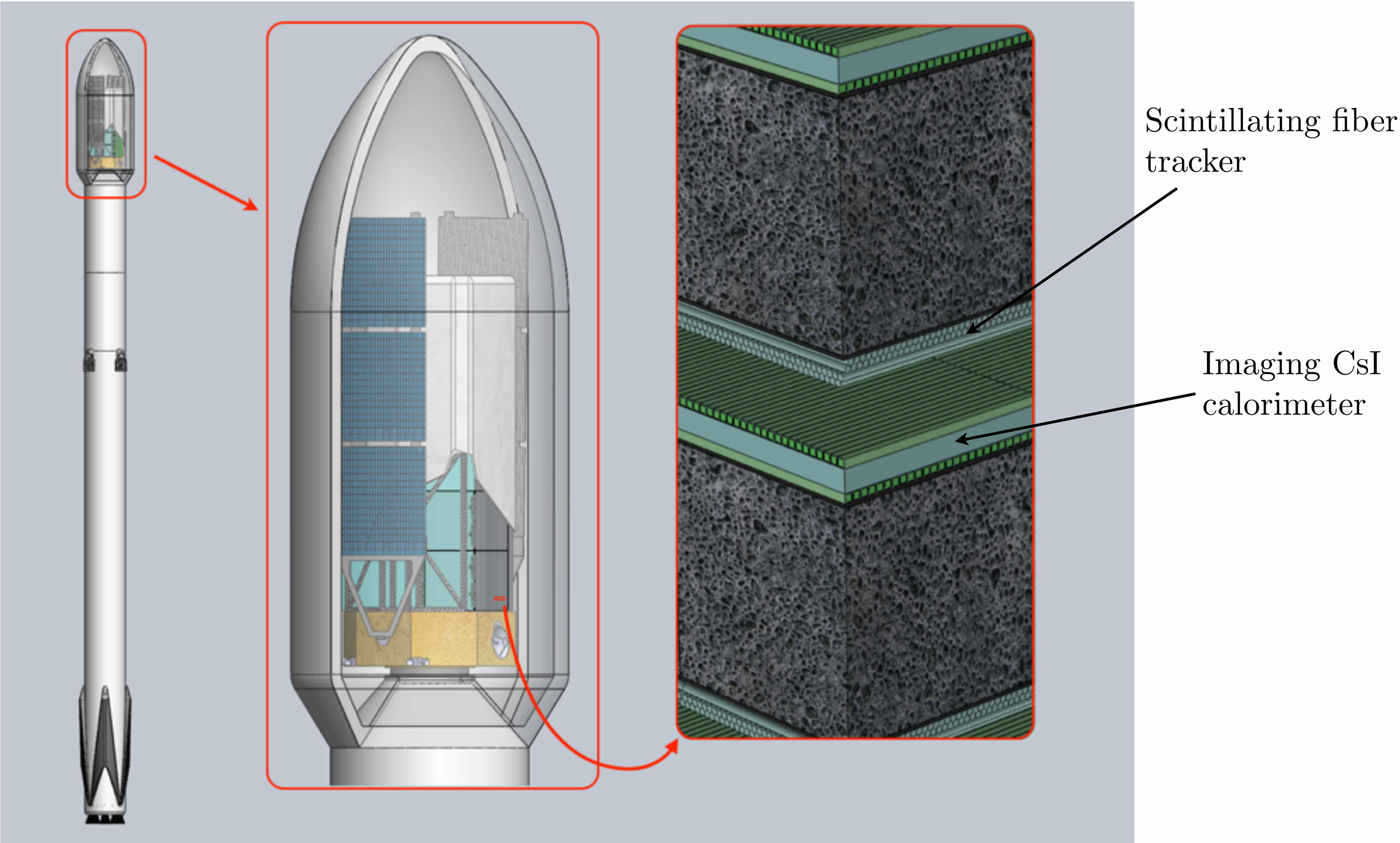

Gamma-Ray Transients with APT

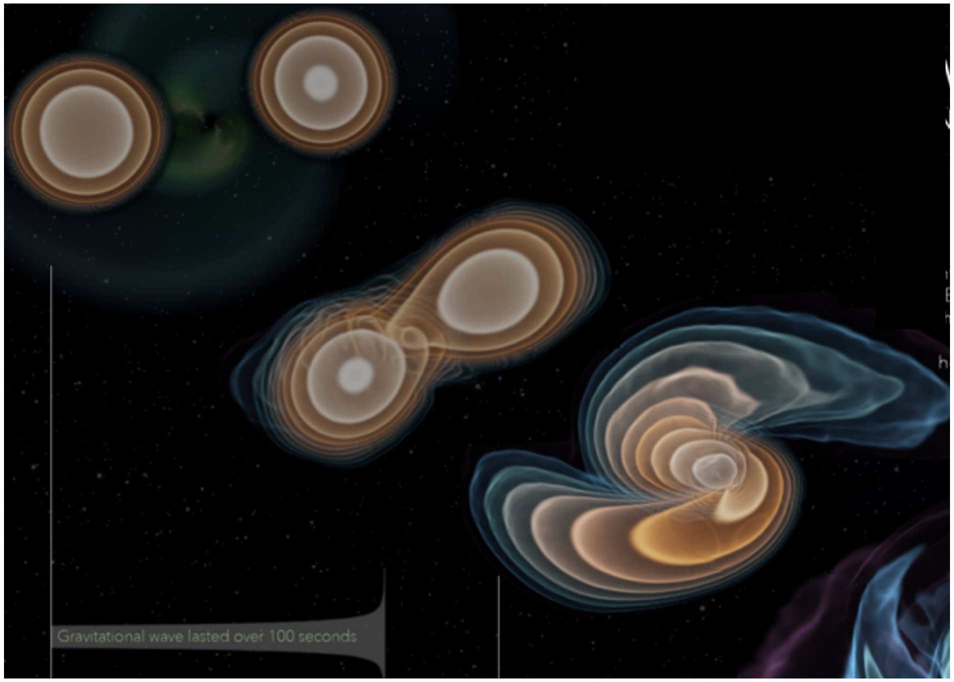

- Large area, almost all-sky coverage for MeV gamma-rays threshold could provide the best instrument for localizing astrophysical transients out to the edge of the visible universe.
  - Short gamma-ray bursts
  - NS merger gravitational wave sources

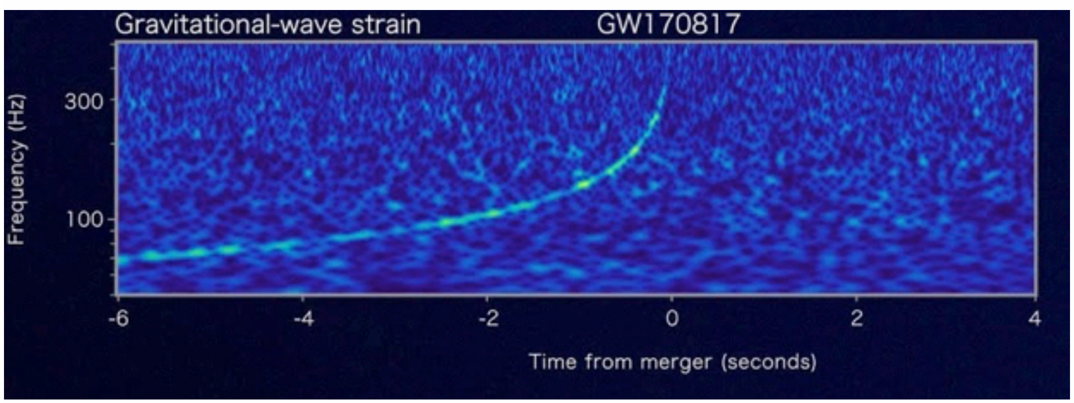

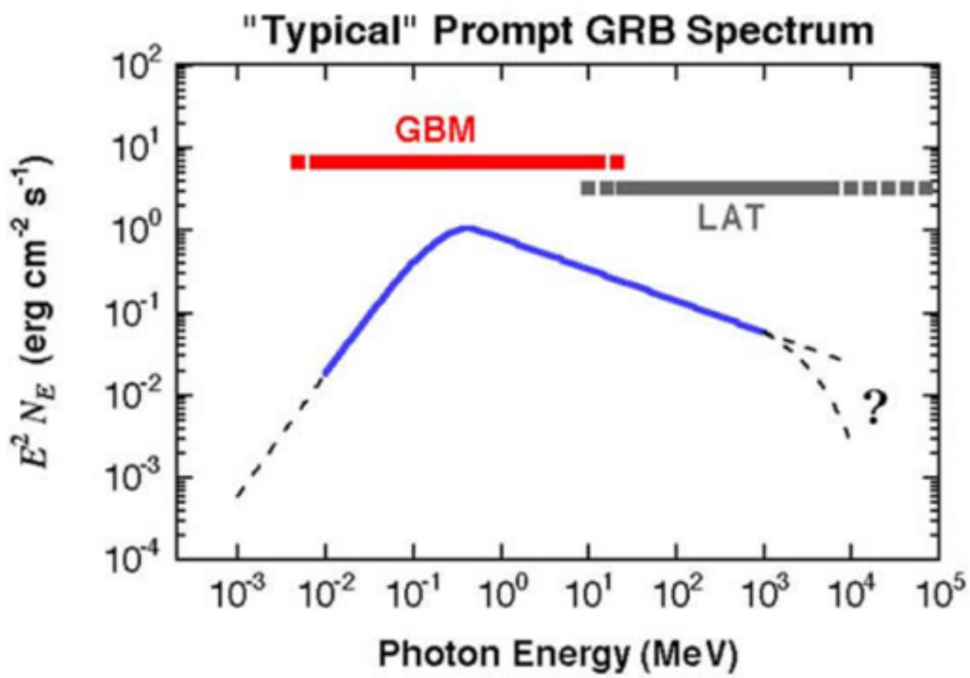

Gamma-Ray Transients with APT

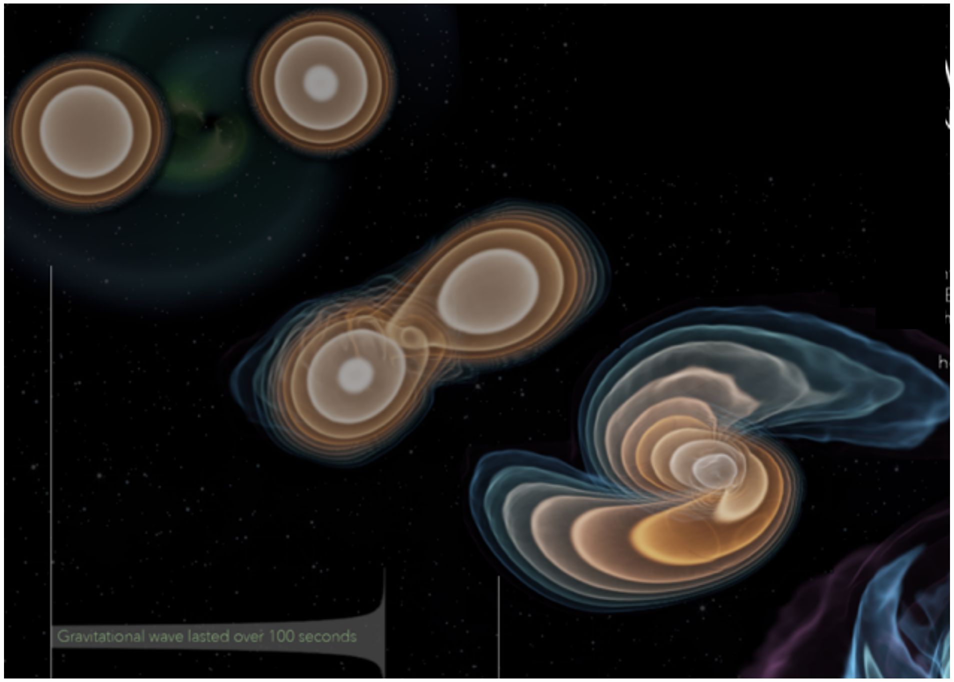

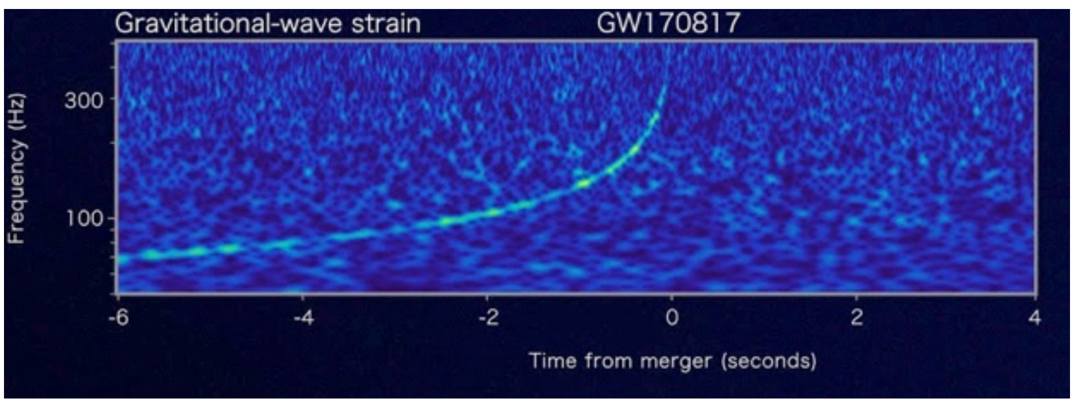

- Large area, almost all-sky coverage for MeV gamma-rays threshold could provide the best instrument for localizing astrophysical transients out to the edge of the visible universe.
  - Short gamma-ray bursts
  - NS merger gravitational wave sources

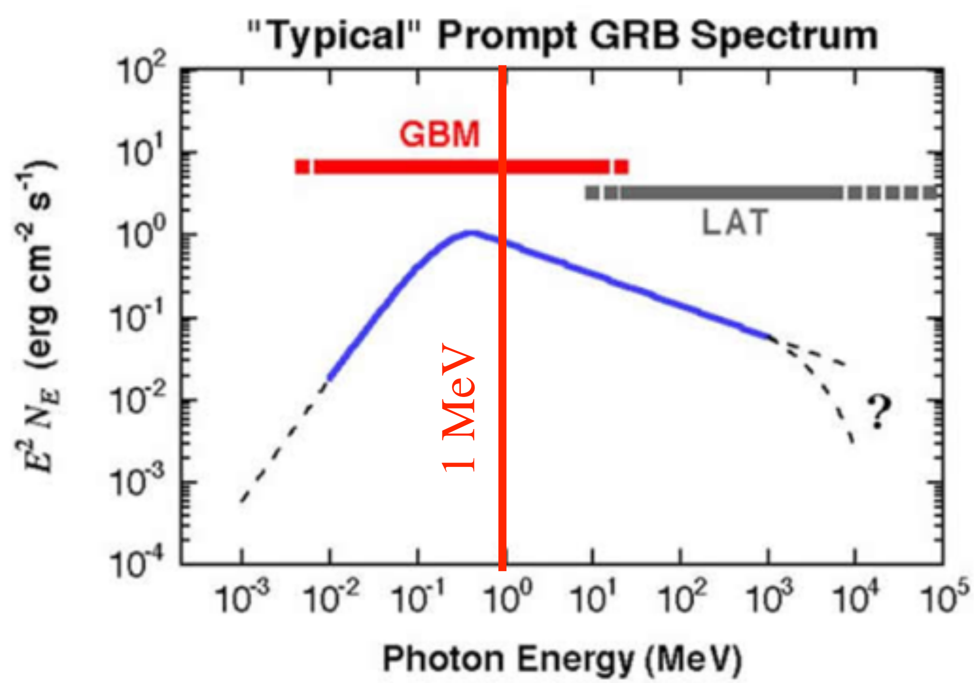

Pair Telescope Mode

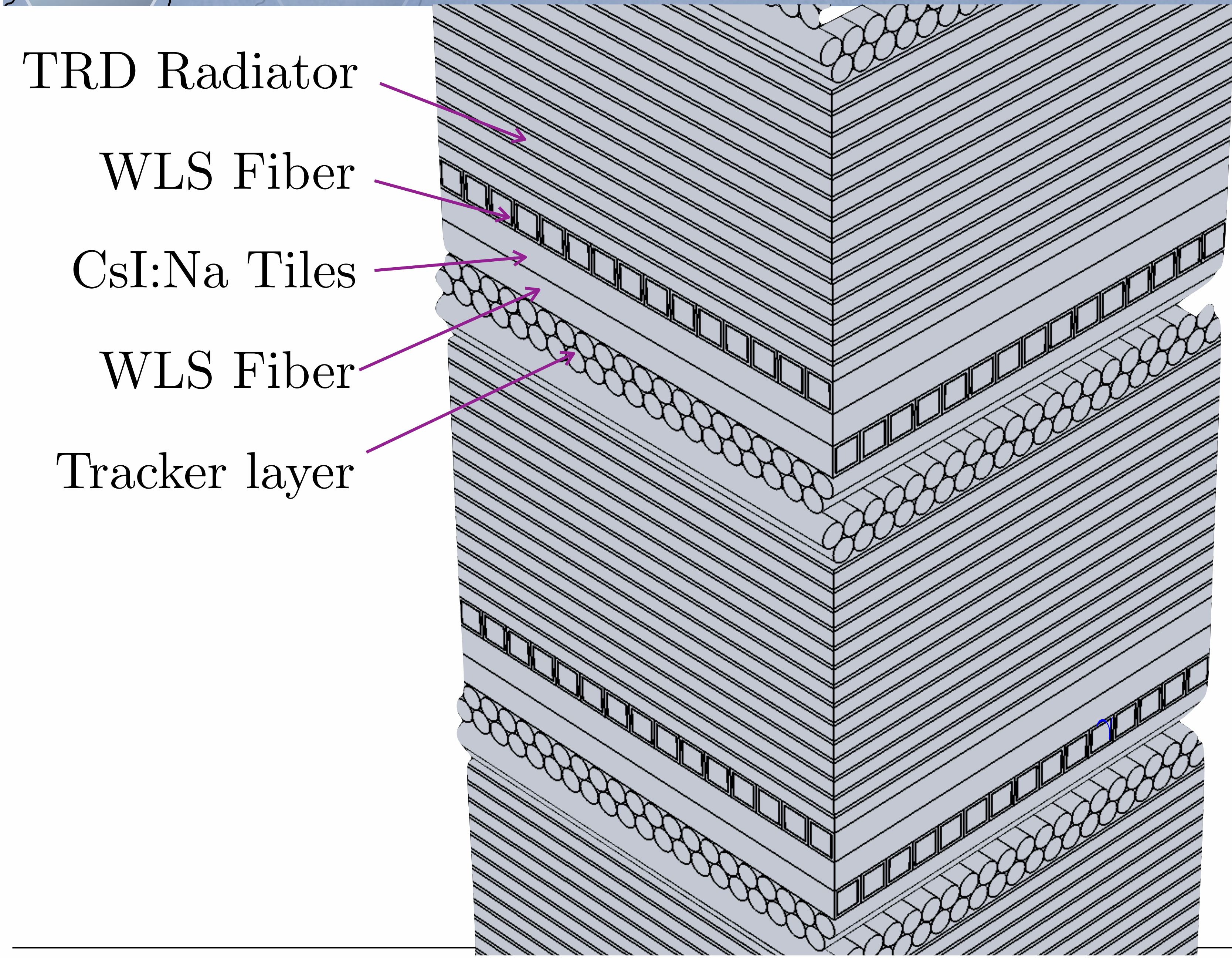

Pair Telescope Mode

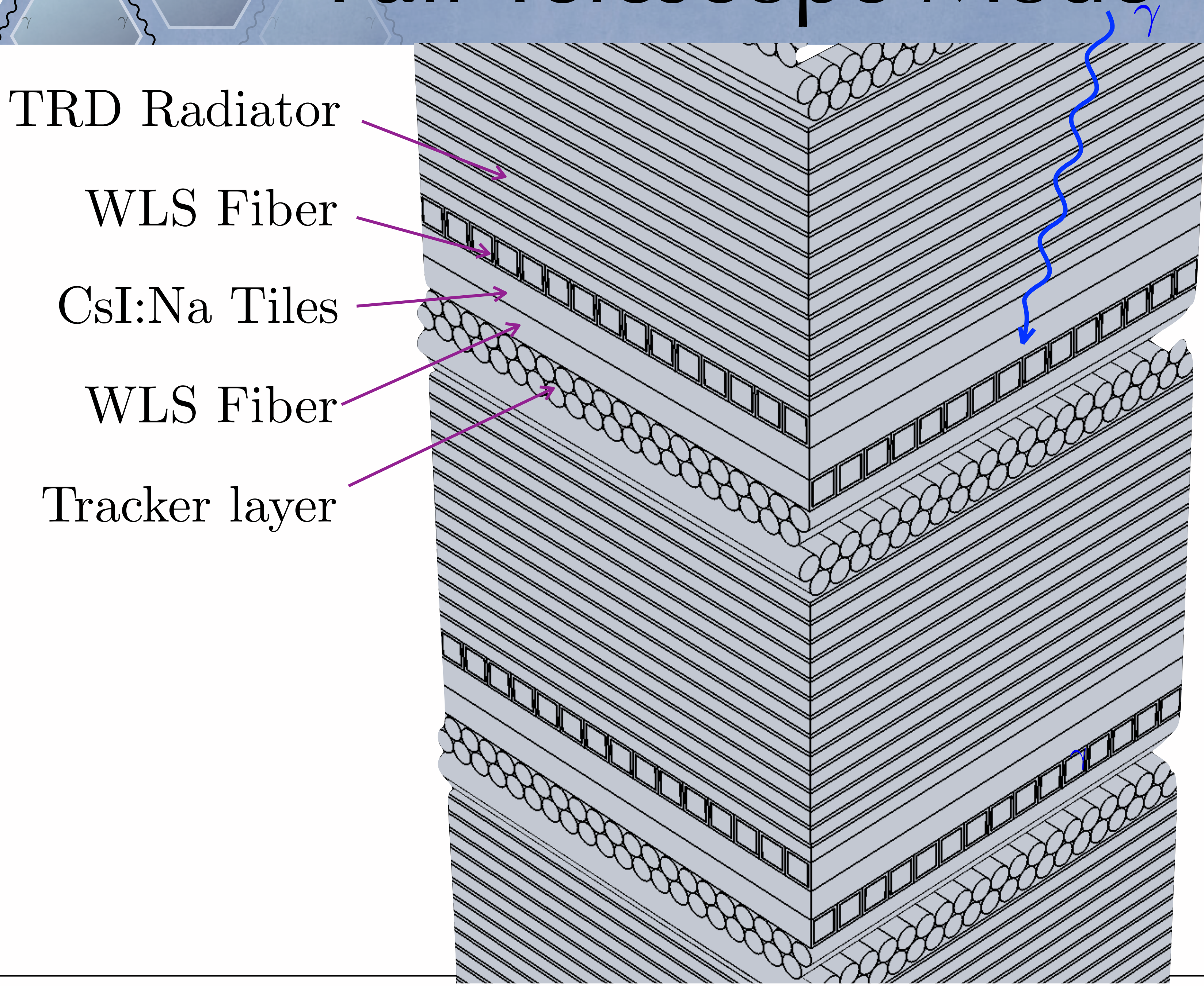

Pair Telescope Mode

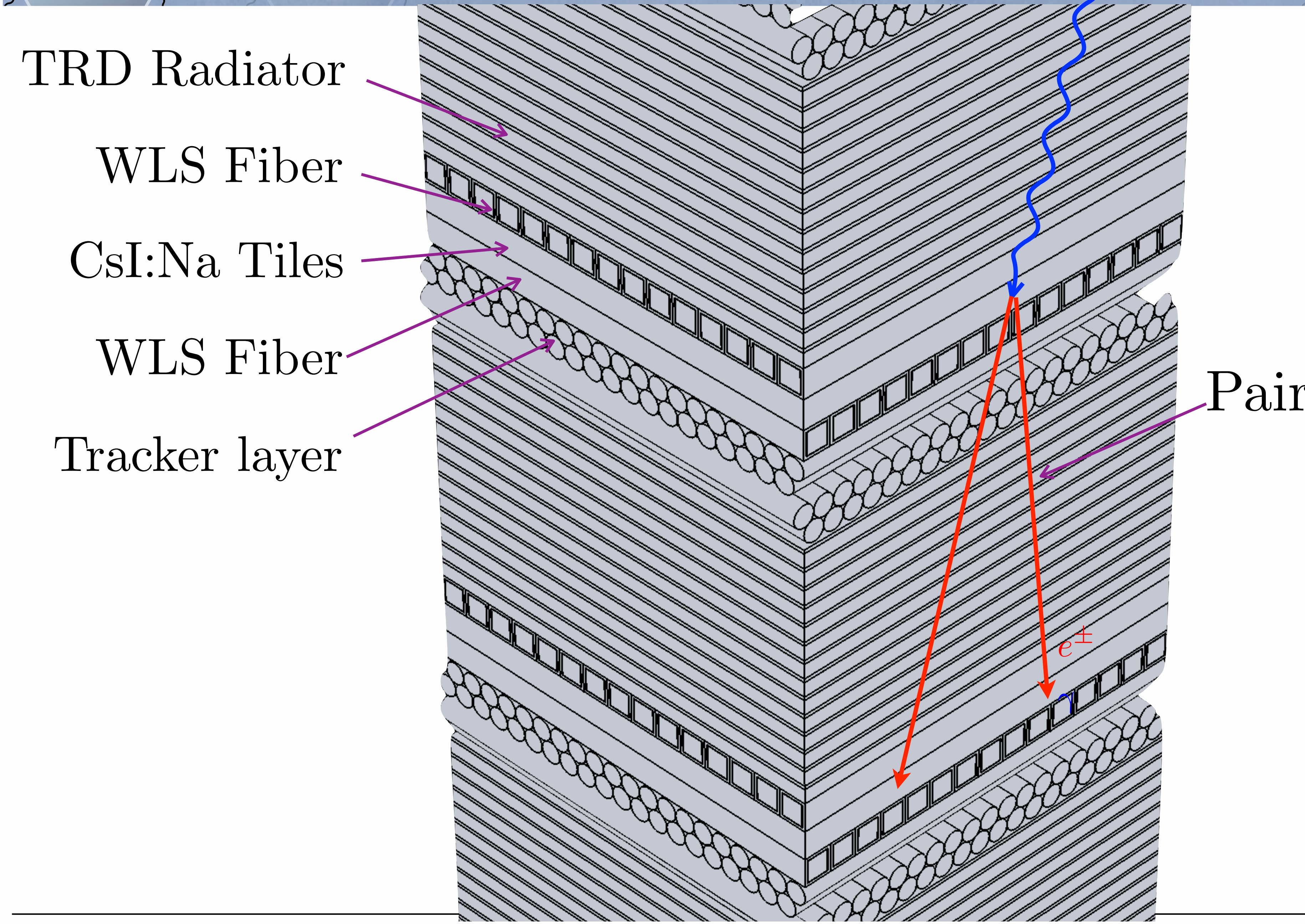

Pair Telescope Mode

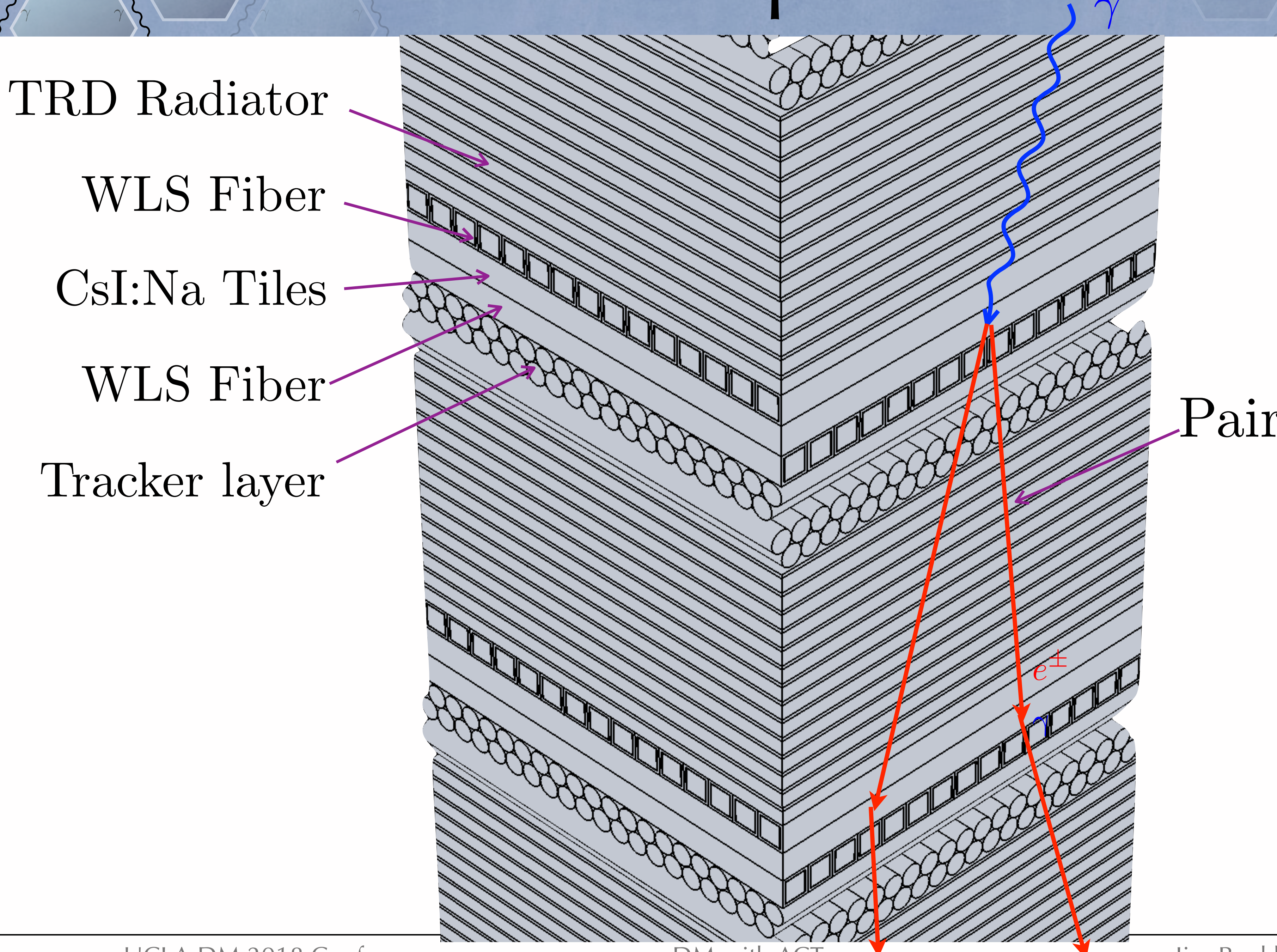

Pair Telescope Mode

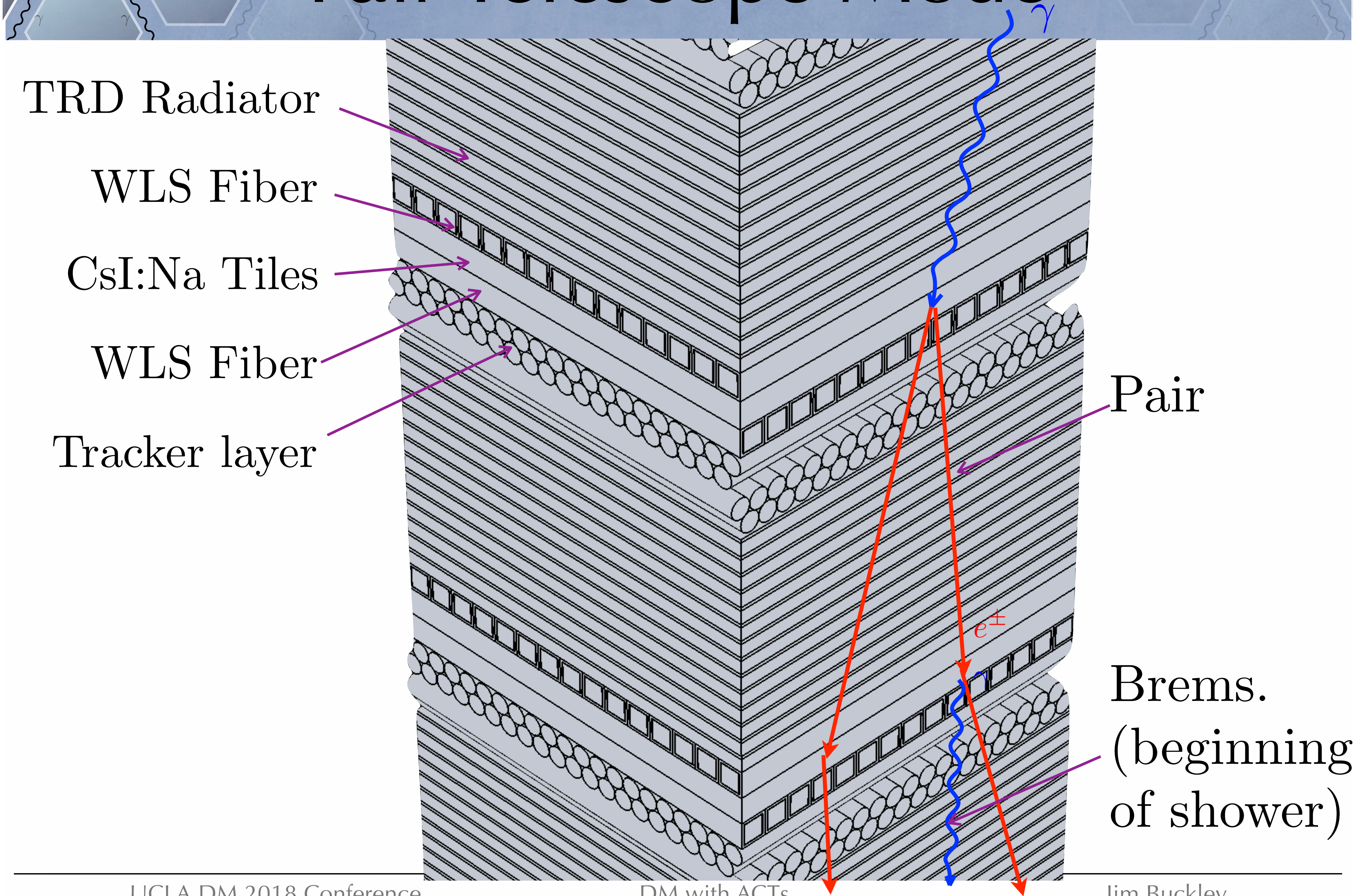

Compton Telescope

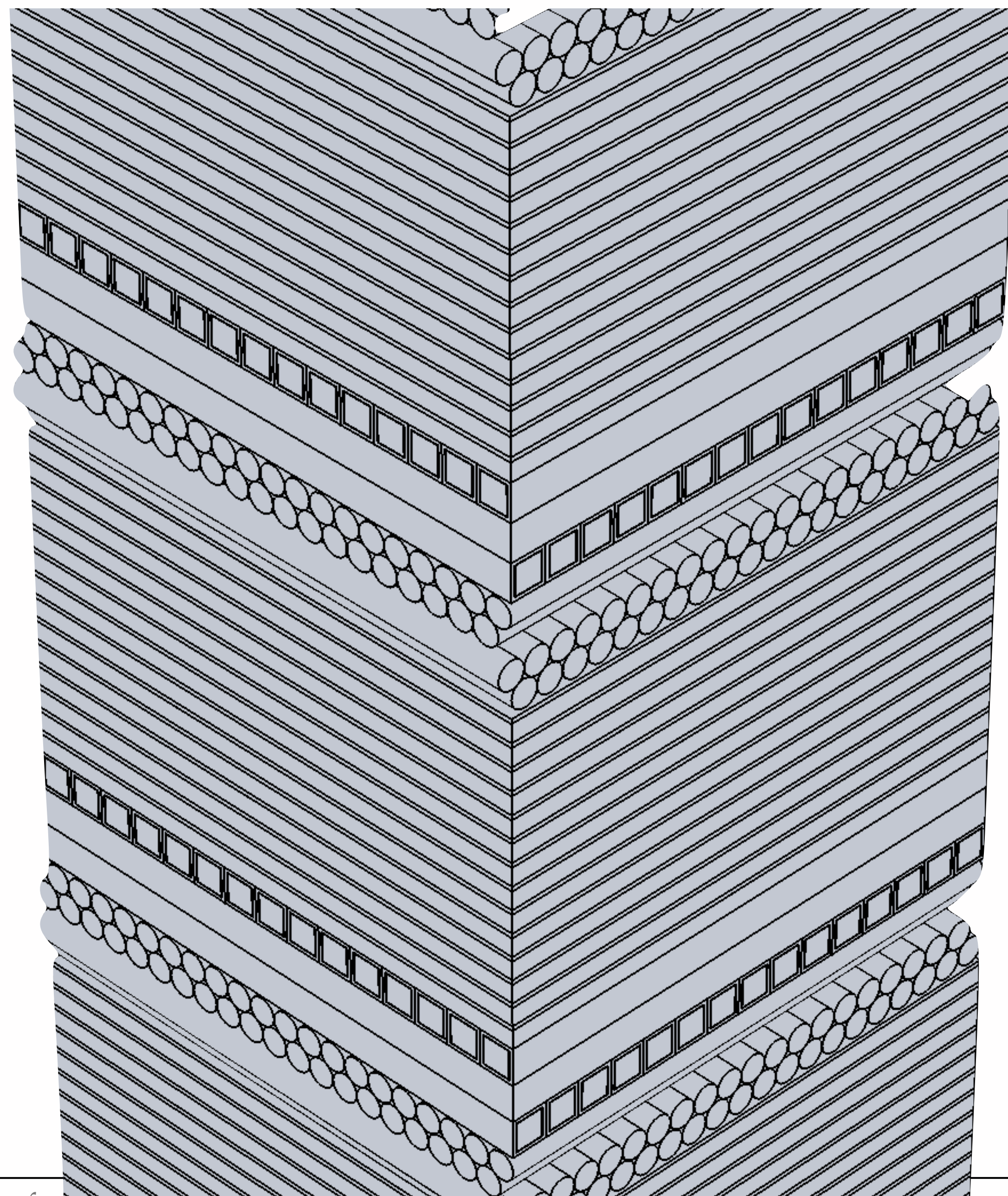

Compton Telescope

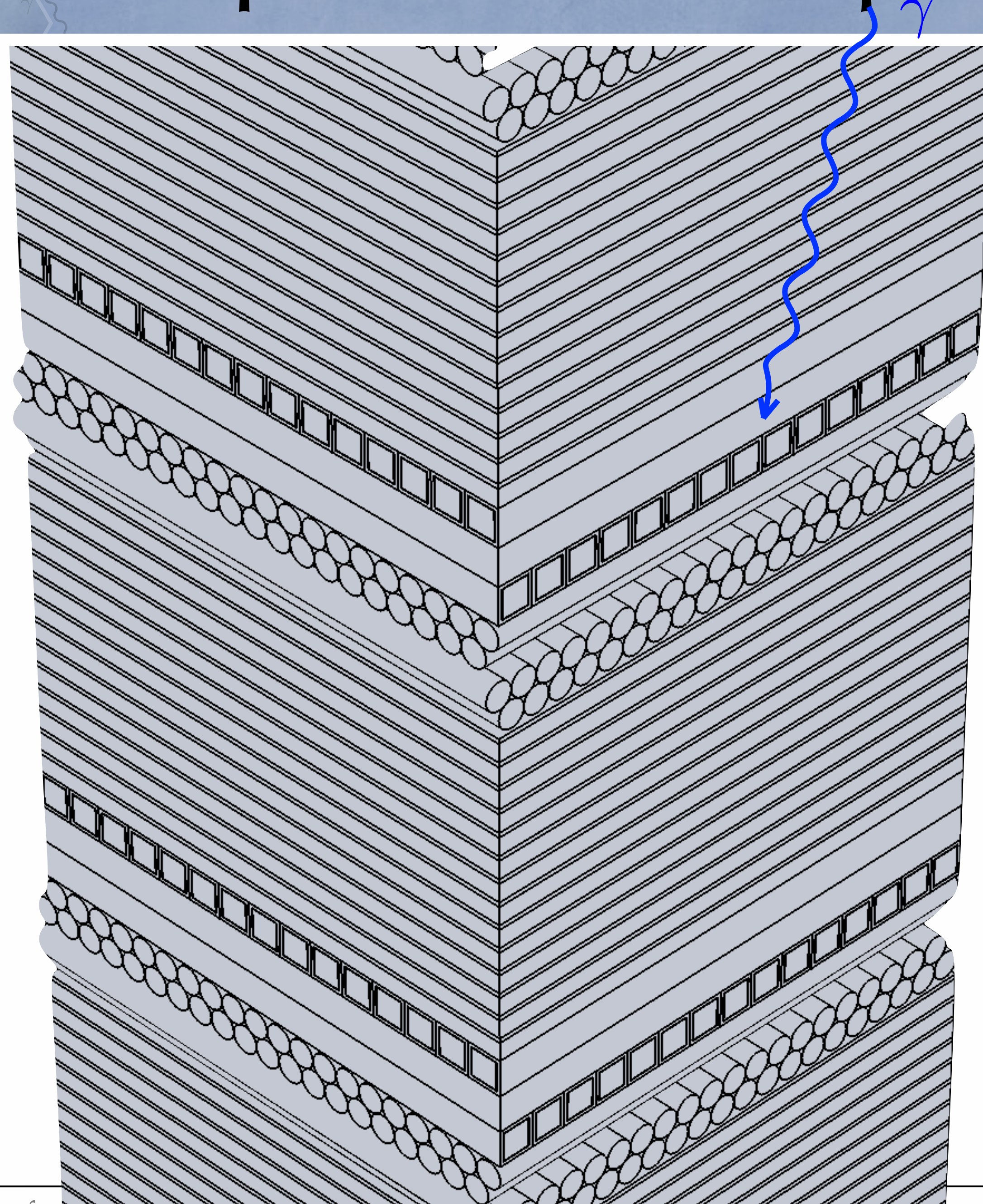

Compton Telescope

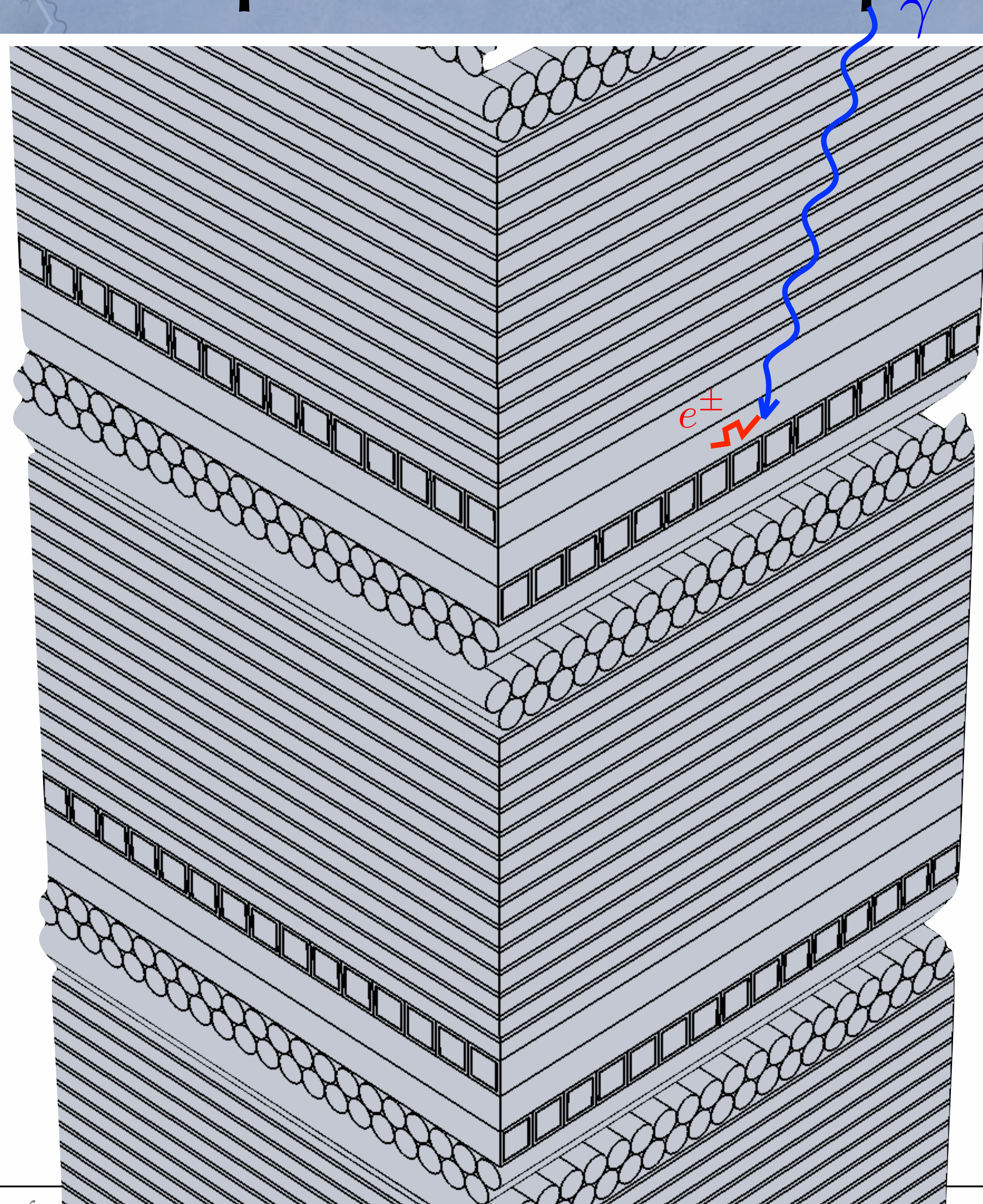

Compton Telescope

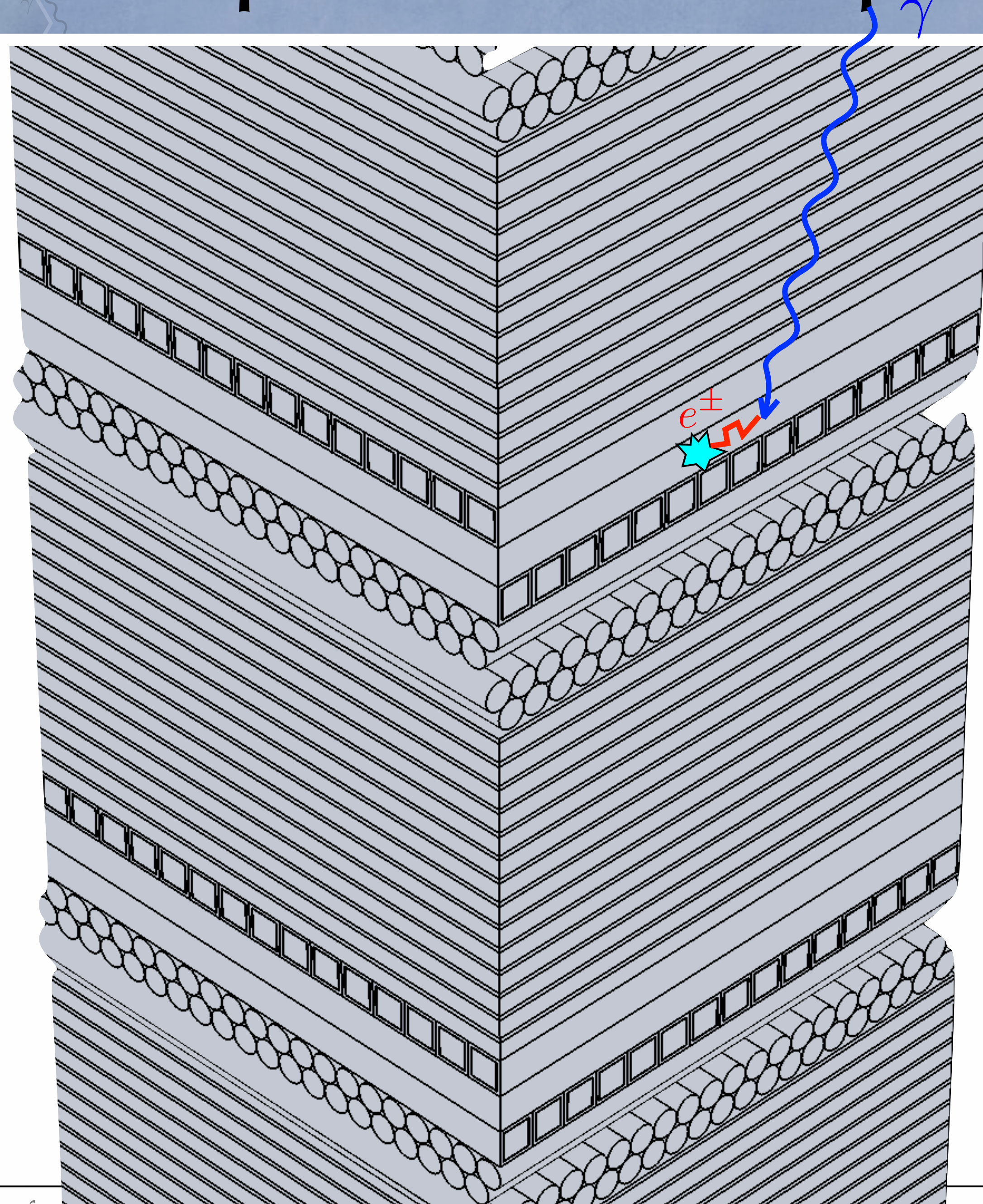

Compton Telescope

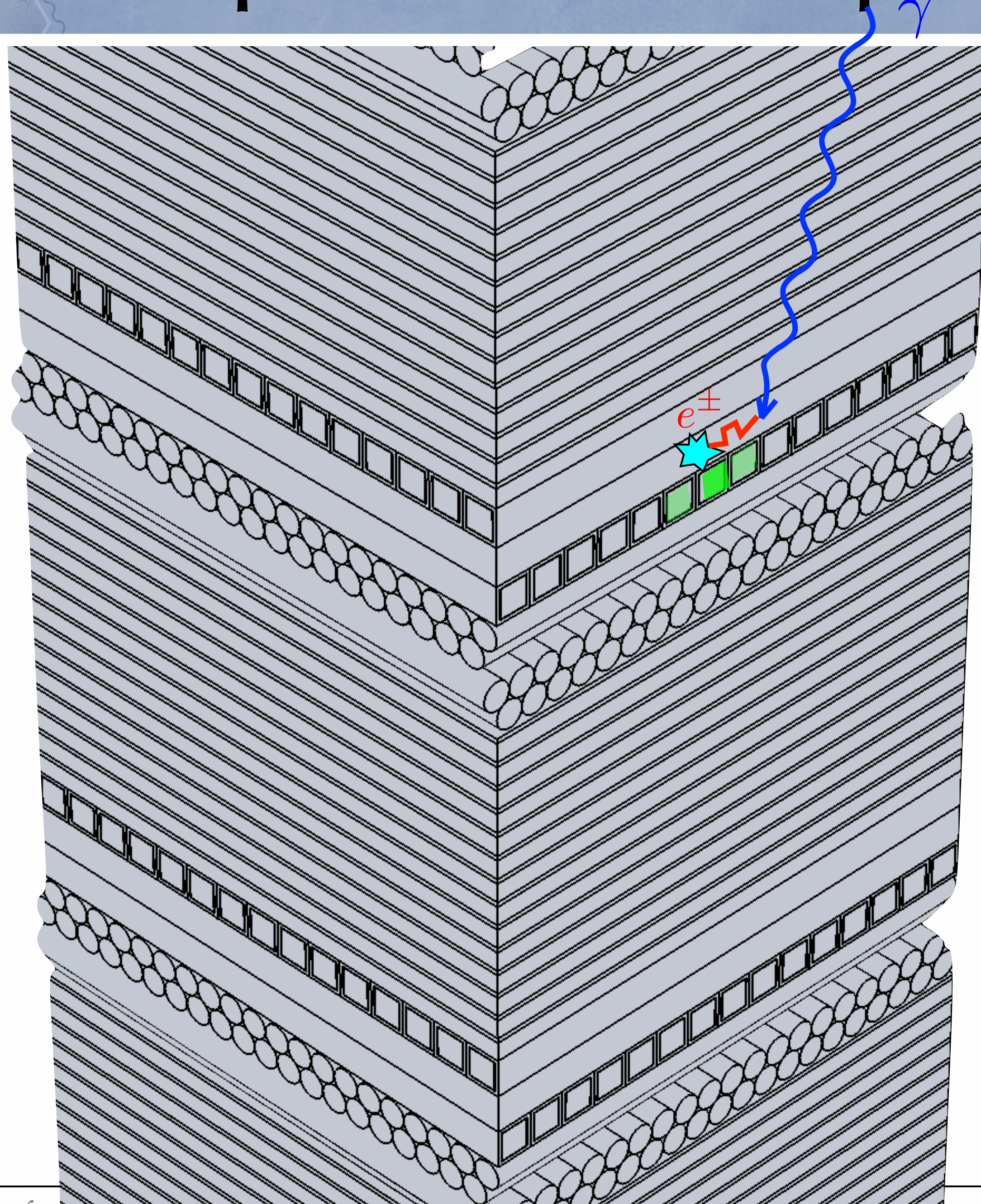

Compton Telescope

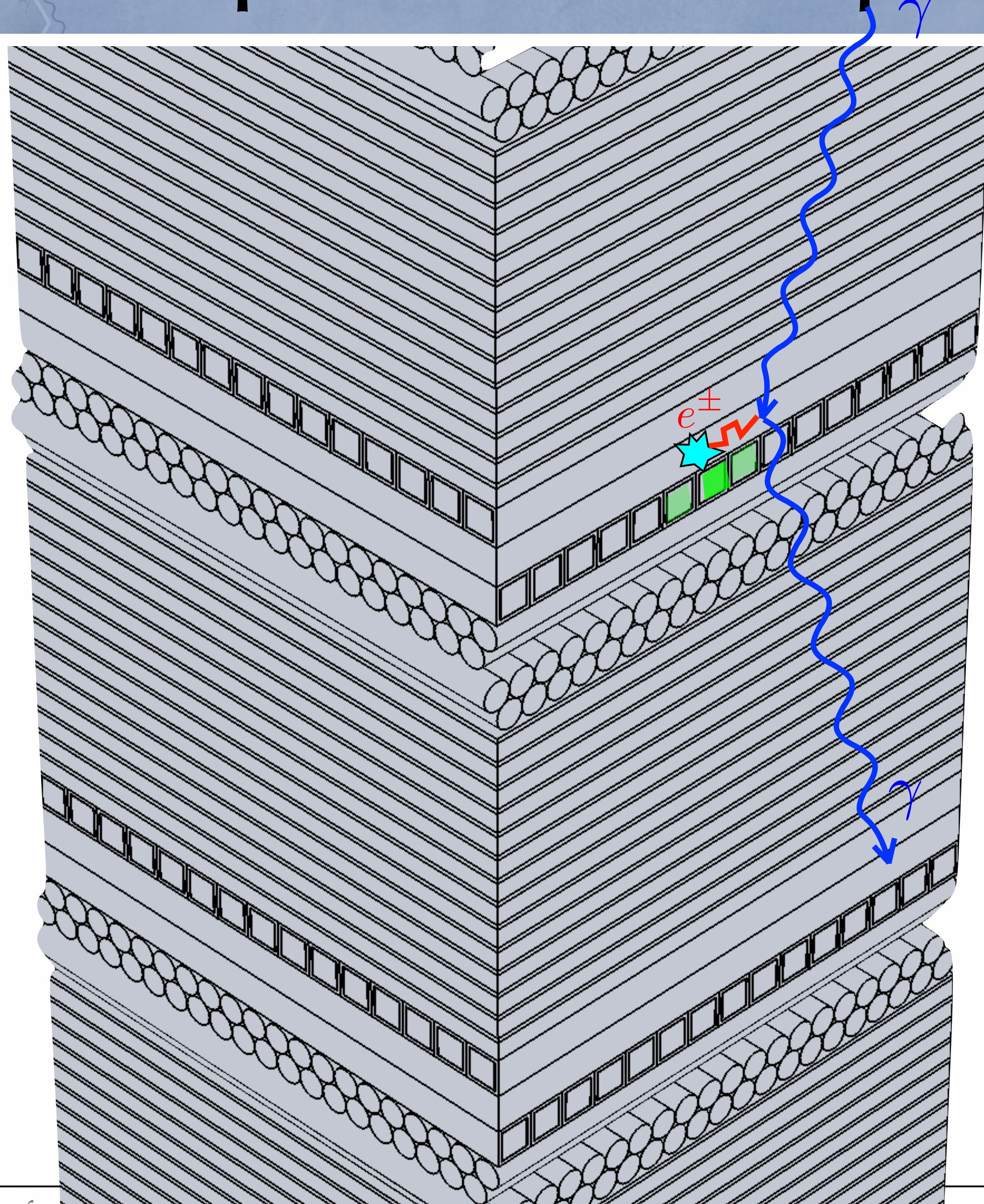

Compton Telescope

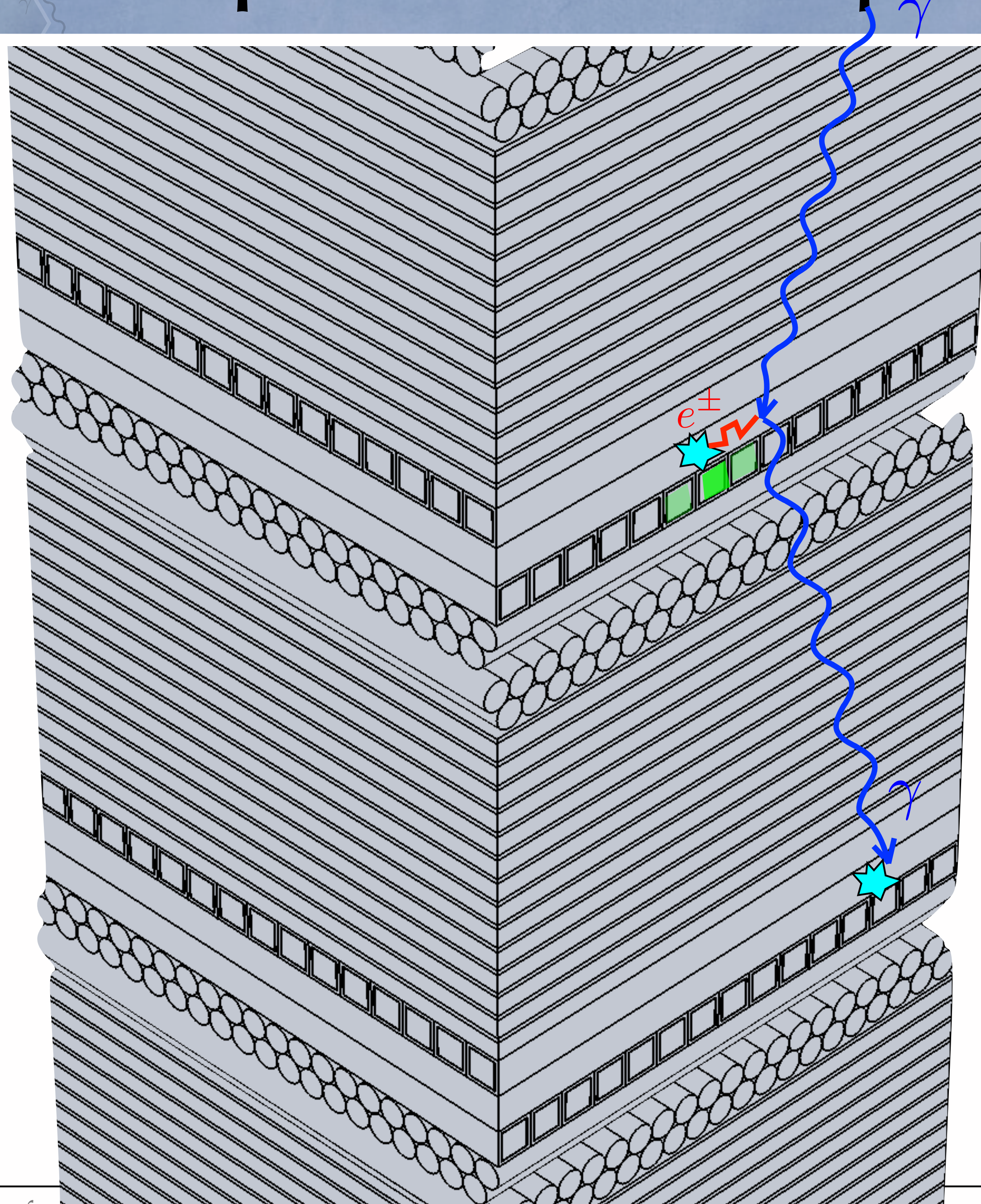

Compton Telescope

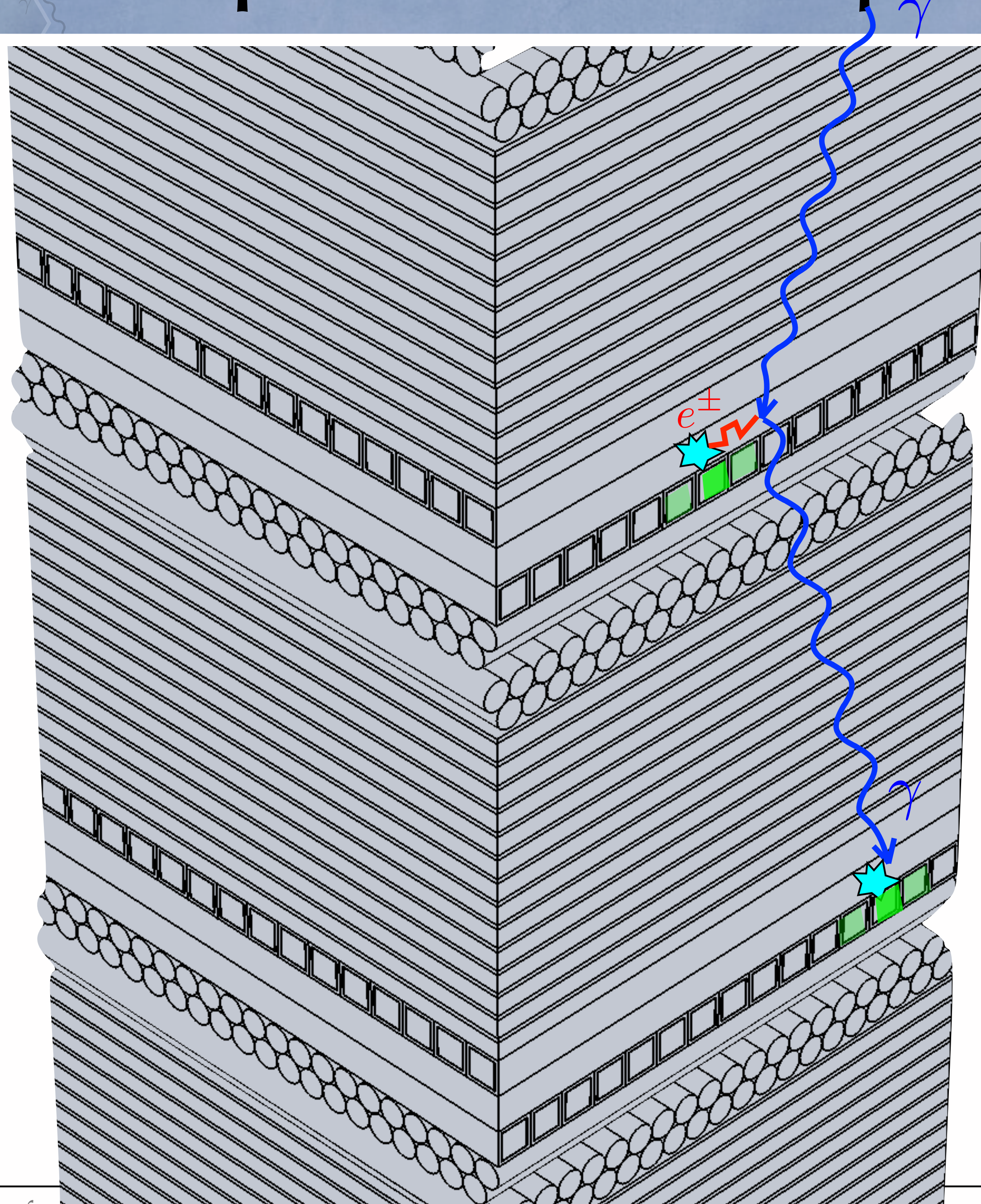

Compton Telescope

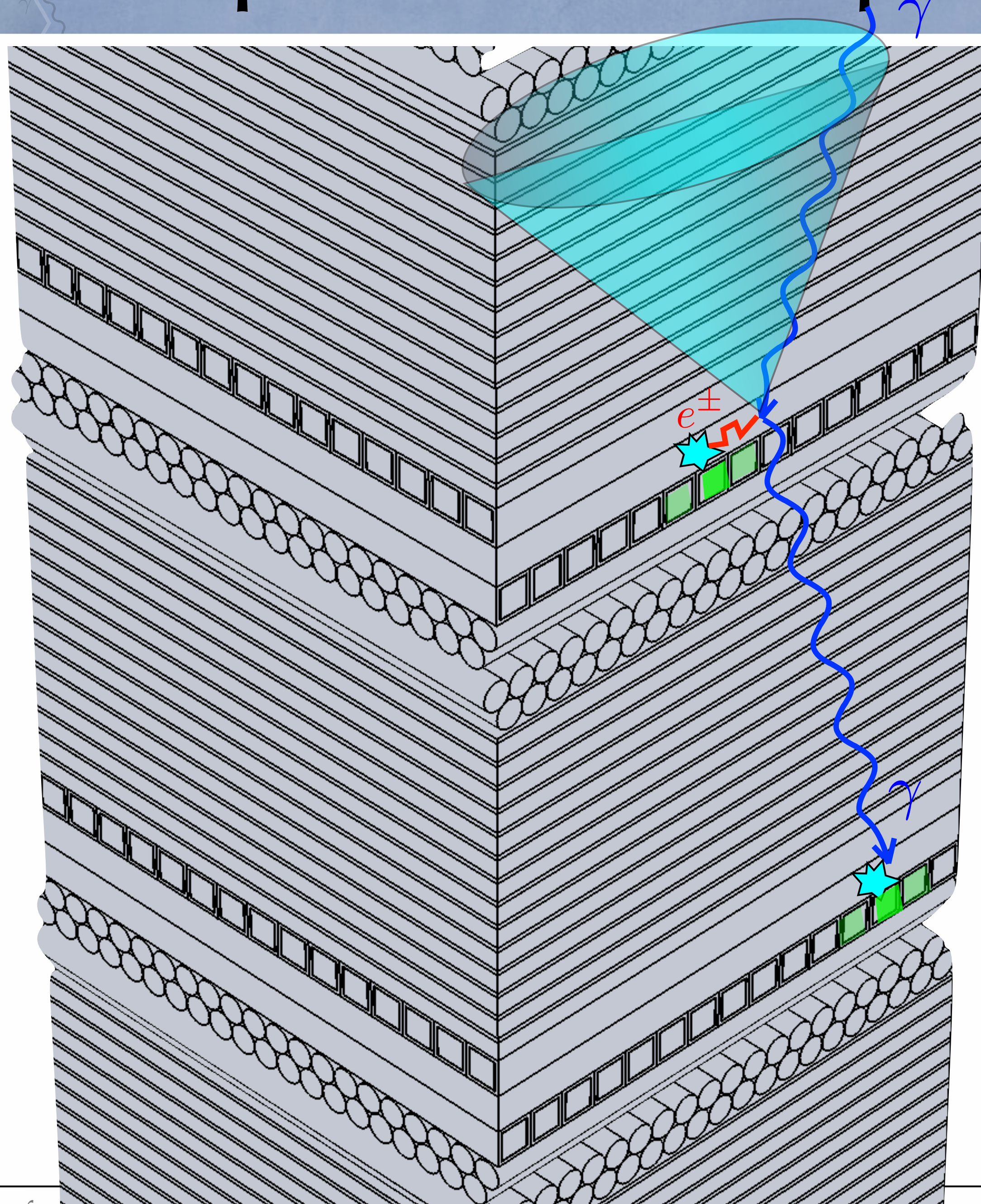

Theory of operation

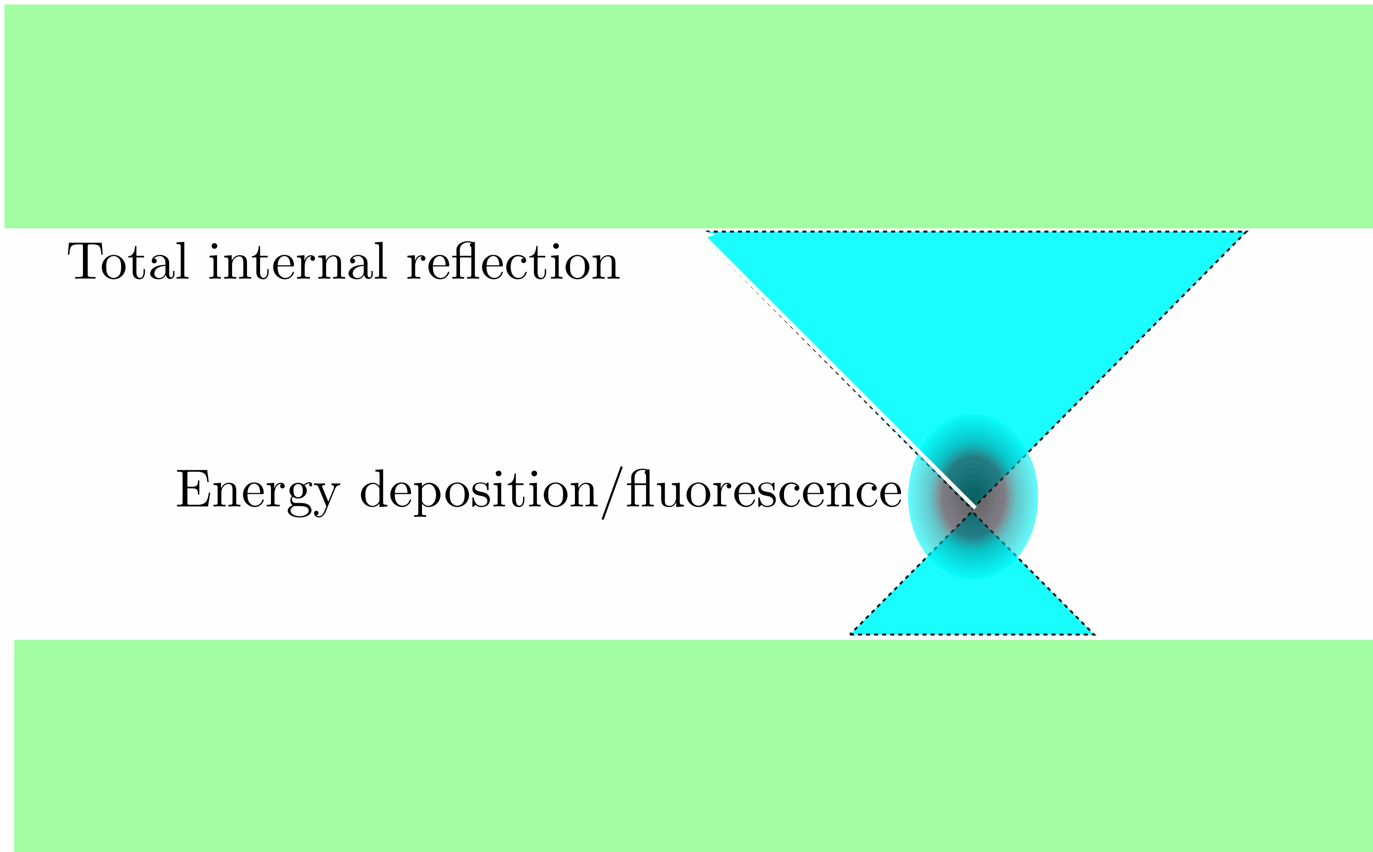

- Slow signals from CsI+WLS can be distinguished from fast signals from ionizing particles passing through fibers. *Bow-tie* illumination pattern allows centroiding of x-y coordinates, some information of depth of interaction.

APT Performance

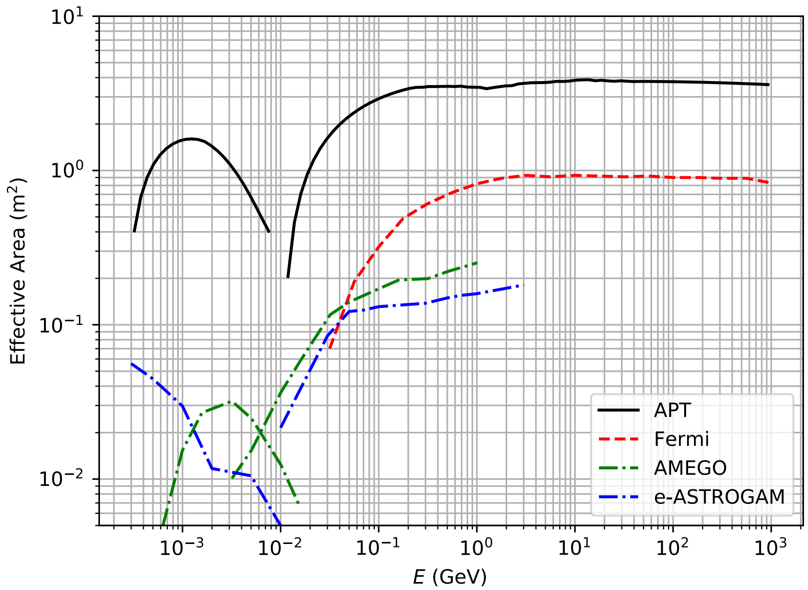

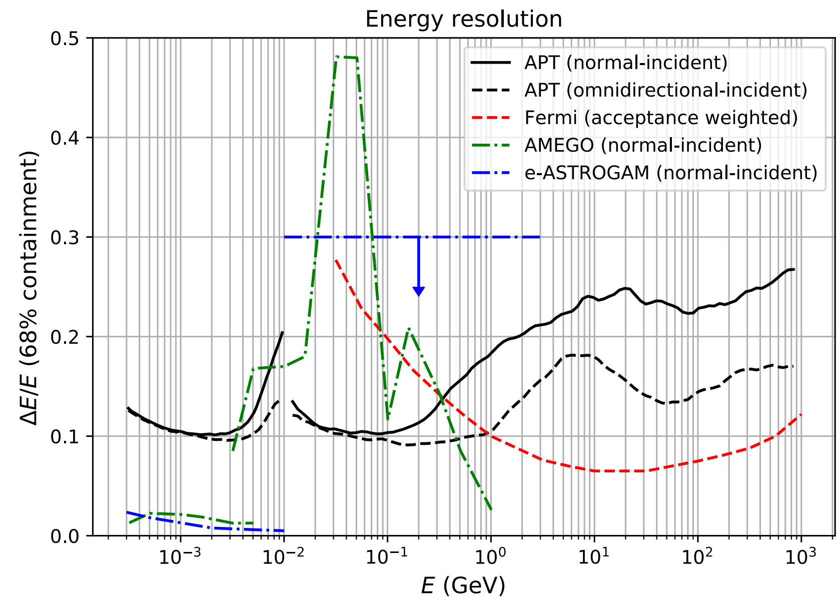

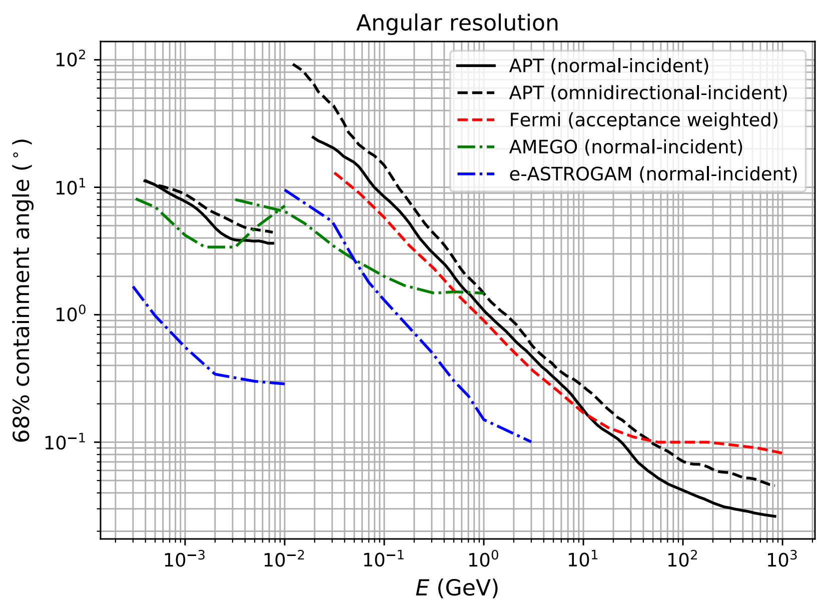

Cosmic Ray Measurements

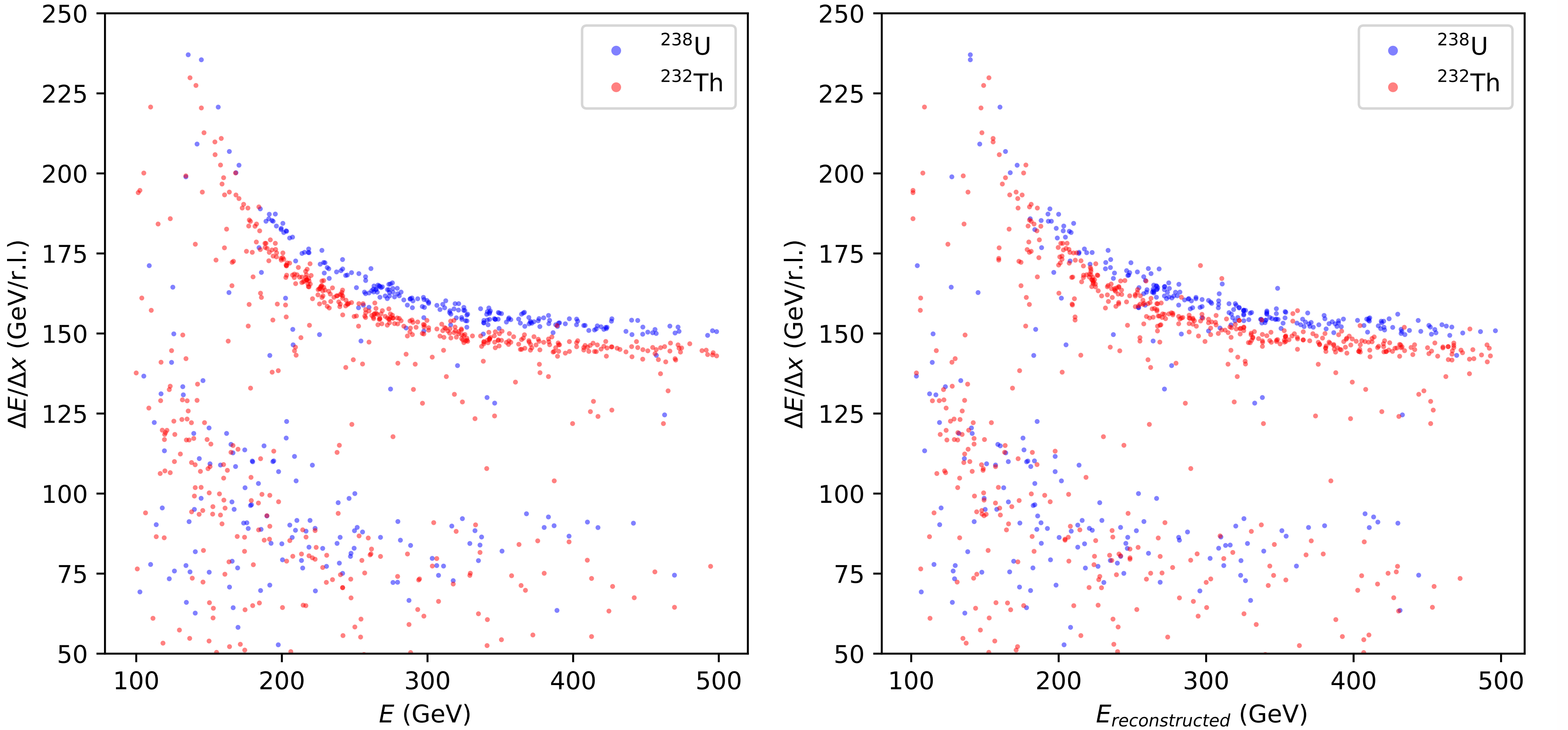

- APT with multiple dE/dx measurements can measure rare, ultra-heavy r-process elemental abundances

Pair Energy Reconstruction

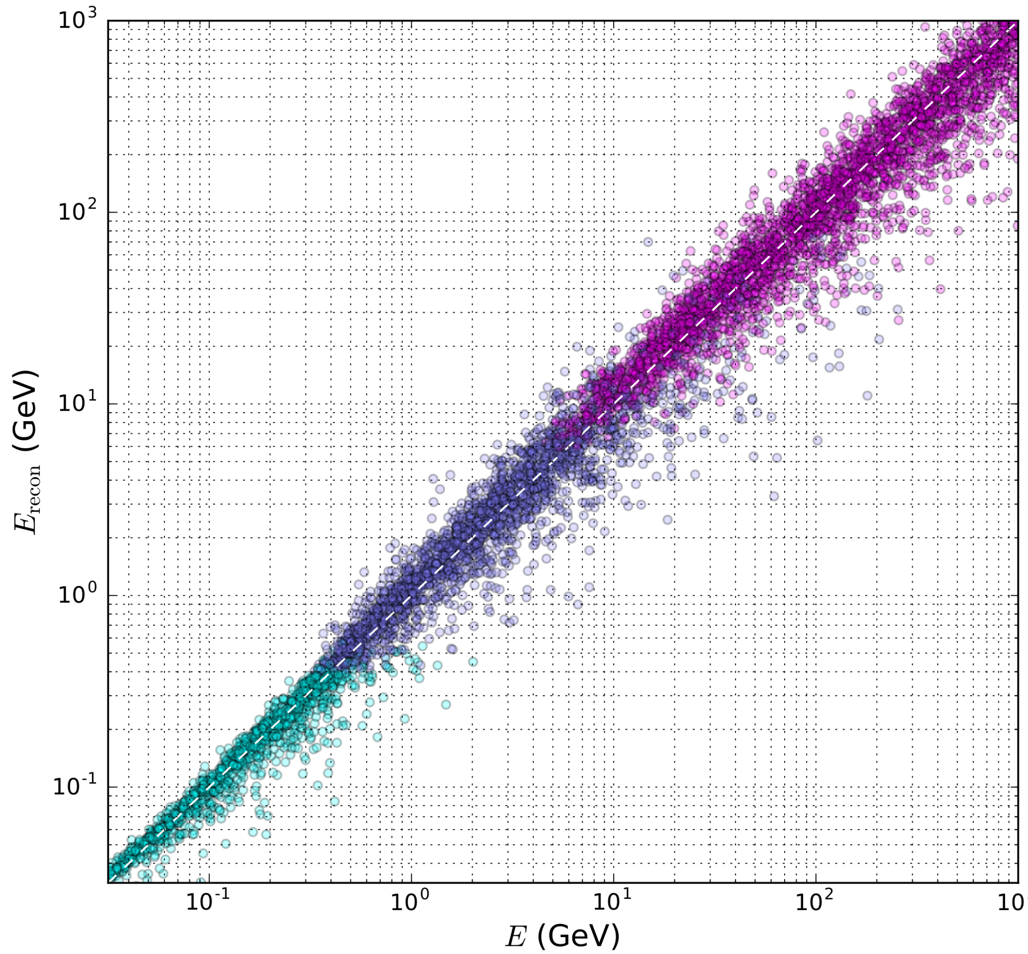

Reconstructed energy as a function of the incoming γ-ray energy. Colors correspond to different reconstruction methods

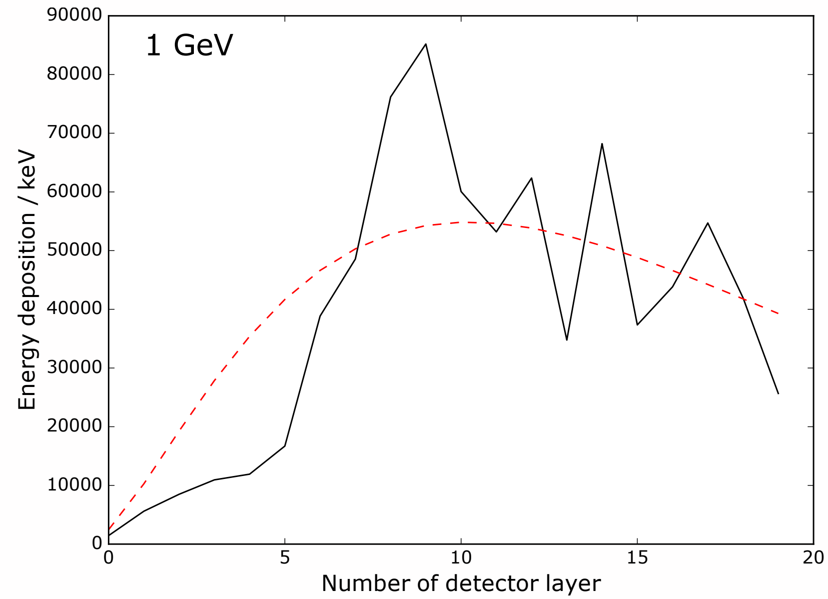

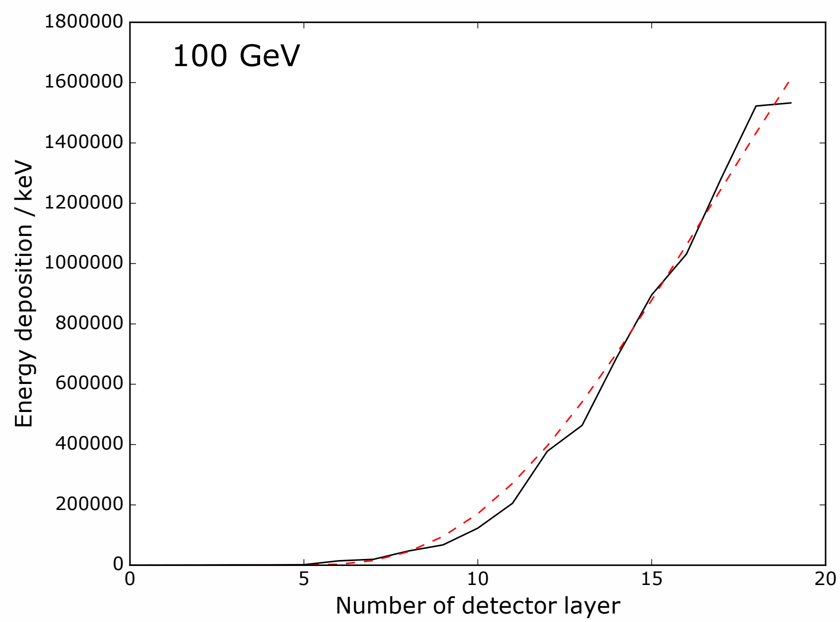

Source Localization

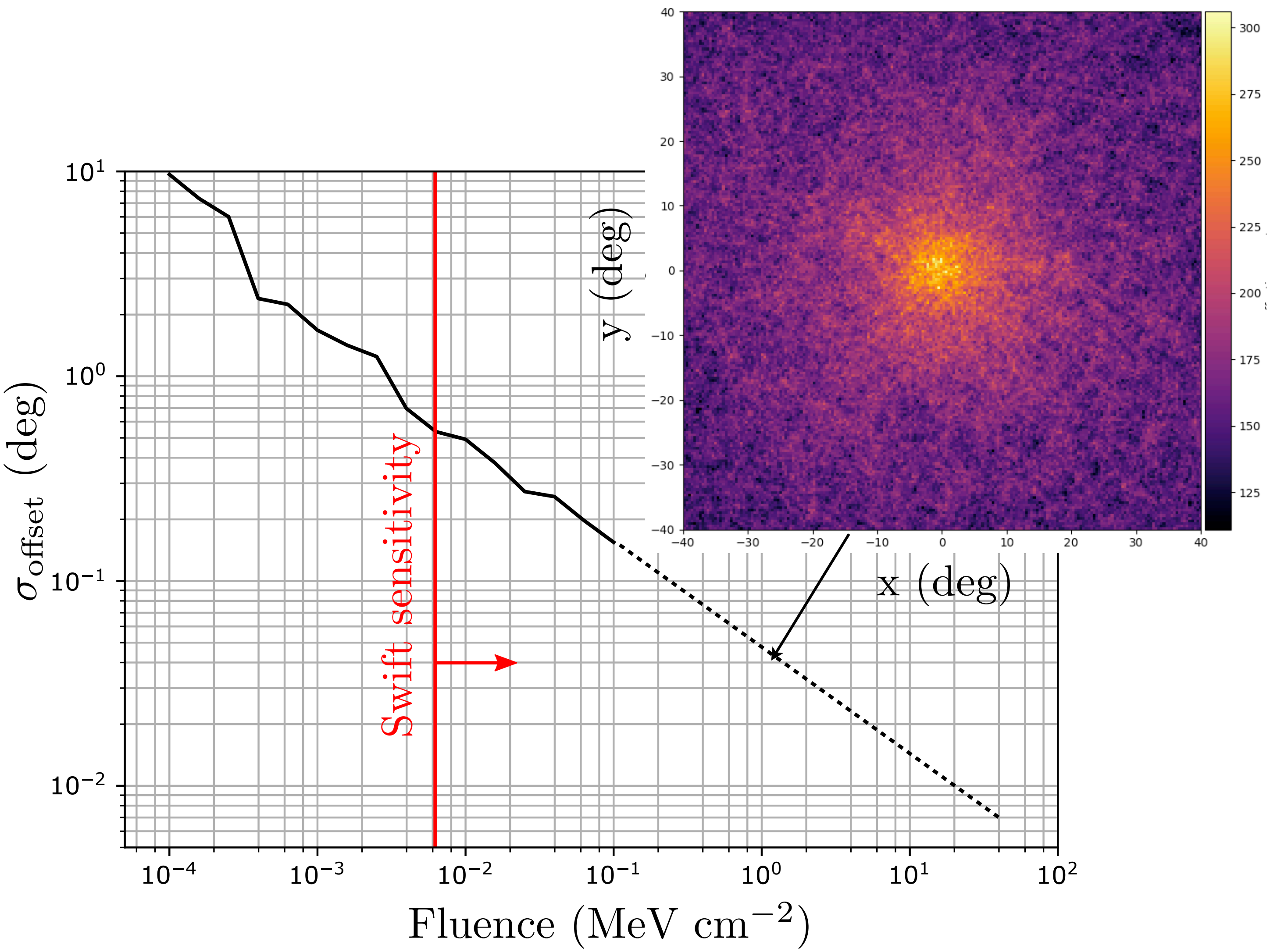

Gravitational Wave

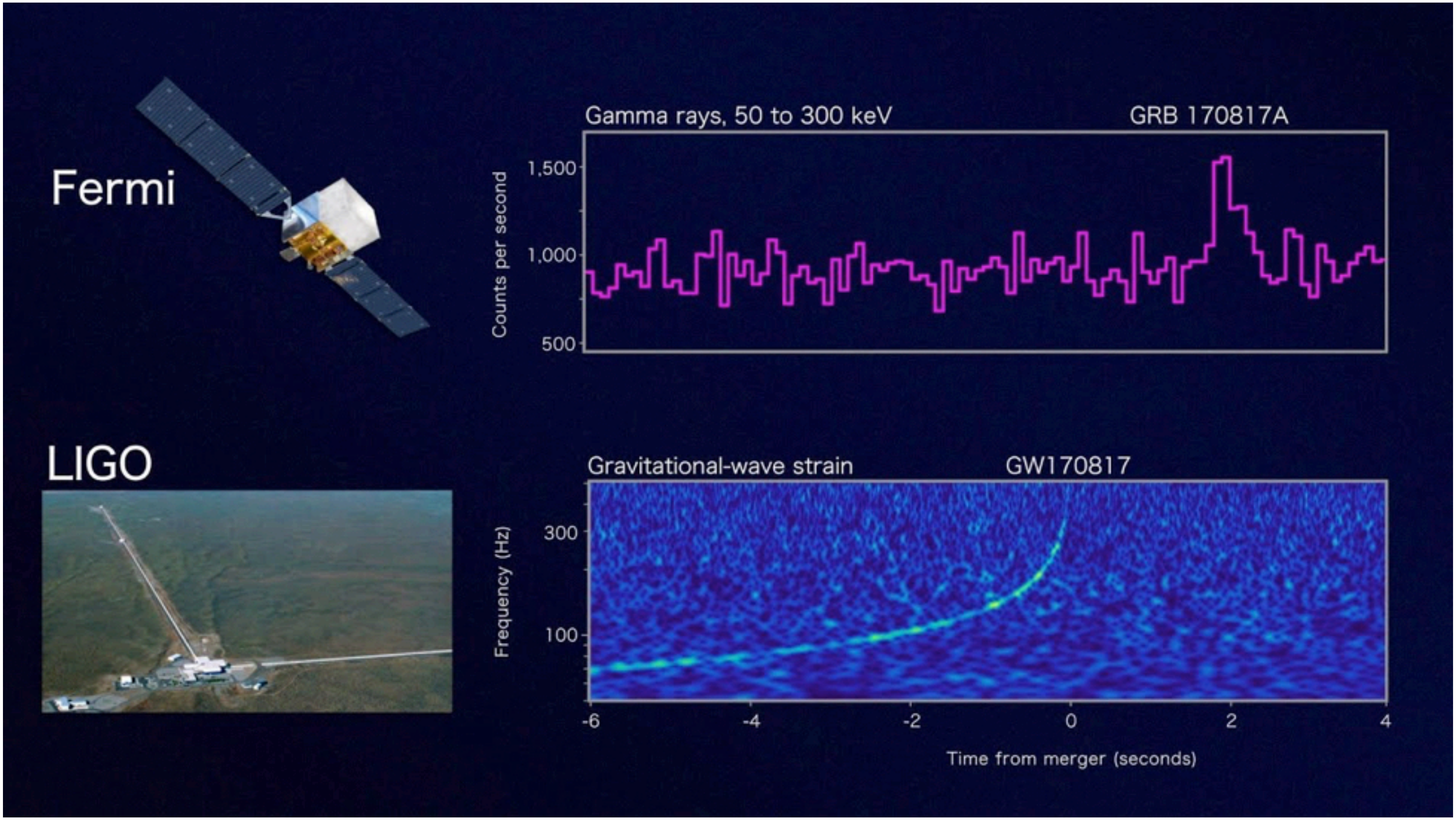

- Electromagnetic counterpart found for recent LIGO event, n-star merger

APT n-star Merger Sensitivity

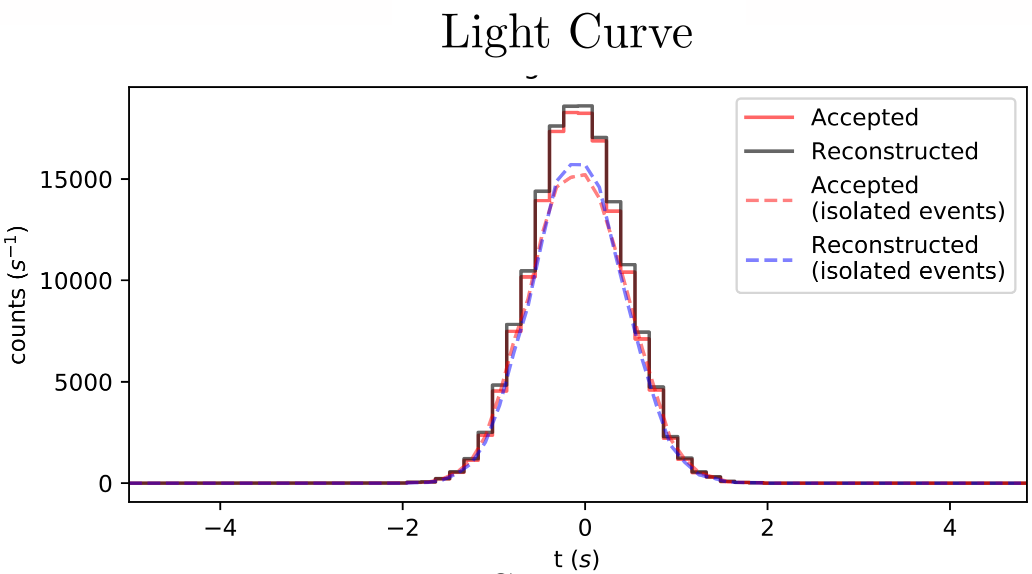

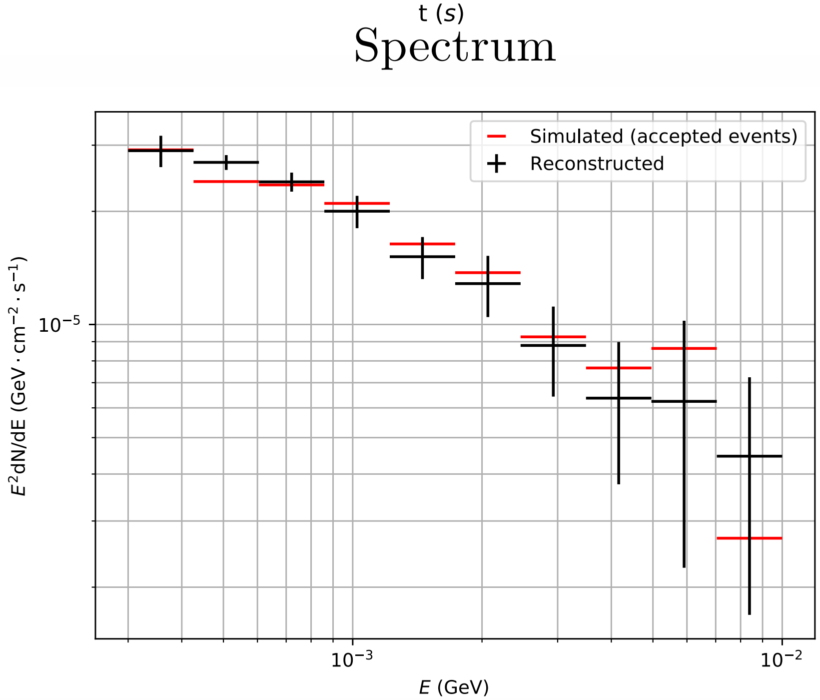

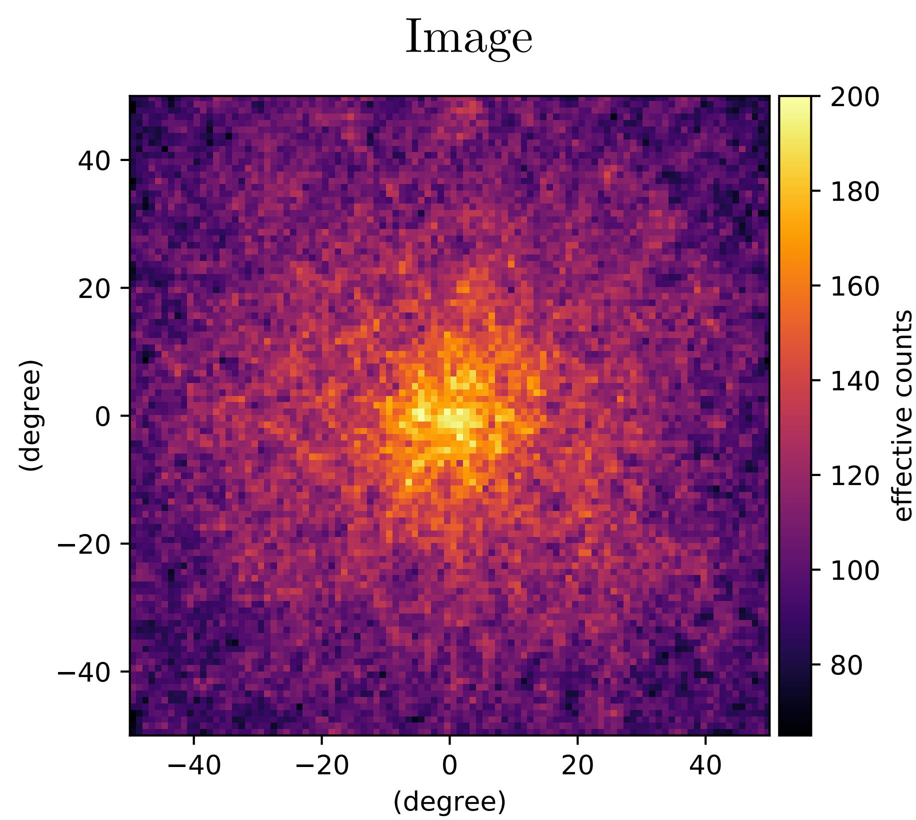

APT GW Performance

LIGO et al., ApJL, **848**, L12 (2017)

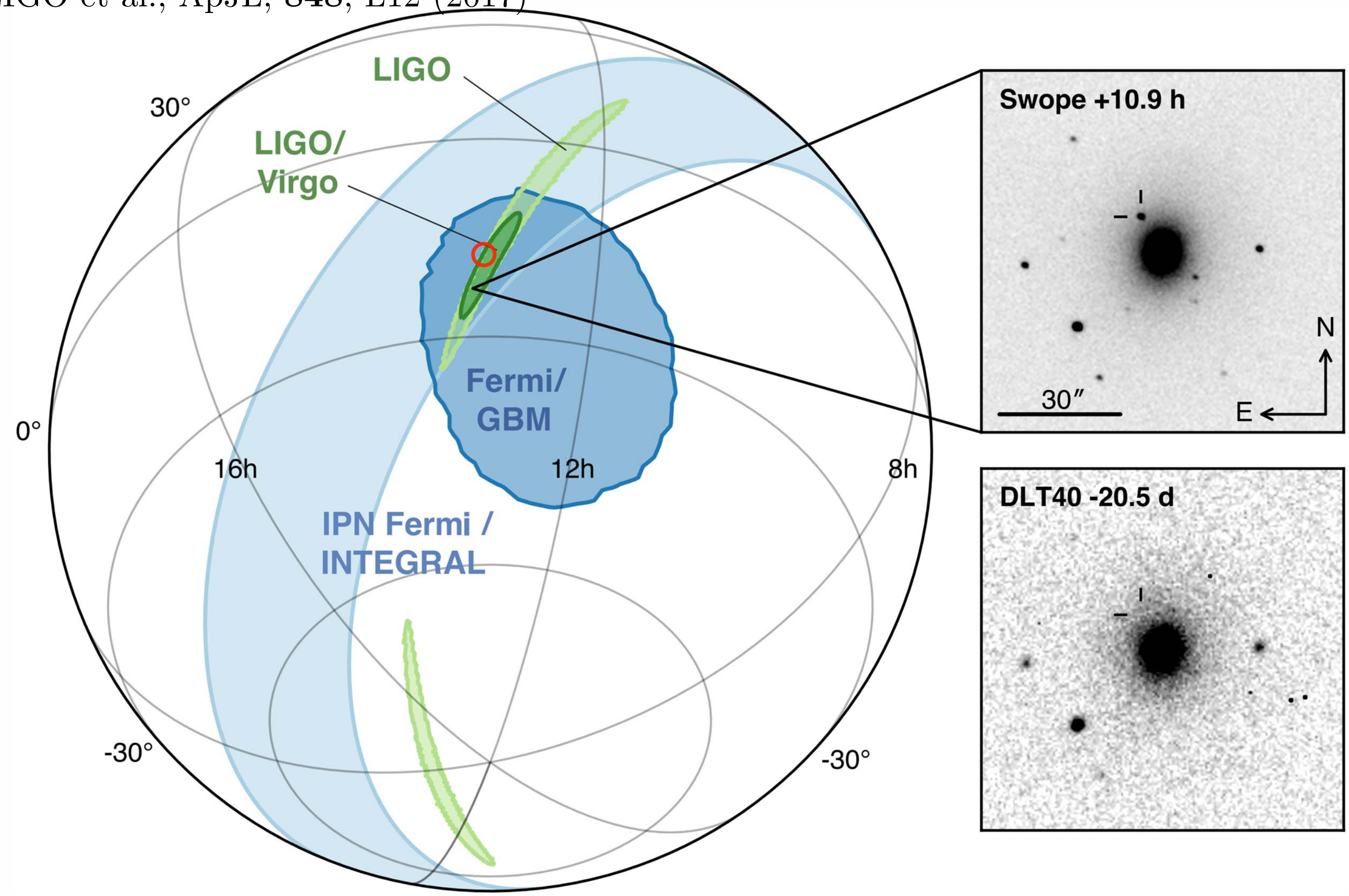

APT GW Performance

LIGO et al., ApJL, **848**, L12 (2017)

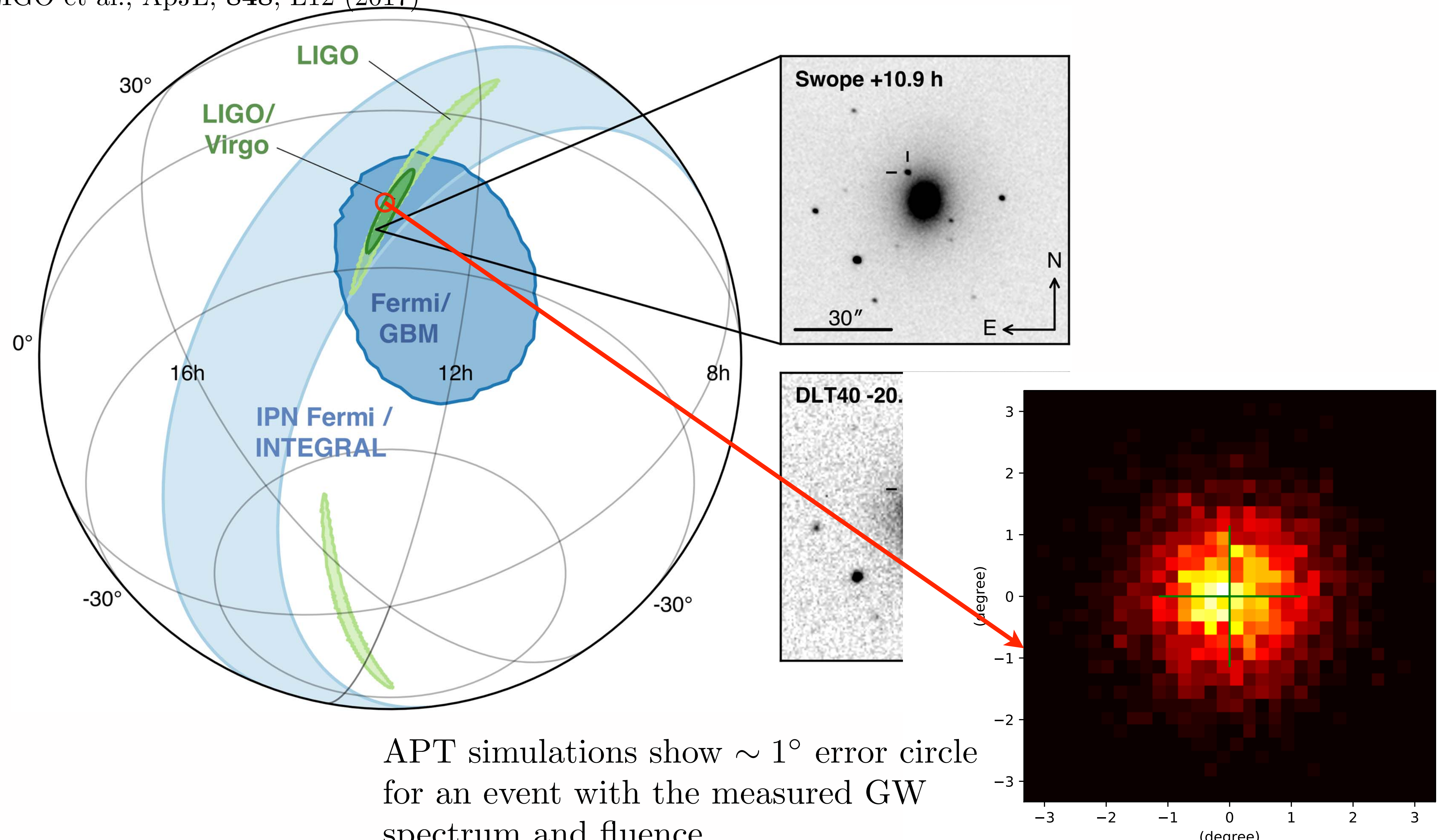

APT simulations show $\sim 1^\circ$ error circle for an event with the measured GW spectrum and fluence

CTA Phases & Timeline

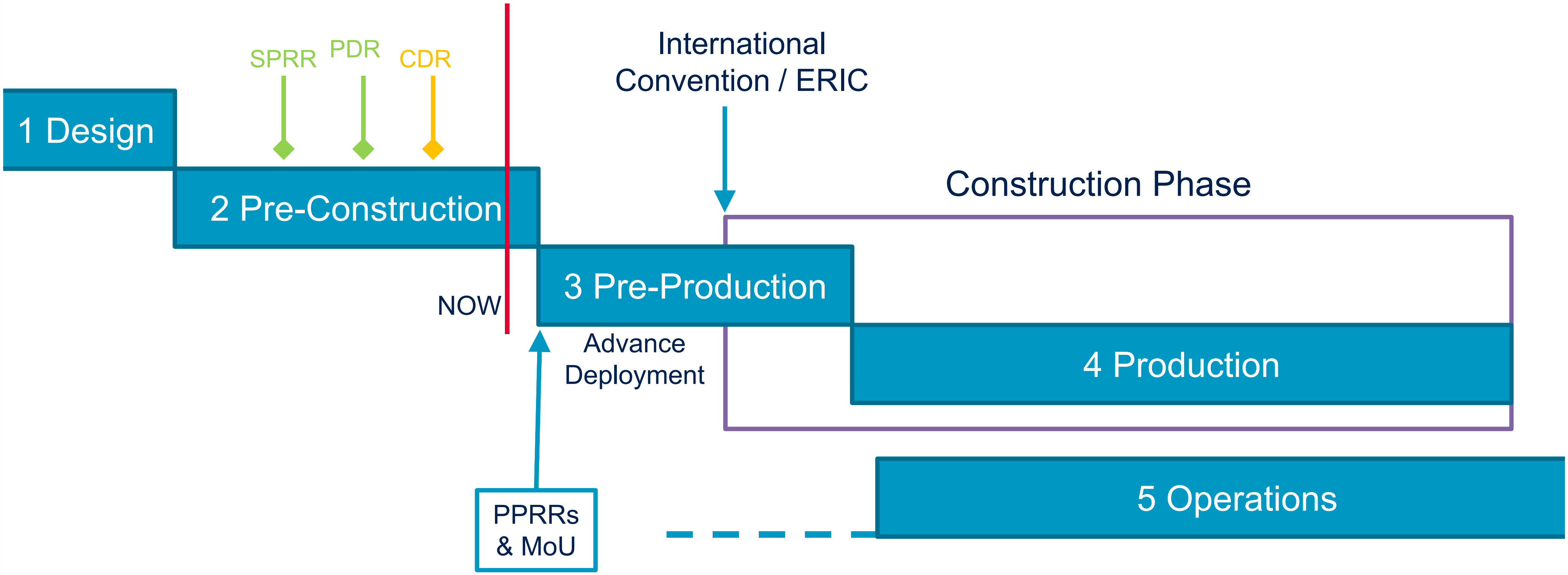

- 2016: Hosting agreement, site preparations start (N)
- 2017: Hosting agreement, site preparations start (S)
- Funding level at ~65% of required for *baseline implementation*
  → start with *threshold implementation*
  → additional funding, telescopes needed to complete CTA
- Construction period of 5-6 years
- Initial science with partial arrays possible before construction end

(credit R. Ong)